U.S. DEPARTMENT OF COMMERCE
National Technical Information Service

PB-261 075

Application of Foam Scrubbing to Fine Particle Control, Phase I

Monsanto Research Corp, Dayton, Ohio

Prepared for

Industrial Environmental Research Lab, Research Triangle Park, N C

May 76

TECHNICAL REPORT DATA

(Please read Instructions on the reverse before completing)

1. REPORT NO. EPA-600/2-76-125	2.	3. RECIPIENT'S ACCESSION NO.
4. TITLE AND SUBTITLE Application of Foam Scrubbing to Fine Particle Control--Phase I		5. REPORT DATE May 1976
		6. PERFORMING ORGANIZATION CODE
7. AUTHOR(S) T.E. Ctvrtnicek, T.F. Walburg, C.M. Moscowitz, and H.H.S. Yu		8. PERFORMING ORGANIZATION REPORT NO. MRC-DA-556
9. PERFORMING ORGANIZATION NAME AND ADDRESS Monsanto Research Corporation 1515 Nicholas Road Dayton, Ohio 45407		10. PROGRAM ELEMENT NO. 1AB012; ROAP 21ADL-029
		11. CONTRACT/GRANT NO. 68-02-1453
12. SPONSORING AGENCY NAME AND ADDRESS EPA, Office of Research and Development Industrial Environmental Research Laboratory Research Triangle Park, NC 27711		13. TYPE OF REPORT AND PERIOD COVERED Phase I Final; 6/74-12/75
		14. SPONSORING AGENCY CODE EPA-ORD

15. SUPPLEMENTARY NOTES IERL-RTP project officer for this report is Geddes H. Ramsey, Mail Drop 61, Ext 2298.

16. ABSTRACT

The report summarizes knowledge and data obtained during the first phase of investigations into foam scrubbing. It gives detailed information concerning foam scrubber theory, experimentation, and economics, The theory pertains to mechanisms influencing the behavior of fine particles and the possibilities of their capture by foam. Collection efficiencies obtained on a bench scale foam scrubber show that foam scrubbing can be a viable fine particle control device. Preliminary economic analysis indicates that foam scrubbing can be competitive with other fine particle collection devices if the surfactant solution is recycled effectively. The report recommends that surfactant recycle be verified, using a bench scale foam scrubber.

17. KEY WORDS AND DOCUMENT ANALYSIS

a. DESCRIPTORS	b. IDENTIFIERS/OPEN ENDED TERMS	c. COSATI Field/Group
Air Pollution	Air Pollution Control	13B
Dust	Stationary Sources	11G
Scrubbers	Fine Particulate	07A
Foam	Foam Scrubbing	

18. DISTRIBUTION STATEMENT Unlimited	19. SECURITY CLASS *(This Report)* Unclassified	21. NO. OF PAGES 156
	20. SECURITY CLASS *(This page)* Unclassified	22. PRICE 4.75

EPA Form 2220-1 (9-73)

350105

PB 261 075

EPA-600/2-76-125
May 1976

Environmental Protection Technology Series

UNITED STATES ENVIRONMENTAL PROTECTION AGENCY

REPRODUCED BY
NATIONAL TECHNICAL
INFORMATION SERVICE
U. S. DEPARTMENT OF COMMERCE
SPRINGFIELD, VA. 22161

RESEARCH REPORTING SERIES

Research reports of the Office of Research and Development, U.S. Environmental Protection Agency, have been grouped into five series. These five broad categories were established to facilitate further development and application of environmental technology. Elimination of traditional grouping was consciously planned to foster technology transfer and a maximum interface in related fields. The five series are:

1. Environmental Health Effects Research
2. Environmental Protection Technology
3. Ecological Research
4. Environmental Monitoring
5. Socioeconomic Environmental Studies

This report has been assigned to the ENVIRONMENTAL PROTECTION TECHNOLOGY series. This series describes research performed to develop and demonstrate instrumentation, equipment, and methodology to repair or prevent environmental degradation from point and non-point sources of pollution. This work provides the new or improved technology required for the control and treatment of pollution sources to meet environmental quality standards.

EPA REVIEW NOTICE

This report has been reviewed by the U.S. Environmental Protection Agency, and approved for publication. Approval does not signify that the contents necessarily reflect the views and policy of the Agency, nor does mention of trade names or commercial products constitute endorsement or recommendation for use.

This document is available to the public through the National Technical Information Service, Springfield, Virginia 22161.

EPA-600/2-76-125
May 1976

APPLICATION OF FOAM SCRUBBING TO FINE PARTICLE CONTROL

PHASE I

by

T.E. Ctvrtnicek, T.F. Walburg,
C.M. Moscowitz, and H.H.S. Yu

Monsanto Research Corporation
1515 Nicholas Road
Dayton, Ohio 45407

Contract No. 68-02-1453
ROAP No. 21ADL-029
Program Element No. 1AB012

EPA Project Officer: Geddes H. Ramsey

Industrial Environmental Research Laboratory
Office of Energy, Minerals, and Industry
Research Triangle Park, NC 27711

Prepared for

U.S. ENVIRONMENTAL PROTECTION AGENCY
Office of Research and Development
Washington, DC 20460

ia/

ABSTRACT

This report summarizes the knowledge and the data obtained during the first phase of investigations into foam scrubbing. Detailed information is presented concerning foam scrubber theory, experimentation, and economics. The theory pertains to mechanisms influencing the behavior of fine particles and the possibilities of their capture by foam. Collection efficiencies obtained on a bench scale foam scrubber show that foam scrubbing can be a viable fine particle control device. Preliminary economic analysis indicates that foam scrubbing can be competitive with other fine particle collection devices provided that surfactant solution is recycled effectively. Verification of surfactant recycle is recommended using a pilot scale foam scrubber.

CONTENTS

Page

1. Summary 1
2. Conclusions and Recommendations 3
3. Introduction 7
4. Theoretical Aspects of Foam Scrubber Application 9
   4.1 Foam Formation 9
   4.2 Diffusion Phenomena in Foam 15
   4.3 Particle Capturing by Other Mechanisms 23
      4.3.1 Impaction and Sedimentation 27
      4.3.2 Thermophoresis and Diffusiophoresis 43
      4.3.3 Electrostatic Force 56
5. Experimental Work 59
   5.1 Experimental Foam Scrubber 60
   5.2 Foam Generation 60
   5.3 Foam Destruction 63
   5.4 Surfactant Selection 66
   5.5 Particle Monitoring Equipment 66
   5.6 Experimental Aerosol Generation 68
   5.7 Foam Scrubber Fine Particle Collection Efficiency 68
6. Foam Scrubber Economics 79
   6.1 Accuracy of Estimate 79
   6.2 Base Collection Efficiencies 81
   6.3 Results 88
7. References 93

Appendixes 97

FIGURES

Number		Page
1	Schematic of spray foam generator	10
2	Schematic of perforated plate foam generator	11
3	Cunningham slip correction for liquid and solid particles	19
4	Displacement of particles in air by diffusion	21
5	Particle collection efficiency	24
6	Particle collection efficiency	25
7	Particle collection efficiency	26
8	Initial and boundary conditions	28
9	Particle collection efficiency	33
10	Particle collection efficiency	34
11	Particle collection efficiency	35
12	Particle collection efficiency	36
13	Particle collection efficiency	37
14	Particle collection efficiency	38
15	Particle collection efficiency	39
16	Particle collection efficiency	40
17	Particle collection efficiency	41
18	Schematic diagram of exhaust gas treatment	46
19	Schematic diagram of air washer using directly recirculated spray water	52
20	The thermophoretic velocity in air as a function of temperature gradient	55
21	The diffusiophoretic velocity in air as a function of water-vapor pressure gradient	55
22	Schematic of electrostatic force between particles and bubble wall	57
23	Experimental foam scrubber	61
24	Destruction chamber of the foam scrubber	62

FIGURES (continued)

Number		Page
25	Foam destruction chamber	64
26	Monodispersed aerosol generating system	69
27	Foam scrubber collection efficiency of polypropylene glycol 425 using 2% Tergitol foam with rotating disk for foam destruction	72
28	Collection of DOP aerosol using foam scrubbing with rotating disk for foam destruction	73
29	Foam scrubber collection efficiency of polypropylene glycol 425 and DOP using large-celled (3.9 mm) foam	76
30	Collection efficiency values for distilled water sprayed on the screen versus water flow rate, DOP particle size: 0.7 - 1.0 μm	78
31	Extrapolated fine particulate control efficiencies	82
32	Capital cost for fine particulate control	90
33	Operating cost for fine particulate control	91
A-1	Bubble diameter versus air flow rate observed for 1% Tergitol foam	100
A-2	Bubble diameter versus screen opening for 1% Tergitol foam constant air and liquid flow	101
A-3	Bubble diameter versus surfactant concentration	102
A-4	Photos of foam for bubble size determinations	104
B-1a	Air flow 1.08 x 10^{-3} m^3/s (2.28 cfm), 1% Tergitol	107
B-1b	Air flow 2.32 x 10^{-3} m^3/s (4.91 cfm), 1% Tergitol	107
B-2a	Air flow 2.32 x 10^{-3} m^3/s (4.91 cfm), 1% Alkanol	109
B-2b	Air flow 1.08 x 10^{-3} m^3/s (2.28 cfm), 1% Alkanol	109
B-3	Foam viscosity measured on Brookfield viscometer	110
C-1	Foam drainage rates	115
C-2	Drainage rates for foams of varying stability	119
C-3	Portable sand blast device used for foam stability measurement	121
C-4	Stability versus concentration for Tergitol foam	123
C-5	Stability of foam generated using Tergitol with 250 mesh screen	126
D-1	Air jet whistle used by Branson for foam breakage	131

FIGURES (continued)

Number		Page
D-2	Deflectojet nozzle from Spraying Systems Company. Nozzle has 180° spray angle	132
D-3	Modified and unmodified Teflon disk	135
E-1	Expansion ratios for Tergitol foams	137
E-2	Expansion ratios for several surfactants	138
F-1	Sample dilution system	142
F-2	Characterization of dilution system	144
G-1	Particles generated by foam destruction with rotating disk	146

TABLES

Number		Page
1	Typical Sedimentation Velocity and Coefficient of Sedimentation	32
2	Typical Coefficient of Impaction	43
3	Surfactant Types	67
4	Sample Data for DOP Particle Collection with Foam Scrubber Using Rotating Disk - High Quality Foam	71
5	Cost Assumptions	84
6	Foam Scrubbing Assumptions	85
7	Electrostatic Precipitation Assumptions	86
8	Fabric Filter Assumptions	86
9	High Energy Wet Scrubber Assumptions	87
10	Foam Scrubbing Capital Costs for 23.6 m^3/s (50,000 acfm) Unit as a Function of Residence Time	89
11	Foam Scrubbing Operating Costs for 23.6 m^3/s (50,000 acfm) Unit as a Function of Surfactant Cycle	89
A-1	Mean Bubble Diameter for Various Flow Conditions	98
A-2	Bubble Size of Foam Generated with Tergitol	105
B-1	Threshold Air Flow Rates	112
C-1	Results of Experimental Measurements	117
C-2	Bubble Volume vs. Diameter	124
D-1	Destruction with Knockdown Spray	128

SECTION 1

SUMMARY

This report summarizes the results of research work investigating the application of foam to fine particle removal from the gaseous phase. The foam is generated using aerosol gas; hence the aerosol particles are enclosed inside the small foam bubbles. Given enough time, the particles diffuse or settle to the bubble wall and are removed from the gas phase. Upon foam destruction the particles remain in the foam liquid and the cleaned gas is discharged.

Section 2 summarizes the conclusions and recommendations resulting from the first phase of this program involving the foam scrubber theoretical evaluations, bench scale testing, and preliminary economics. An introduction to the rationale behind foam scrubbing is given in Section 3. Theories and theoretical correlations describing the significance of mechanisms that might be involved in the fine particle collection process by foam are included in Section 4.

Application of foam to fine particle removal was experimentally verified on a 1.2×10^{-3} m^3/s (2.5 cfm) bench scale scrubber. The results are presented in Section 5 and indicate that 80% or higher collection efficiencies for particles between 0.2 and 1 μm are obtainable using this device and depend mainly on foam bubble size, scrubber residence time, particle and surfactant type, and particle size. Preliminary economics are presented in Section 6.

SECTION 2

CONCLUSIONS AND RECOMMENDATIONS

Based on the results of this program's first phase involving the foam scrubber theoretical evaluation, bench scale development, and preliminary economic analysis the following is concluded and recommended:

1. The foam scrubber is a viable method to remove fine particles from gaseous streams. The method is simple consisting of basic operations such as pumping the liquid and gas and spinning the disk to destroy the foam. The foam is generated by forcing aerosol gas through a screen sprayed with a surfactant liquid. Particle collection is believed to take place mainly by difussion and sedimentation, the mechanisms that are predictable and rather well understood.

2. Theoretical evaluations and later experimental verification indicated that foam bubble size is an important parameter for fine particle collection. This is due to the diffusion and sedimentation distance a particle has to travel in order to reach the bubble collection surface. Hence, the smaller the foam bubble the shorter the residence time required for particle collection. Uniform and sufficiently stable foams with bubbles ranging in average size from 0.7 to 3 mm were successfully produced in this program.

3. Foam bubble size is mainly dependent on screen size, gas flow rate, and concentration of surfactant. The higher the screen mesh, the gas flow rate, and the surfactant concentration the smaller the size of foam bubbles. The relative position of the screen and the spray nozzle are also critical. With the screen properly wetted the liquid flow rate was found to have little influence on foam bubble size and stability. Generally, the smaller size foam is more stable. Foam stability is further influenced by the foam wetness (density) and surfactant type (the wetter the foam, the higher its stability). Four surfactant types were used in this program, namely Tergitol® TMN, Sterox® NM, Alkanol® DW, and Aerosol® OT. At 1% surfactant concentration, the Alkanol DW foam was found significantly more stable than foams made from the other three surfactants.

4. The particle collection was experimentally verified for fine aerosols of three size categories, 0.56 - 1.0 μm, 0.32 - 0.56 μm, and 0.18 - 0.32 μm, and two aerosol types, dioctyl phthalate (DOP) and polypropylene glycol. In order to obtain 90% polypropylene glycol aerosol collection in Tergitol foam with average size bubbles of 0.8 mm, 20 - 50 second scrubber residence times were required (see Figure 27). The larger particles collected better than the smaller ones. Comparable experiments using foam with bubbles between 3 - 5 mm lowered the collection efficiencies at 50 second residence time to about 76 - 82%, the larger number representing collection of larger particles.

   Collection efficiencies in Tergitol foam with average bubble size of 0.8 mm using the DOP aerosol were determined at 55 - 64% for 20 second scrubber residence time. The collection increased to 70 - 79% at scrubber residence time of 50 seconds. The smaller DOP particles collected better than the large ones (see Figure 28). Larger bubble foam (3 - 5 mm) reduced the DOP collection at 50 seconds to about 35 - 40%.

5. A good agreement was found between theoretical collection efficiencies and those determined experimentally. The collection efficiencies are a function of particle size, particle density, foam bubble size, and particle residence time in the bubble. The effect of temperature on collection efficiency was not experimentally investigated. Due to a proportional relationship of the particle diffusion coefficient and the temperature an increase in collection efficiency with an increased temperature may be expected. Change in the gas relative humidity from 5% to 45% did not influence the particle collection significantly.

6. Preliminary economics indicate that the foam scrubber can be competitive in terms of capital investment costs with other conventional particle collection devices including fabric filter, high energy scrubber, and high efficiency electrostatic precipitator. However, the operating costs for the foam scrubber appear substantially higher than those required for the aforementioned conventional devices, mainly due to the cost of surfactants. While the economic data produced useful comparisons, their applicability must be considered with respect to the presently limited availability of reliable information on fine particle collection by the conventional devices and lack of accurate economic information when these devices are collecting significant amounts of fine particulates. Also, the cost data for foam scrubber are based on experimental data observed on a bench scale using non-industrial aerosols.

7. Based on the results of the experimental phase of this program, we recommend that further evaluation of foam scrubbing be made on a pilot scale preferably with 14 m^3/hr (500 cfm) foam scrubber capacity. Additional pilot scale information is needed in several areas. These are listed below:

   (a) Foam scrubber operation and collection capability using an industrial fine aerosol.

   (b) Surfactant recycle and recovery for reuse in foam generation.

   (c) Generation of uniform and sufficiently stable foam on a large scale.

   (d) Uniform foam transportation in large scale duct.

   (e) Effective destruction of large volumes of foam.

   (f) Scrubber collection ability of industrial aerosols at elevated temperatures.

SECTION 3

INTRODUCTION

A variety of air pollution equipment is available to industry for containing solid particulate emissions (e.g., electrostatic precipitators, baghouses, inertial separators, wet scrubbers, settling chambers, impingement separators, and panel filters). In terms of mass removal efficiency, a majority of the commercially available particulate control devices are adequate, with mass removal efficiencies up to +99%. However, submicrometer particles are not captured by this equipment; they pass readily into the atmosphere, creating hazards to human health, as well as visibility and smog problems.

New concepts and technology for the control of fine particles are needed to help remedy this situation. In this category is foam scrubbing. Prior investigations suggested that foam capture of fine particles may be possible.[1] However, in order to effectively utilize this concept for fine particulate control in industrial effluents, better understanding of the mechanism of foam formation, behavior, and destruction and mechanisms controlling the particle collection in foam are needed.

---

[1] Shannon, L. J. Control Technology for Fine Particulate Emissions. Midwest Research Institute. Kansas City. U.S. Environmental Protection Agency, EPA-650/2-74-027 (PB 236 646). May 1974. 225 p.

This program in its first phase has attempted to (1) establish the theoretical basis for fine particle collection mechanisms using foam, (2) experimentally verify the established theories, and (3) assess the preliminary economics of foam scrubbing. The results are presented below.

SECTION 4

THEORETICAL ASPECTS OF FOAM SCRUBBER APPLICATION

4.1 FOAM FORMATION

The most practical ways to generate foam for particulate scrubbing are shown in Figures 1 and 2. Figure 1 shows details of a spray foam generator where foam is generated in gas phase. Figure 2 shows a perforated plate foam generator where foam is generated by forcing gas through a liquid phase.

A detail showing a bubble still attached to a wire screen is also shown in Figure 1. The pressure of the gas stream pushes the bubble forward with surface tension forces acting in the opposite direction. Theoretically, when the pressure force of the gas stream exceeds the surface tension force, the detachment of a foam bubble occurs. The equation describing the two acting forces is presented below.

$$\frac{\rho V^2}{2}(\pi r^2) \geqq 2(2\pi r)\gamma \qquad (1)$$

where ρ = density of gas

V = velocity of gas

r = radius of screen opening

γ = surface tension of liquid

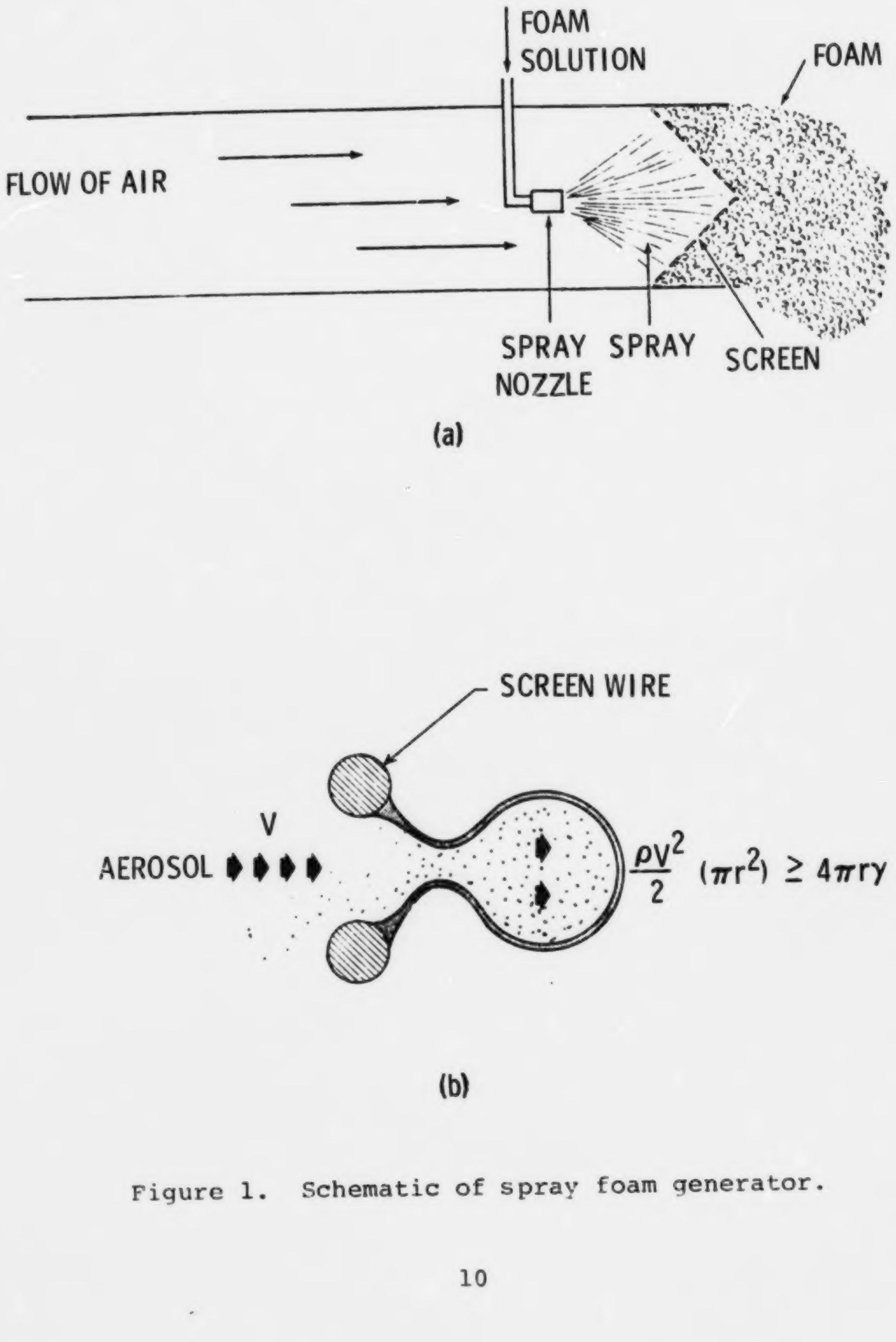
FOAM SOLUTION
FOAM
FLOW OF AIR
SPRAY NOZZLE
SPRAY
SCREEN
(a)
SCREEN WIRE
V
AEROSOL
$\frac{\rho V^2}{2} (\pi r^2) \geq 4\pi r\gamma$
(b)

Figure 1. Schematic of spray foam generator.

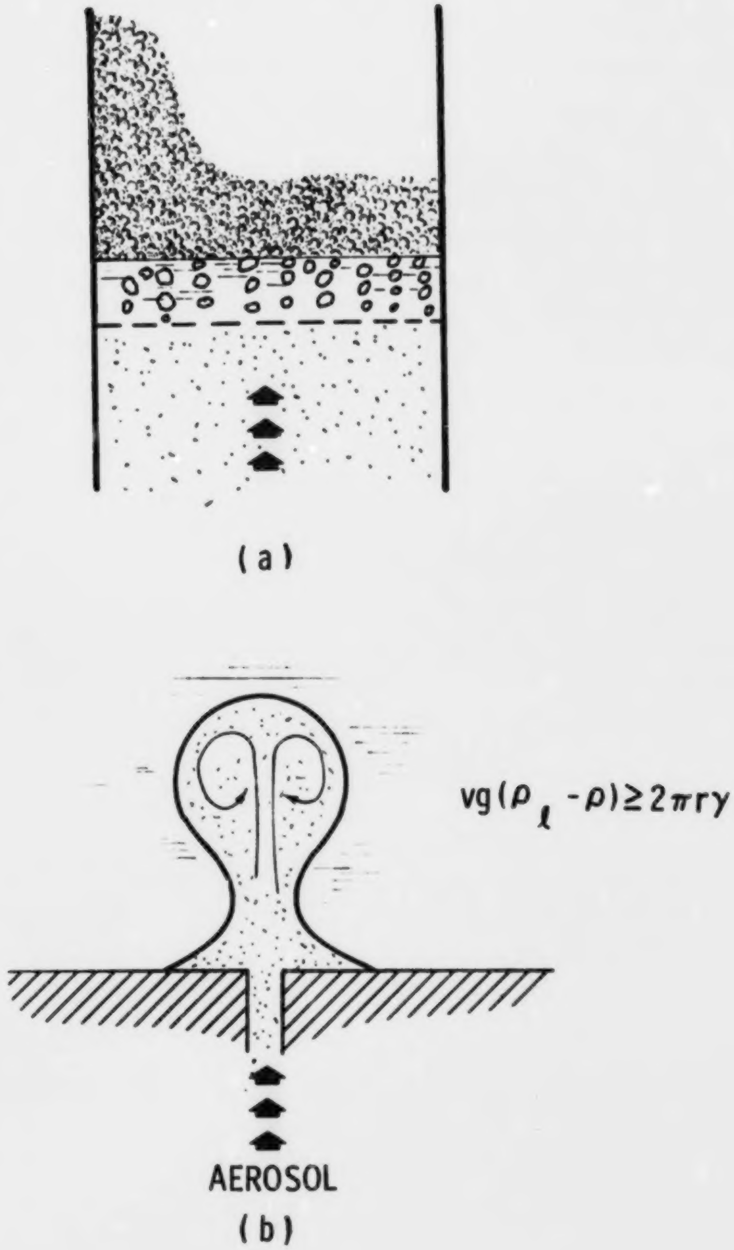
(a)
$vg(\rho_l - \rho) \geq 2\pi r\gamma$
AEROSOL
(b)

Figure 2. Schematic of perforated plate foam generator.

The factor of 2 on the right hand side of Equation 1 accounts for two surfaces on both sides of foam film. Hence, the minimum gas velocity, V_{min}, required for the generation of foam bubble by spray foam generator may be calculated as follows:

$$V_{min} = 2\sqrt{\frac{2\gamma}{\rho r}} \qquad (2)$$

In the case of multiple bubbles, due to sharing of film by neighboring bubbles, the surface tension term in Equation 1 should be $(2\pi r\gamma)$ instead of $2(2\pi r\gamma)$, and Equation 2 becomes

$$V_{min} = 2\sqrt{\frac{\gamma}{\rho r}} \qquad (2a)$$

Knowing the minimum gas velocity, the theoretical minimum power requirement, N_{min}, for the gas blower needed for bubble formation may be determined according to the following equation:

$$N_{min} = \frac{1}{2}\rho A V_{min}^3 \qquad (3)$$

where A = duct cross-section area

In addition to energy for the blower, the foam scrubber would require energy for liquid spray, foam destruction, and other frictional losses.

In the process of bubble formation in a liquid phase (Figure 2) the buoyancy force of gas tends to lift the bubble with surface tension forces acting again in the opposite direction. When the bubble grows, the buoyancy increases more rapidly than does the surface force, and it finally overtakes the latter; at this moment, bubble detachment takes place. Equation 4 describes the two forces for the perforated plate foam generator.

$$vg(\rho_\ell - \rho) \geqq (2\pi r)\gamma \tag{4}$$

where v = volume of bubble

ρ_ℓ = density of liquid

ρ = density of gas

r = radius of orifice

γ = surface tension of liquid

Since $\rho << \rho_\ell$ and it is assumed that a spherical bubble with radius R is formed, further treatment of Equation 4 will yield:

$$R = \left(\frac{3r\gamma}{2g\rho_\ell}\right)^{1/3} \tag{5}$$

In this case, the energy requirement for the blower is simply to overcome the static head of liquid layer and pressure drop through perforated plate. Our discussion illustrated the minimum energy requirement for the generation of foam. Let us now consider how much surface energy is stored in foam per unit volume of foam. Assuming uniform size bubbles, it is reasonable to assume that bubbles are arranged in such a way as to obtain maximum packing density. The maximum number of spheres packed per unit volume can be determined:

$$N = \left(\frac{1}{2R}\right)\left(\frac{1}{\sqrt{3}R}\right)\left(\frac{1}{\sqrt{\frac{8}{3}}R}\right) = \frac{1}{4\sqrt{2}R^3} \tag{6}$$

The total surface area of the bubble per unit volume can now be calculated using Equation 6:

$$\text{Total area} = (4\pi R^2)\ \frac{1}{4\sqrt{2}R^3} = \frac{\pi}{\sqrt{2}R} \qquad (7)$$

The total surface energy involved is, area x surface tension,

$$\text{Total surface energy per unit volume} = \frac{\pi\gamma}{\sqrt{2}R} \qquad (8)$$

The conditions existing in real life situations are far more complicated than our equations can describe. Consider now the order of magnitude of Reynolds number of gas in an actual scrubber. At typical scrubber flow velocity of 2.5 m/s (∿500 fpm), duct diameter, d, of 1 meter (∿3 ft), gas viscosity $\mu = 0.02 \times 10^{-3}$ Pa•s, and gas density $\rho = 1.2\ \text{kg/m}^3$, the Reynolds number (Re) is determined:

$$Re = \frac{Vd\rho}{\mu} = \frac{2.5 \times 1 \times 1.2}{0.02 \times 10^{-3}} \simeq 150{,}000 \text{ (turbulent)} \qquad (9)$$

Consequently, turbulent conditions are present in the main gas stream. At the moment of the formation of bubbles, if the bubble diameter is about 2 mm, the initial Reynolds number of gas movement inside the bubble is:

$$Re = \frac{2.5 \times 2 \times 10^{-3} \times 1.2}{0.02 \times 10^{-3}} \simeq 300 \text{ (laminar)} \qquad (10)$$

This suggests that at the formation of foam bubbles, the transient phenomena of turbulent to laminar flow occurs. The description and analysis of the phenomena under such unsteady conditions is extremely complicated.

4.2 DIFFUSION PHENOMENA IN FOAM

The summary of governing equations describing general flow conditions, assuming constant gas properties, is presented below.

Continuity equation:

$$\frac{D\rho}{Dt} + \rho \, \mathrm{div}\vec{V} = 0 \tag{11}$$

Momentum equation (Navier-Stokes equation; incompressible):

$$\rho\frac{DV}{Dt} = \rho\vec{g} - \mathrm{grad}\ p + \mu\nabla^2\vec{V} \tag{12}$$

Energy equation (for normal engineering process):

$$\rho C_v \frac{DT}{Dt} = k\nabla^2 T \tag{13}$$

Diffusion equation (2nd Fick's Law):

$$\rho\frac{DV}{Dt} = \rho D\nabla^2\vec{C} \tag{14}$$

where t = time

$\vec{V}$ = gas velocity

ρ = gas density

p = pressure

μ = viscosity of gas

C_v = specific heat of gas

k = conductivity of gas

D = diffusion coefficient

T = temperature

C = concentration

The above equations are very often difficult and tedious to solve. In the following paragraphs, some simplifying assumptions appropriate for particle collection by foam will be made. Let us first consider the idealized case of a bubble formation as shown in Figure 1. Aerosol with constant concentration C rushes into a foam bubble and the detachment of the bubble (assuming spherical shape) occurs at the time $t = 0$. As long as the cross-sectional areas of foam generator and the foam scrubber remain constant, the mass of aerosol moves with the same velocity before and after the formation of a bubble. It is therefore reasonable to assume that the aerosol inside the bubble and the foam bubble surface progress with the same velocity through the scrubber. Consequently, the impaction mechanism of aerosol on foam surface is negligible.

As opposed to the case just mentioned (i.e., Figure 1), the formation of a rising bubble through a liquid layer tends to create a gas circulation pattern inside the bubble. This is illustrated in Figure 2. The gas velocity at the surface of the bubble is approximately given by classical inviscid flow around a sphere. The conditions of perforated plate foam generation will further be evaluated in the following section.

Assuming isothermal system (i.e., gas temperature = bubble film temperature) and for a very small bubble, if the motion of gas is negligible inside the bubble after the bubble has been formed, the set of Equations 11, 12, 13, and 14 reduces to a single equation:

$$\frac{\partial C}{\partial t} = D\nabla^2 C \qquad (15)$$

which after its transformation to spherical coordinates becomes:

$$\frac{\partial C(r,t)}{\partial t} = D\left[\frac{1}{r^2}\ \frac{\partial}{\partial r}\ (r^2\ \ \frac{\partial C}{\partial r}\ )\right] \qquad (16)$$

To solve Equation 16 the initial and boundary conditions must be summarized:

(a) $C(r,0) = C_o$ initial concentration at $t = 0$ is constant (16a)

(b) $C(R,t) = 0$ on the surface of the sphere at $t > 0$ (16b)

(c) $C(r,t) \neq \infty,\ t \geq 0$ (16c)

The diffusion coefficient for small particles may be expressed by:

$$D = \frac{k'T}{6\pi\mu r_p}\left[1 + A(\frac{\lambda}{r_p}) + Q'(\frac{\lambda}{r_p})\ e^{-br_p/\lambda}\right] \qquad (17)$$

where k' = Boltzmann's constant (1.38×10^{-22} kg m/s^2 ^{o}K)

T = temperature (23^{o}C)

μ = viscosity of gas (1.85×10^{-5} Pa·s)

r_p = radius of diffusing particle, μm

λ = mean free path of the gas (0.653×10^{-5} cm at 23^{o}C, 760 mm Hg)

A, Q', b = empirical constants

The quantity inside the brackets in Equation 17 is called Cunningham slip correction factor, K.

The constants A, Q', and b in Cunningham slip correction depend on the value selected for the mean free path of the gas molecules and the nature of the surface of the particles (i.e., influenced by degree of specular reflection and diffuse reflection of gas molecule at the surface of particles).

The calculated Cunningham correction factors are shown in Figure 3 for particles of glass spheres and oil droplets. The constants for glass spheres and oil droplets are presented below:

Glass spheres	Oil droplets
$A = 0.77$	$A = 0.86$
$Q' = 0.40$	$Q' = 0.29$
$b = 1.62$	$b = 1.25$

Using the diffusion equations one can determine the distance which a particle of a specific size can travel in a selected period of time. This estimation is of interest to indicate the size of foam bubbles that would be desirable for practical foam scrubber applications. Basically, the diffusion of small particles is caused by Brownian motion, the random movement of particles as they are bombarded by surrounding gas molecules. This motion can be expressed by the following equation:

$$\overline{X}^2 = 2Dt \qquad (18)$$

where $\overline{X}^2$ = mean square displacement

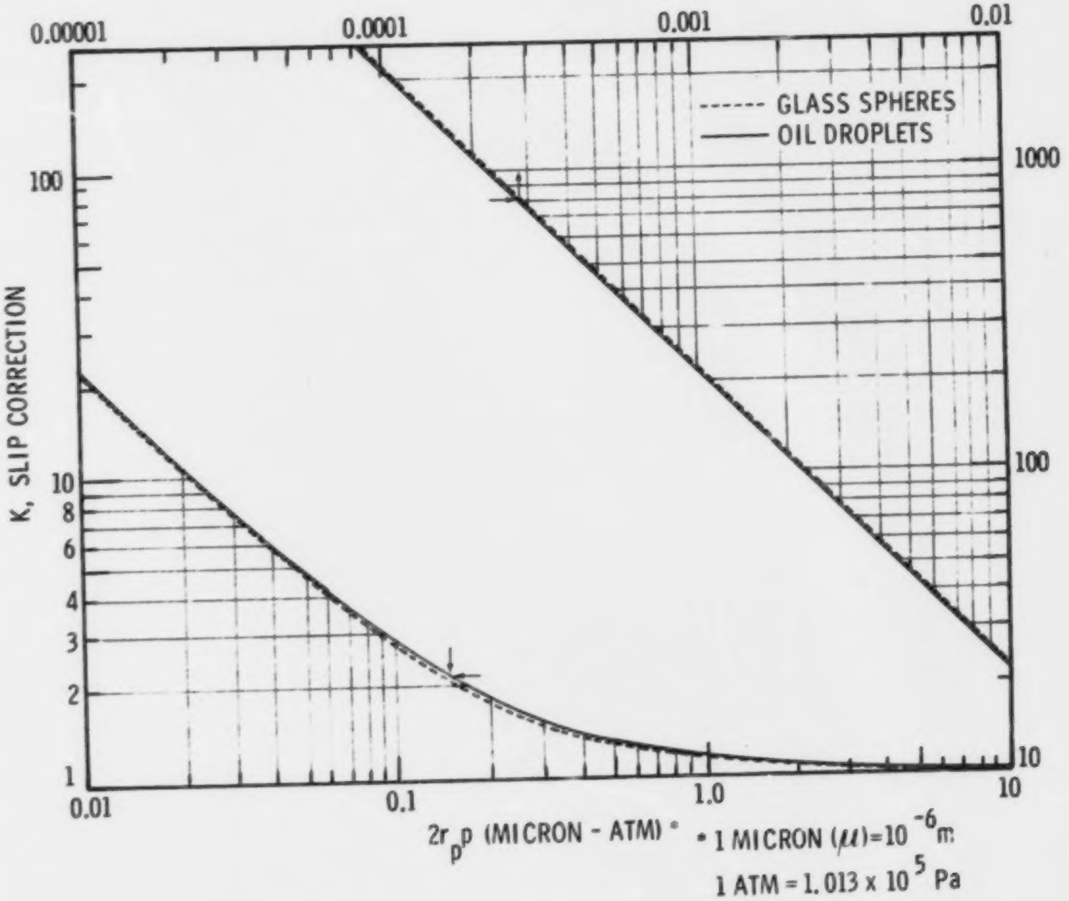

Figure 3. Cunningham slip correction for liquid and solid particles.

Figure 4 shows the calculated variations of $\overline{X}^2$ with r_p and t, with and without the Cunningham slip correction. The calculations are based on oil droplets in air at 23°C and 760 mm Hg.

The data are plotted on a logarithmic paper to demonstrate basic relationships between particle size, bubble size, and probability of particle impaction with the bubble. It is evident from Figure 4 that the Cunningham correction is relatively unimportant for a 10 μm diameter particle but of great importance for a 0.01 μm diameter particle.

Figure 4 can be used to get a qualitative idea of the behavior of a foam scrubber. The following arbitrary example will demonstrate this. Assuming that the foam is composed of 100 μm diameter bubbles, a 0.01 μm particle in the center of the bubble will diffuse to the bubble surface in less than 0.1 second. A 0.1 μm particle will take 2.3 seconds, while a 10 μm particle will take more than 100 seconds.

Equation 17 does not apply accurately to particles as small as gas molecules. The uncertainty in the value due to different particle substance does not usually exceed 2 - 3%. With the above information available, the solution of Equation 16 will give particle concentration distribution inside a bubble as a function of time for various particle sizes, assuming that the particulate cloud is monodisperse and at given concentration the coagulation of particles is negligible.

The partial differential equation, Equation 16 can be solved by the separation-of-variables method. The general solution will have a form as follows:

$$C(r,t) = (C_1 e^{-\alpha^2 Dt} + C_2 e^{\alpha^2 Dt}) \left[C_3 \frac{1}{\sqrt{r}} J_{\frac{1}{2}}(\alpha r) + C_4 \frac{1}{\sqrt{r}} J_{-\frac{1}{2}}(\alpha r) \right] \tag{19}$$

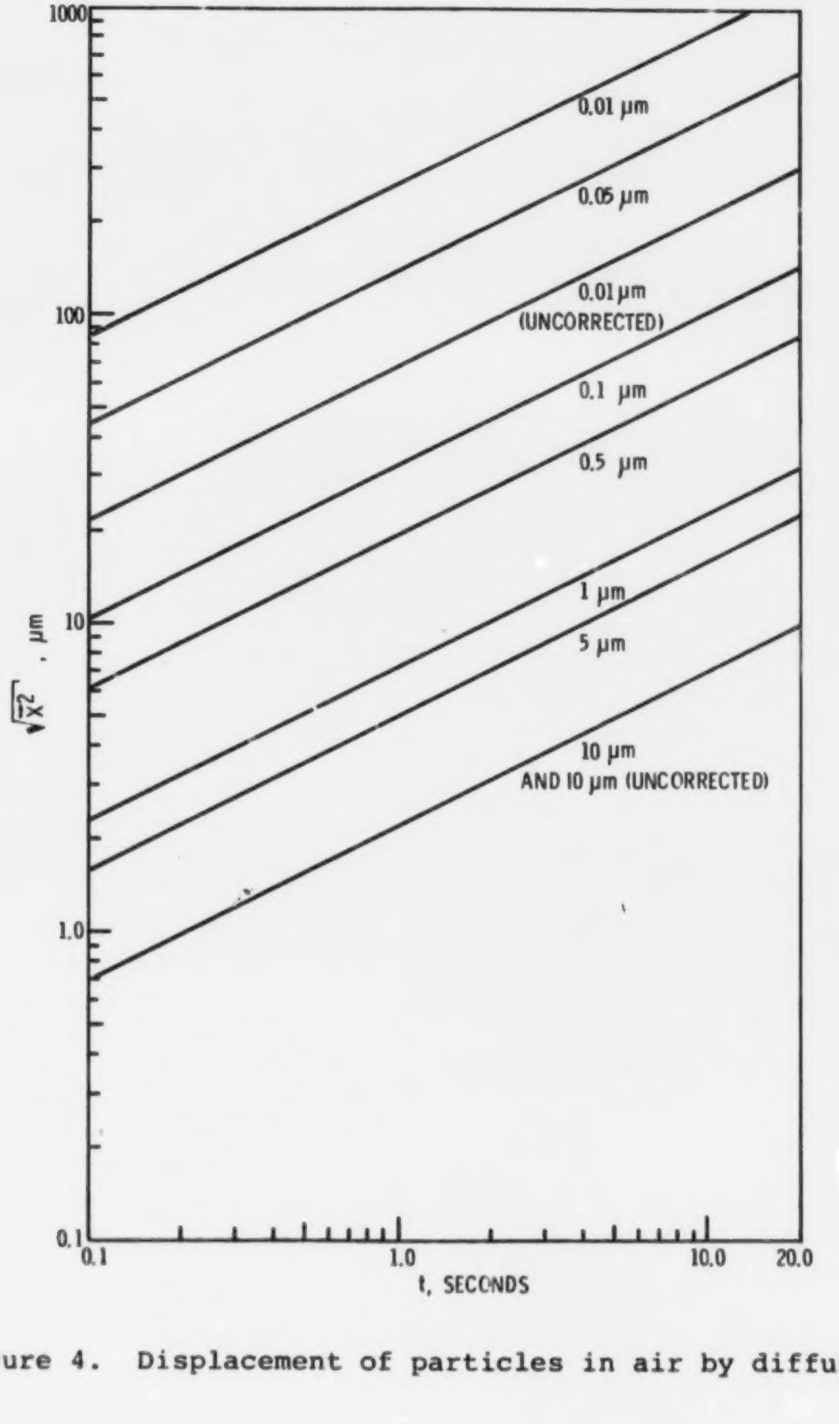

Figure 4. Displacement of particles in air by diffusion.

where α, C_1, C_2, C_3, C_4 = constants

J_n = Bessel's functions

By use of boundary conditions, Equations 16a, 16b, and 16c, and lengthy derivation and transformation, Equation 19 becomes:

$$\frac{C(r,t)}{C_o} = \frac{2}{\pi} \left(\frac{R}{r} \right) \sum_{n=1}^{\infty} \frac{(-1)^{n+1}}{n} e^{-\left(\frac{n\pi}{R}\right)^2 Dt} \sin\left(n\pi\frac{r}{R}\right) \quad (19a)$$

This equation gives instantaneous particle concentration inside the bubble.

The instantaneous rate of loss of particles to bubble surface is now given by:

$$q(R,t) = -D(4\pi R^2) \left.\frac{\partial C}{\partial t}\right|_{r=R} = 8\pi RDC_o \sum_{n=1}^{\infty} e^{-\left(\frac{n\pi}{R}\right)^2 Dt} \quad (20)$$

The total loss of particles in time t from time t = 0 is:

$$Q(t) = \int_0^t q(R,t)dt = \frac{8R^3C_o}{\pi} \sum_{n=1}^{\infty} \frac{1}{n^2} \left[1 - e^{-\left(\frac{n\pi}{R}\right)^2 Dt} \right] \quad (21)$$

Hence, the particle collection efficiency, E (%), in time t may be determined as follows:

$$E = \frac{Q}{4/3\pi R^3 C_o} 100 = \frac{6}{\pi^2} \sum_{n=1}^{\infty} \frac{1}{n^2} \left[1 - e^{-(\frac{n\pi}{R})^2 Dt} \right] \times 100 \qquad (22)$$

note: $\sum_{n=1}^{\infty} \frac{1}{n^2} \equiv \frac{\pi^2}{6}$

Particle collection efficiency, Equation 22, was plotted for various bubble sizes (0.5, 1.0, and 2.0 mm diameter) and particle sizes (0.01, 0.1, and 1 μm diameter) as a function of foam residence time in Figures 5, 6, and 7. Inspection of Equation 22 shows that bubble diameter R is of primary importance (appears as square term in denominator of expotential term). Also, Figure 3 and Equation 17 reveal that the diffusion coefficient of 0.01 μm diameter particle is about 2,000 times larger than that of 1.0 μm particle.

Figures 5, 6, and 7 show that the collection efficiency of 0.01 μm particles within a reasonable practical residence time (say 5 seconds) is very high. However, for 1.0 μm particle, even a foam bubble diameter of 0.5 mm would not appear to provide acceptable collection efficiency in most practical engineering applications.

4.3 PARTICLE CAPTURING BY OTHER MECHANISMS

Other particle collection mechanisms (such as particle impaction, sedimentation, etc.) were neglected in the above analysis. Consequently, the results presented represent the lowest collection efficiency in the practical foam scrubbing, except for adverse temperature or vapor gradient conditions. (For non-isothermal system, the diffusion collection efficiency

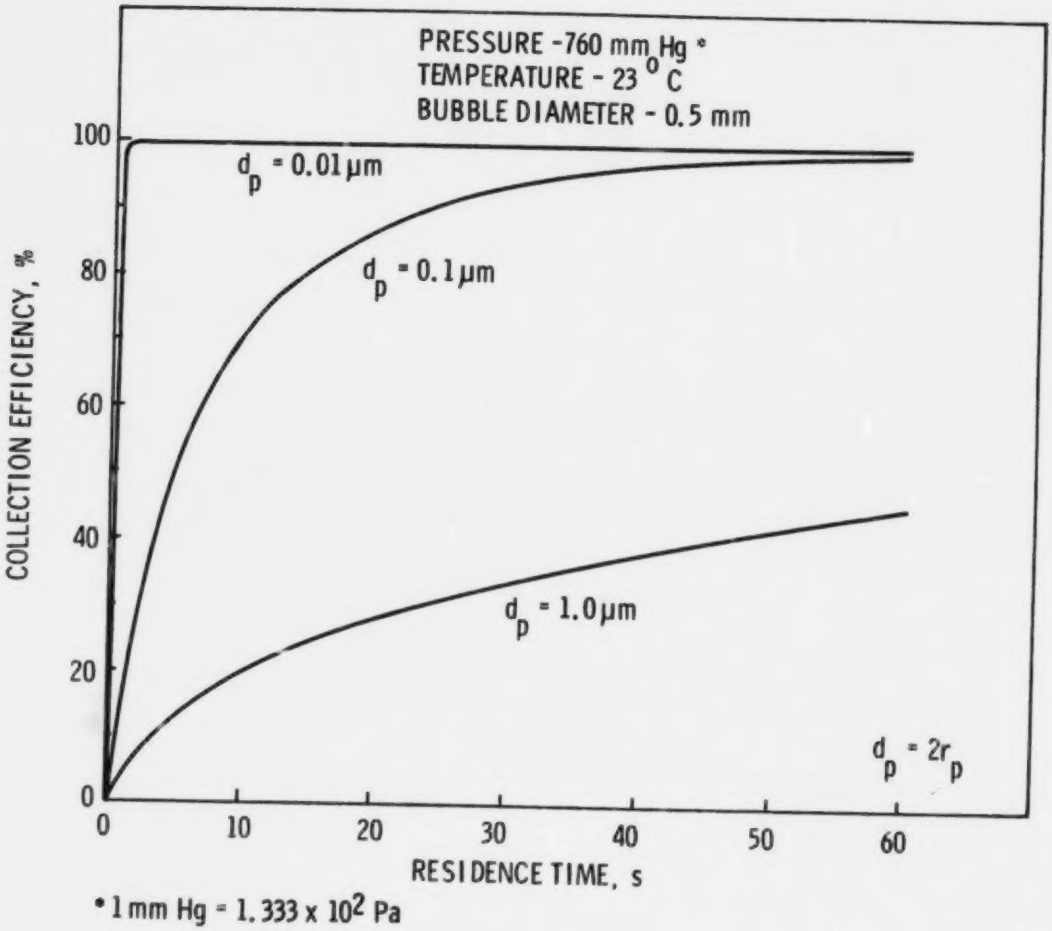

Figure 5. Particle collection efficiency.

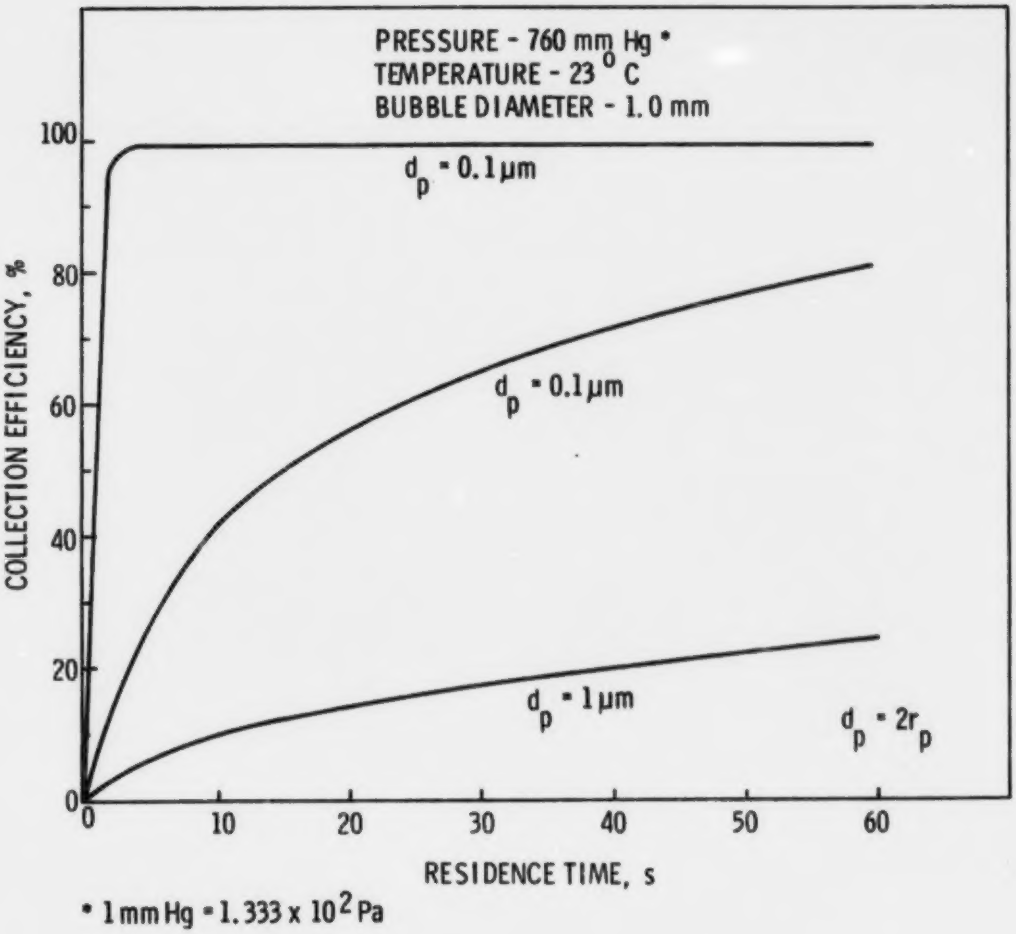

Figure 6. Particle collection efficiency.

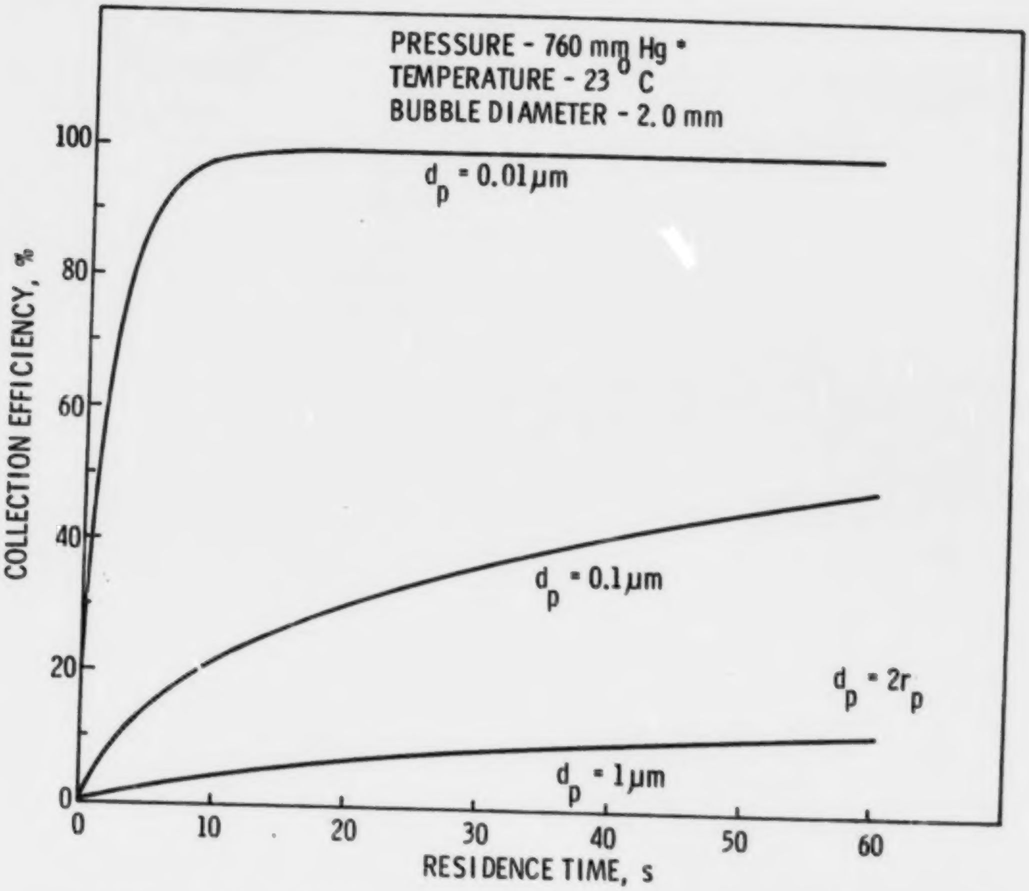

* 1 mm Hg = 1.333×10^2 Pa

Figure 7. Particle collection efficiency.

may fall as the temperature of foam rises, on account of repulsion of particles from the walls of the bubble owing to Stefan flow and thermophoresis.) For very small particles (e.g., 0.1 μm or larger) however, other mechanisms may influence the collection efficiency.

4.3.1 Impaction and Sedimentation

In order to evaluate the effect of impaction and sedimentation on the particle collection efficiency, the flow development inside the bubbles during the period from foam generation to final destruction must be known for the specific foam generation technique. In the isothermal system, the flow development can be obtained by solving Navier-Stokes equations with appropriate initial and boundary conditions. Thus, the momentum equation is as follows:

$$\frac{\partial V}{\partial t} = \mu\left[\frac{\partial}{\partial r}\left(r^2\frac{\partial V}{\partial r}\right) + \frac{1}{\sin\theta}\,\frac{\partial}{\partial\theta}\left(\sin\theta\,\frac{\partial V}{\partial\theta}\right)\right] \qquad (23)$$

where θ = angular direction

The initial and boundary conditions for two foam generating techniques are shown in Figure 8. The solution of Equation 23 would give instantaneous velocity profile inside a bubble as a function of time and coordinates. The solution can only be obtained by numerical analysis, using a computer. It was felt that it was outside the scope of this program to obtain the solution of Equation 23.

However, as the first approximation, the order of magnitude of relaxation time for gas flow inside the bubbles to reach steady state can be estimated. This should provide an

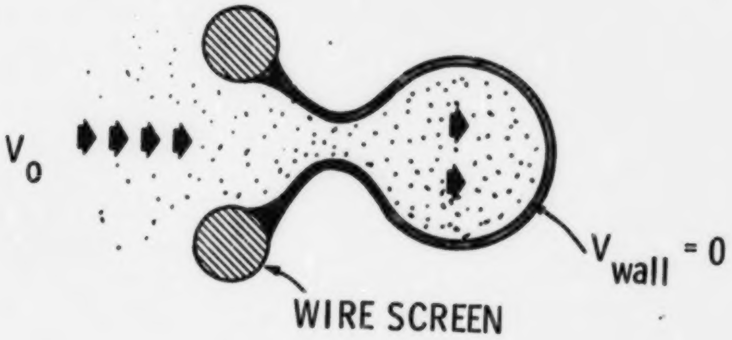
V_0
$V_{wall} = 0$
WIRE SCREEN

(a) bubble formation over wire screen

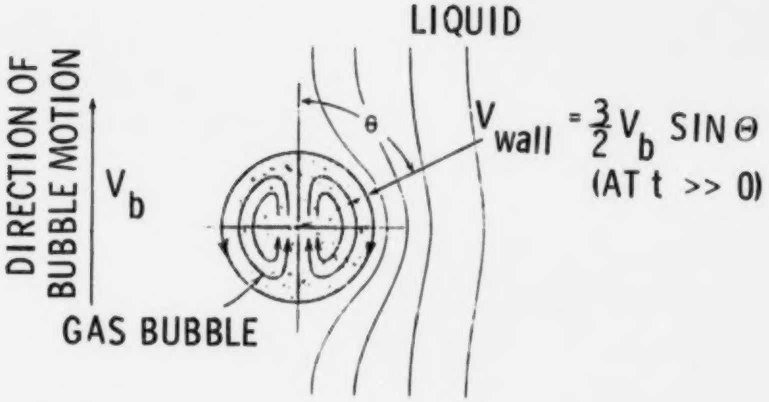
LIQUID
DIRECTION OF BUBBLE MOTION
V_b
θ
$V_{wall} = \frac{3}{2} V_b \sin\Theta$
(AT t >> 0)
GAS BUBBLE

Figure 8. Initial and boundary conditions.

indication of significance of the unsteady state on the overall collection process.

Let us determine how fast the steady flow profile can be attained in a bubble shown in Figure 8-b. The gas velocity at the surface of the bubble is given by:

$$V_{wall} = 3/2\ V_b \sin\theta \tag{24}$$

where V_b = velocity of bubble rise

From the result of the analysis of Couette flow between the annulus with one moving wall, the value required for the flow to reach 95% of final velocity profile from the start was investigated by H. S. Yu and E. M. Sparrow:[2]

$$\frac{x}{R} = 0.32\ Re \tag{25}$$

where x = entrance length

R = channel width, or in this case, radius of bubble

Re = Reynolds number

The time required for flow to reach 95% of final profile is therefore:

$$t = \frac{x}{V_b} = 0.32R(Re)/V_b \tag{26}$$

---

[2] Yu, H. S., and E. M. Sparrow. Flow Development in a Channel Having a Longitudinally Moving Wall. Journal of Applied Mechanics. 37(2):498-507, June 1970.

For bubble size of 1 mm in diameter, rate of rise of bubble at 0.30 m/s, and Reynolds number of 100, Equation 21 gives $t = 0.05$ seconds. That means the gas flow in 1 mm bubble would reach the steady state almost immediately, say in less than 0.1 second. The motion of gas, however, would persist as long as the bubbles are rising through the liquid layer. By the same reasoning, as soon as foam bubble is out of liquid, the internal gas motion would subside immediately in the same relaxation time (<0.1 s) due to absence of surface film motion. The impaction mechanism would, therefore, be applicable only during the period of bubble rise through the liquid. At a rising rate of 0.30 to 3.0 m/s, this amounts to probably less than a second in most of the practical engineering applications.

In the case of screen foam generator (Figure 8-a), initial disturbance of gas movement from the foam generation process would expect to subside in the same short period of time. The pure diffusion process takes over during the rest of foam residence time in the scrubber, which may be 10 seconds or more.

Without computer analysis of initial flow disturbance, Equation 23, the extent of impaction or sedimation is difficult to estimate. However, due to insignificant relative motion between moving bubbles and gas, and short relaxation time as we have just demonstrated, contribution of impaction would appear insignificant for small particles which are of interest in this project.

The number of particles deposited inside the bubble by sedimentation in one second can be expressed as $(\pi R^2)CV_s$. Using this expression we can formulate the coefficient of absorption by sedimentation (ratio of the rate of particles deposited to the total number of particles in the bubble), α_s as follows:

$$\alpha_s = \frac{\pi R^2 C V_s}{(4/3\pi R^3) C} = \frac{3V_s}{4R} \tag{27}$$

where V_s = particle settling velocity

The settling velocity can be expressed by:

$$V_s = \frac{mg}{3\pi\mu d_p}\left(1 + A\frac{2\lambda}{d_p} + Q'\frac{2\lambda}{d_p}e^{-bd_p/2\lambda}\right) \tag{28a}$$

or

$$V_s = \frac{d_p^2 \rho_p g}{18\mu}\left(1 + A\frac{2\lambda}{d_p} + Q'\frac{2\lambda}{d_p}e^{-bd_p/2\lambda}\right) \tag{28b}$$

where m = particle mass
ρ_p = particle density

Combination of Equations 27 and 28b gives:

$$\alpha_s = \frac{d_p \rho_p g}{24\mu R}\left(1 + A\frac{2\lambda}{d_p} + Q'\frac{2\lambda}{d_p}e^{-bd_p/2\lambda}\right) \tag{29}$$

Typical sedimentation velocity of particles, Equation 27, and coefficient of absorption by sedimentation, Equation 29, are listed in Table 1 for bubble diameter of 1 mm and particle density of 1,000 kg/m^3:

Table 1. TYPICAL SEDIMENTATION VELOCITY AND COEFFICIENT OF SEDIMENTATION (for $R = 0.0005$ m, $\rho_p = 1{,}000$ kg/m^3)

	d_p (μm)		
	0.01	0.1	1.0
V_s, m/s	6.5×10^{-8}	8.8×10^{-7}	3.5×10^{-5}
α_s, 1/s	0.0001	0.0013	0.052

Evidently, for particles larger than 1 μm, sedimentation would significantly enhance the collection of particles during the foam scrubbing process. For 1 μm particles, the table indicates that about 5.2% of the remaining particles are removed by sedimentation mechanism every second, assuming uniform particle concentration within the foam bubble. Because of diffusion process, the particle concentration profile, Equation 19, would not be uniform throughout the bubble (i.e., leaner near the wall) and, therefore, the actual sedimentation coefficient would be somewhat less than indicated above.

The combined particle collection efficiency (including diffusion and sedimentation) can now be determined in a step-by-step calculation. Although the results obtained may not be mathematically rigorous, they provide an additional tool for estimating foam scrubber collection efficiency.

The computational results are presented in Figures 9 through 17 for various bubble diameters, particle sizes, and particle densities. For convenience, the diffusion collection curves are also shown in these figures. As evidenced by the collection curves, the enhancement of collection efficiency by the sedimentation mechanism is far more important than the diffusion mechanism for these larger particles. However, for the particles smaller than 0.1 μm, the sedimentation mechanism of particle collection is negligible.

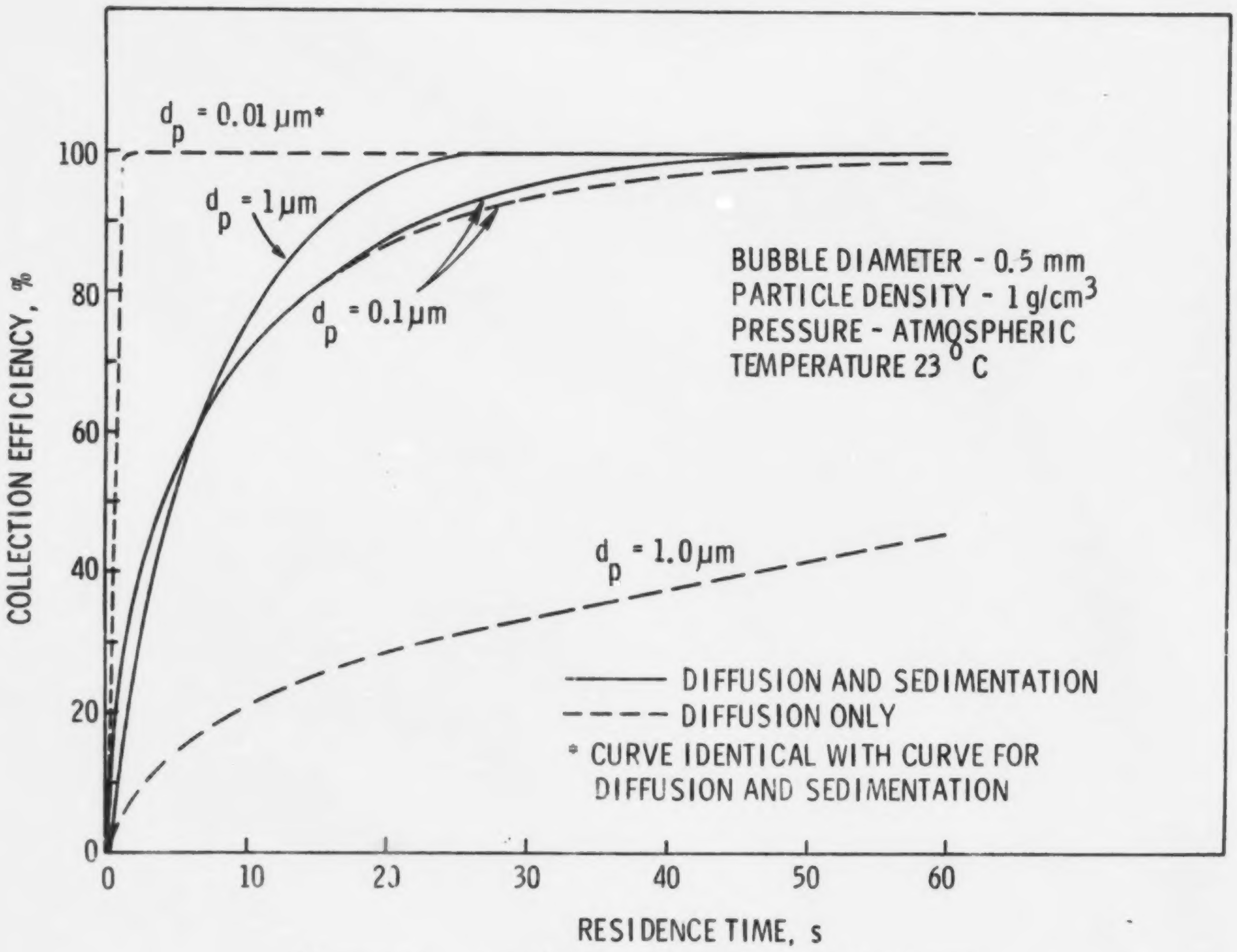

Figure 9. Particle collection efficiency.

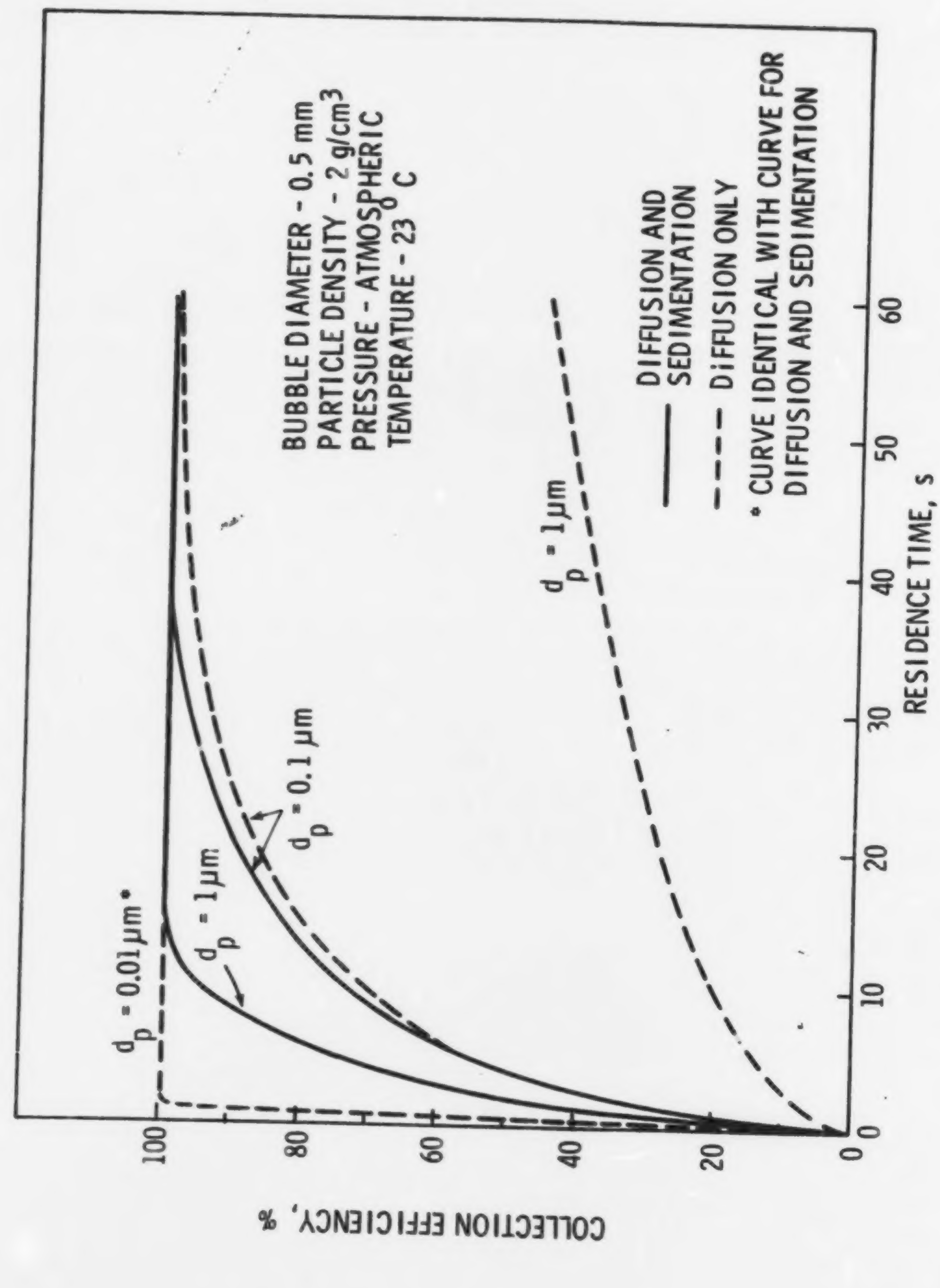

Figure 10. Particle collection efficiency.

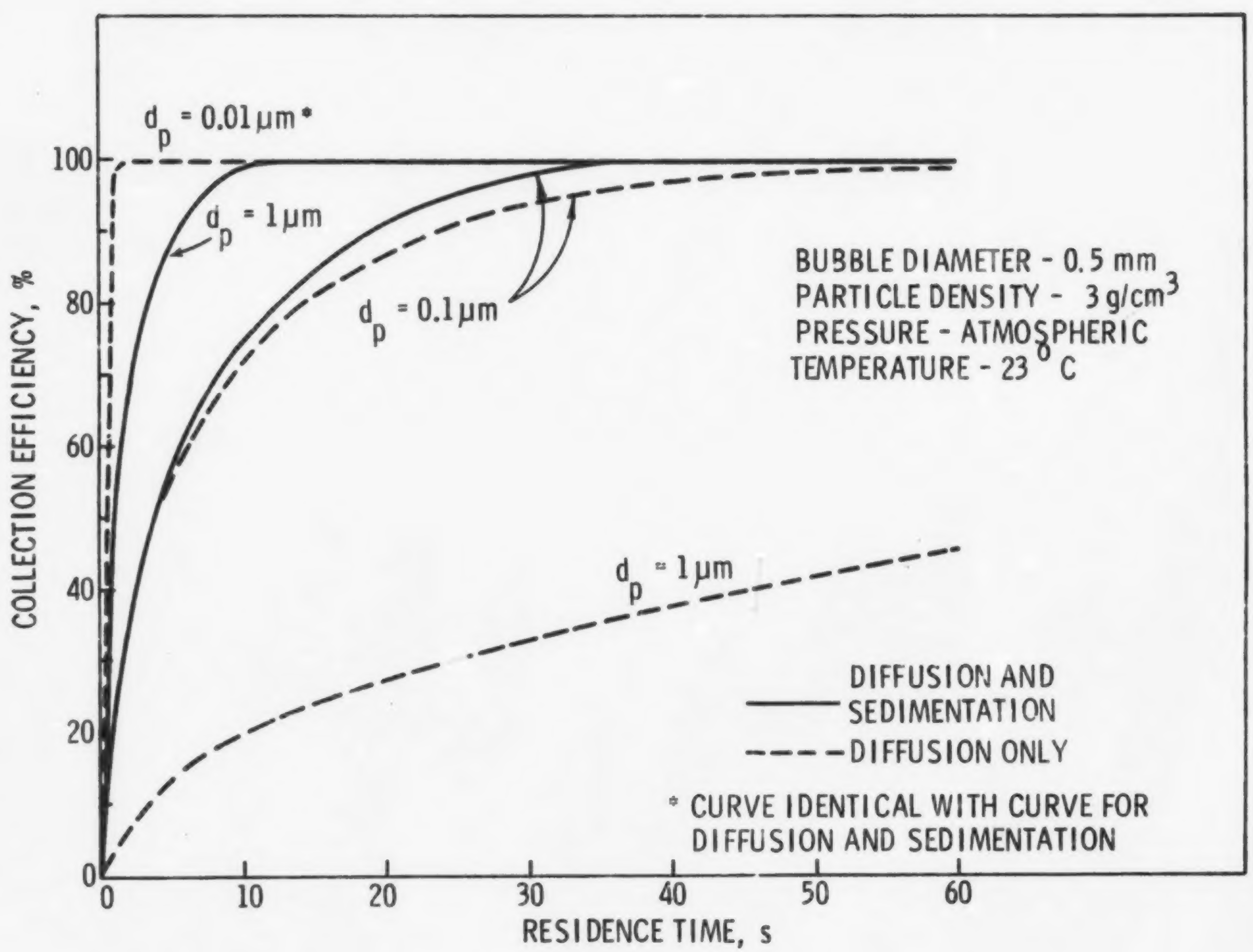

Figure 11. Particle collection efficiency.

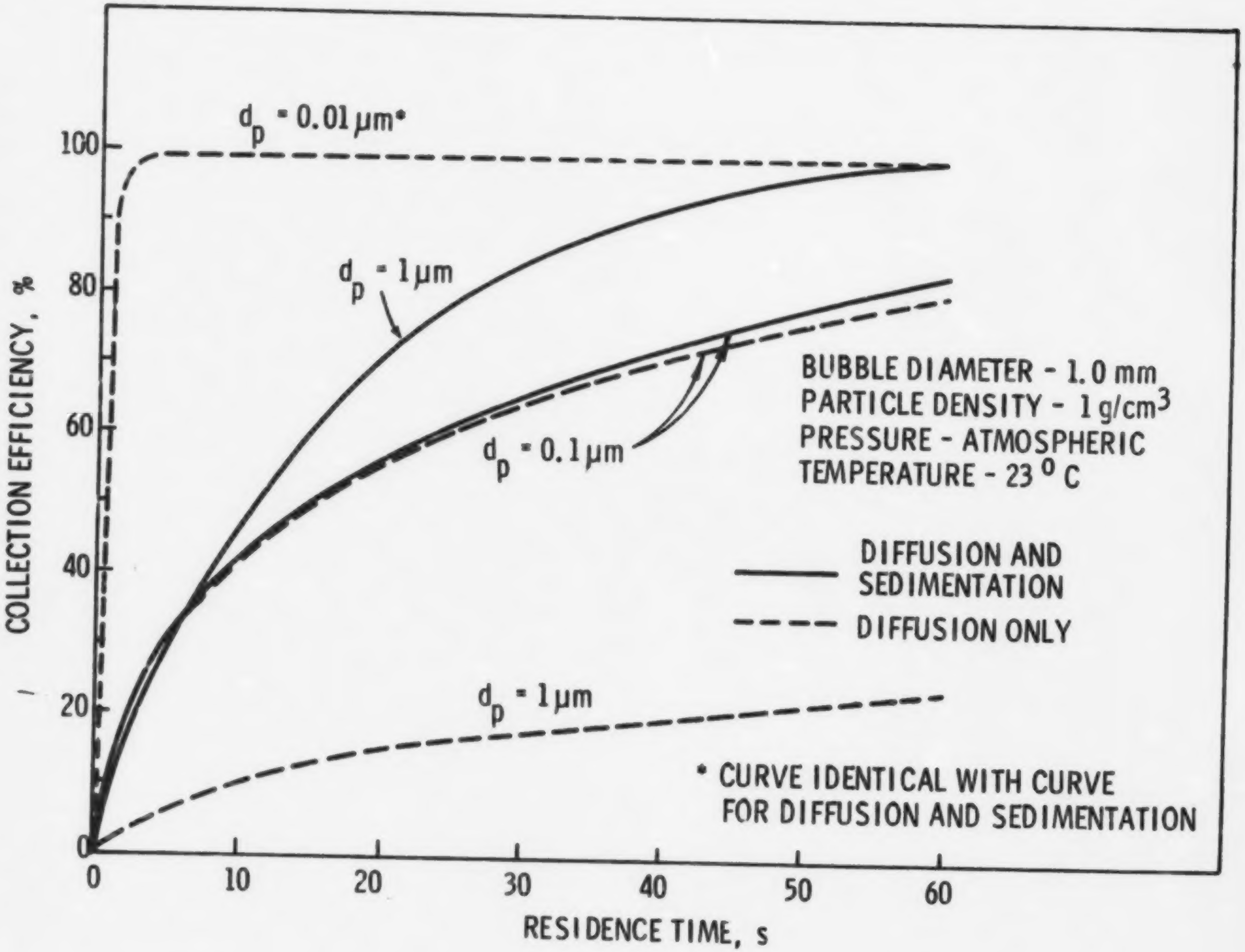

Figure 12. Particle collection efficiency.

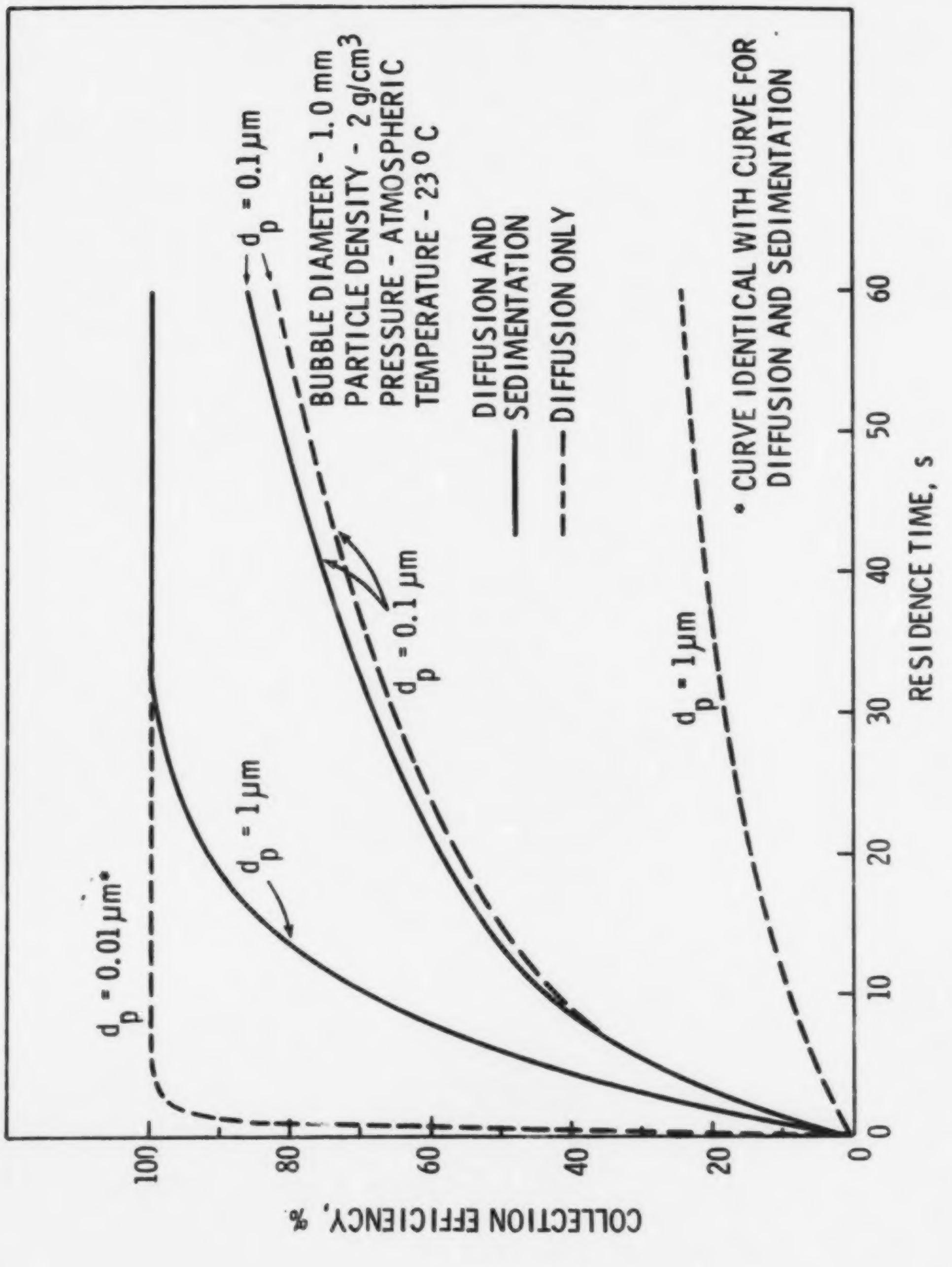

Figure 13. Particle collection efficiency.

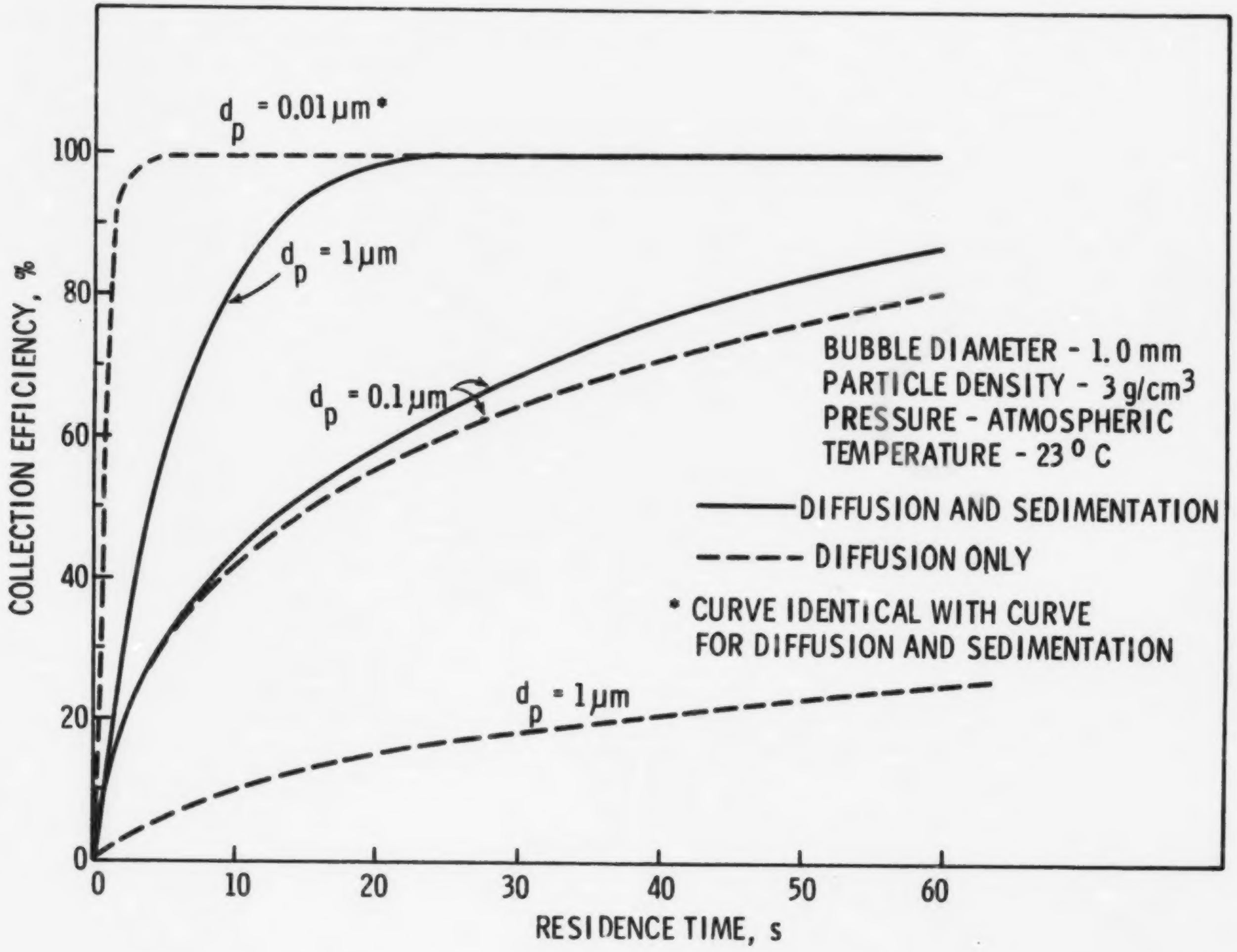

Figure 14. Particle collection efficiency.

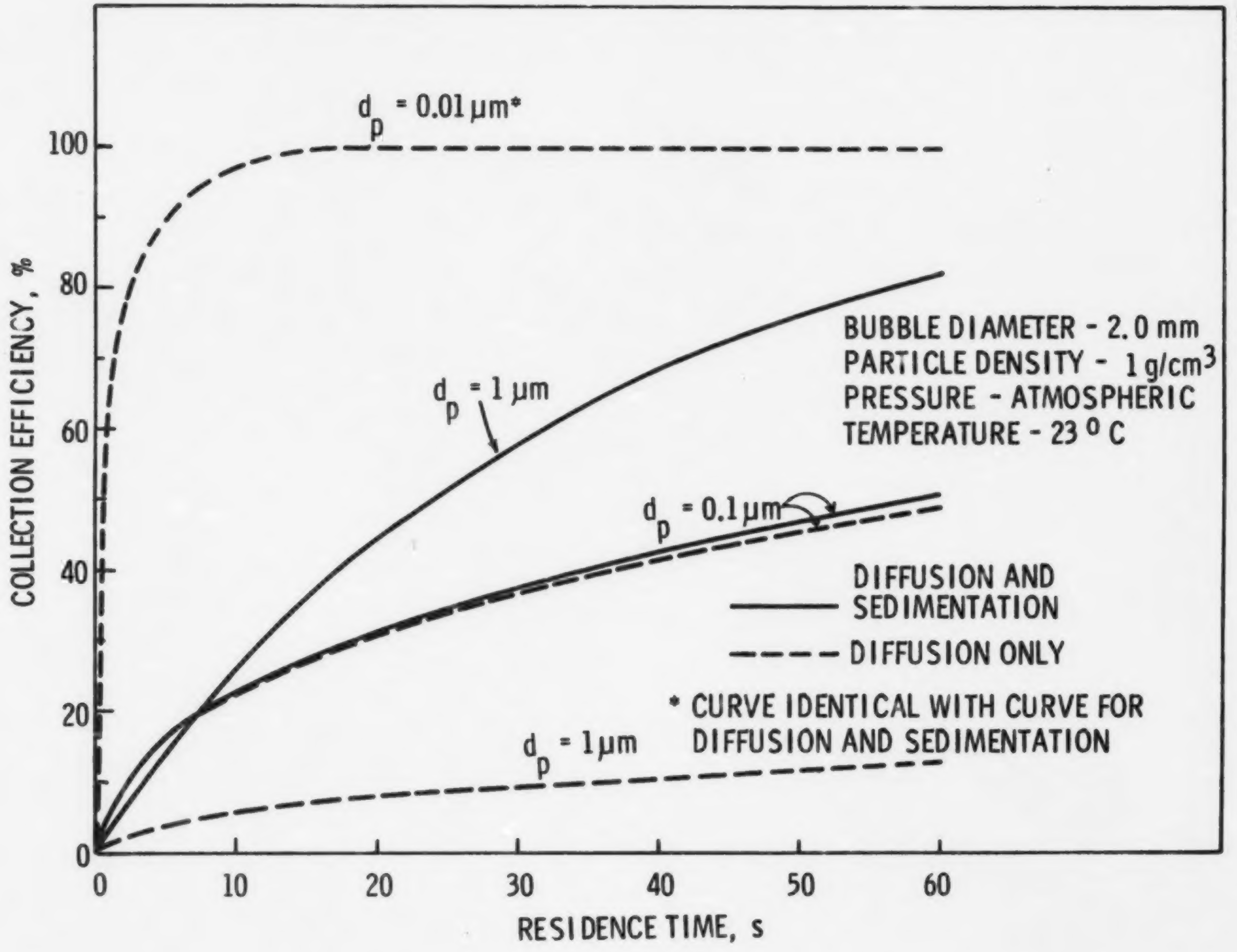

Figure 15. Particle collection efficiency.

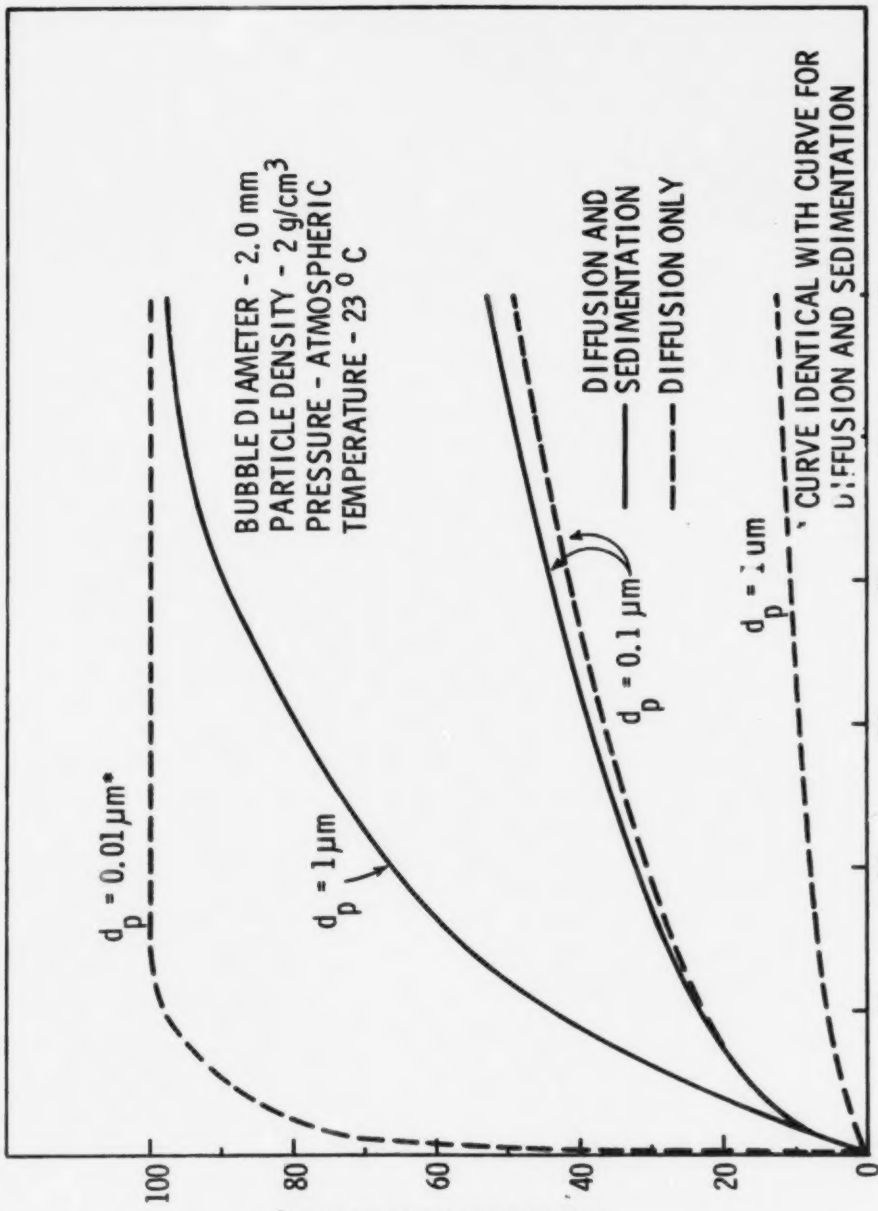

Figure 16. Particle collection efficiency.

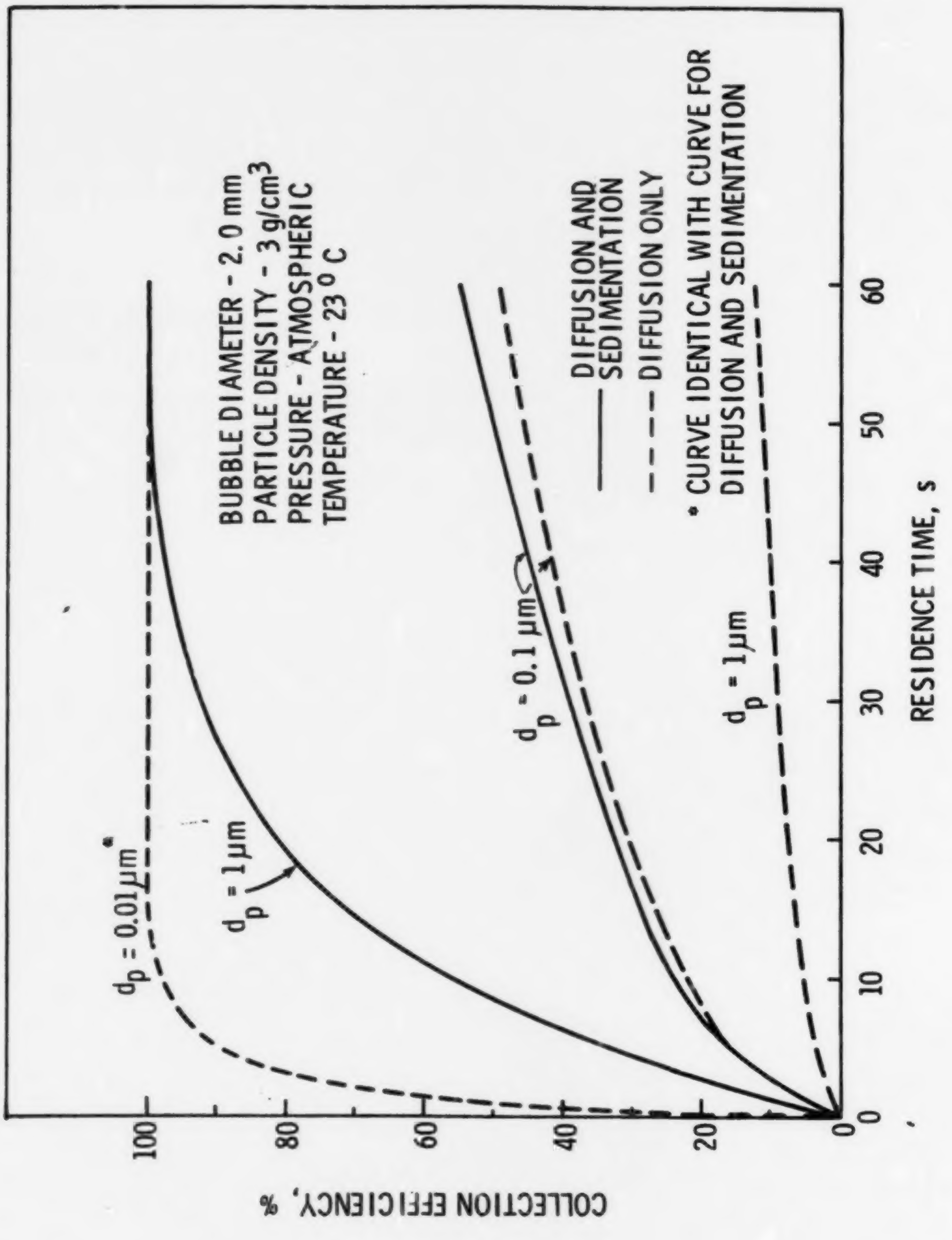

Figure 17. Particle collection efficiency.

Next, let us consider the effect of inertial deposition for the situation shown in Figure 8-b, i.e., during the rising of bubble through the liquid layer. Even though it has been shown that unsteady conditions exist only for a limited period we will attempt to determine whether in this short time any significant particle collection could occur. It is reported that small amounts of surface active agents cause a marked decrease in surface film movement because of the formation of a "skin" around the bubble that effectively prevents circulation.[3] The circulation has only been substantiated for gas bubbles of about 0.003 to 0.005 m in diameter rising through carefully purified water. Nevertheless, further discussion is warranted. In calculation of inertia deposition, the radial velocity of the particles due to the centrifugal force is:

$$V_{rad} = \frac{V_{wall}^2 V_s}{Rg} = \frac{9}{4}\cdot\frac{V_b{}^2 V_s \sin^2\theta}{Rg} \tag{30a}$$

$$= \frac{d_p^2 \rho_p V_b{}^2 \sin^2\theta}{3\mu R}\left(1+A\frac{2\lambda}{d_p} + Q'\frac{2\lambda}{d_p}e^{-bd_p/2\lambda}\right) \tag{30b}$$

Hence, the number of particles deposited on the bubble surface in one second will be:

$$\frac{9V_b{}^2 V_s n}{4Rg}\int_0^{\pi} \sin^2\theta\, 2\pi R^2 \sin\theta\, d\theta = \frac{6\pi V_b{}^2 V_s nR}{g} \tag{31a}$$

or

$$\frac{d_p^2 \rho_p C V_b{}^2 R}{3\mu}\left(1 + A\frac{2\lambda}{d_p} + Q'\frac{2\lambda}{d_p}e^{-bd_p/2\lambda}\right) \tag{31b}$$

---

[3] Bird, R. B., W. E. Stewart, and E. N. Lightfoot. Transport Phenomena. New York, John Wiley and Sons, Inc., 1960. 780 p.

The ratio of the rate of particles deposited per second to the total number in the bubble, or coefficient of inertia deposition α_i, is:

$$\alpha_i = \frac{\dfrac{d_p^2 \rho_p C V_b^{\,2} R}{3}\left(1 + A\dfrac{2\lambda}{d_p} + Q'\dfrac{2\lambda}{d_p}e^{-bd_p/2\lambda}\right)}{(4/3\pi R^3)C}$$

$$= \frac{d_p^2 \rho_p V_b^{\,2}}{4R}\left(1 + A\frac{2\lambda}{d_p} + Q'\frac{2\lambda}{d_p}e^{-bd_p/2\lambda}\right) \qquad (32)$$

Typical coefficient of inertial absorption for case of Figure 8-b is shown below for bubble diameter of 1 mm and particle density of 1,000 kg/m^3, assuming bubble rising velocity of 0.30 m/s.

Table 2. TYPICAL COEFFICIENT OF IMPACTION (for R = 0.0005 m, ρ_p = 1,000 kg/m^3 , V_b = 0.30 m/s)

	d_p (μm)		
	0.01	0.1	1.0
α_i, 1/s	0.011	0.146	5.84

Surprisingly, the above simplified analysis shows that the inertial absorption is quite efficient in removing micrometer (1 μm) size particles in relatively short time. The table shows that all the particles above 1 μm could be removed in less than 0.2 second, only if the circulation of the gas inside the bubble could be maintained.

4.3.2 Thermophoresis and Diffusiophoresis

Other diffusion mechanisms can contribute to the foam scrubbing operation. A small particle in a temperature gradient is subject to thermophoresis: gas molecules striking the side of the particle facing the high temperature region have more kinetic energy on the average than those hitting on the low temperature side and the particle moves toward the low temperature region. As a result, if the particulate-laden air passing through the foam scrubber is warmer than the bubble surface, thermophoresis will aid in particle collection.

Another important phenomenon to consider is Stefan flow caused by the evaporation or condensation of water vapor from or onto a bubble surface. This is a hydrodynamical flow of a vapor-gas mixture, normal to a liquid surface, which compensates for gas diffusion. Because of Stefan flow it is important that air going into a foam scrubber be saturated with water vapor. If warm, saturated air cools and condenses as it passes through a foam scrubber, Stefan flow will sweep particles toward the liquid surface where water vapor is condensing. If unsaturated air is used, evaporation will hinder particle deposition.

However, the water vapor can also condense on fine particles, which act as nucleation sites for water droplets. If this occurs, the now larger particles will diffuse more slowly to the bubble surface, and the particle collection efficiency will be reduced. Of course, if submicron particles grow large enough ($>\sim 1$ μm), they can be collected by gravitation or inertial impaction.

One final diffusion mechanism, called diffusiophoresis, occurs in binary gas-vapor mixtures. In a process analogous to thermophoresis, a small particle suspended in a concentration gradient is struck from one side by a greater number of heavier molecules. As a result, the particle migrates toward the low concentration region of the higher molecular weight species. In contrast to Stefan flow, diffusiophoresis ceases when the molecular weights of gas and vapor are equal, even though a concentration gradient exists. The following discussion will attempt to quantify the diffusional phenomena mentioned above.

The following examples will illustrate some practical aspects of the application of a foam scrubber to industrial gases. A typical foundry furnace exhaust gas temperature is 721°C (1,330°F). In some installations heat is reclaimed from the furnace exhaust gases, and the gas temperature is reduced to within the design limits of applicable pollution control equipment. Further cooling may be accomplished by water spray nozzles, dilution air, or convective radiation cooling.

According to the Air Pollution Engineering Manual (1967), the test results of a typical outlet gas temperature from the waste heat boiler are 238°C (460°F) with a moisture content of 12.4% (or humidity ratio of 0.08).

Figure 18 shows schematically a possible process for a total particulate removal system using a foam scrubber. The temperature and humidity of the dust-laden gas entering the foam scrubber will influence the particle collection efficiency. In previous discussions we have only dealt with the isothermal bubble system and neglected the effect of vapor condensation (or evaporation), temperature gradient, and electrostatic effect inside the foam bubbles. In engineering practice, water spray is used to cool and humidify the gas stream entering wet scrubbers. However, the simple water spray is not always sufficient to saturate the gas with moisture. The psychrometric process of gas inside the foam bubble therefore can be that of vapor evaporation from the bubble film surface or condensation of moisture from the gas phase

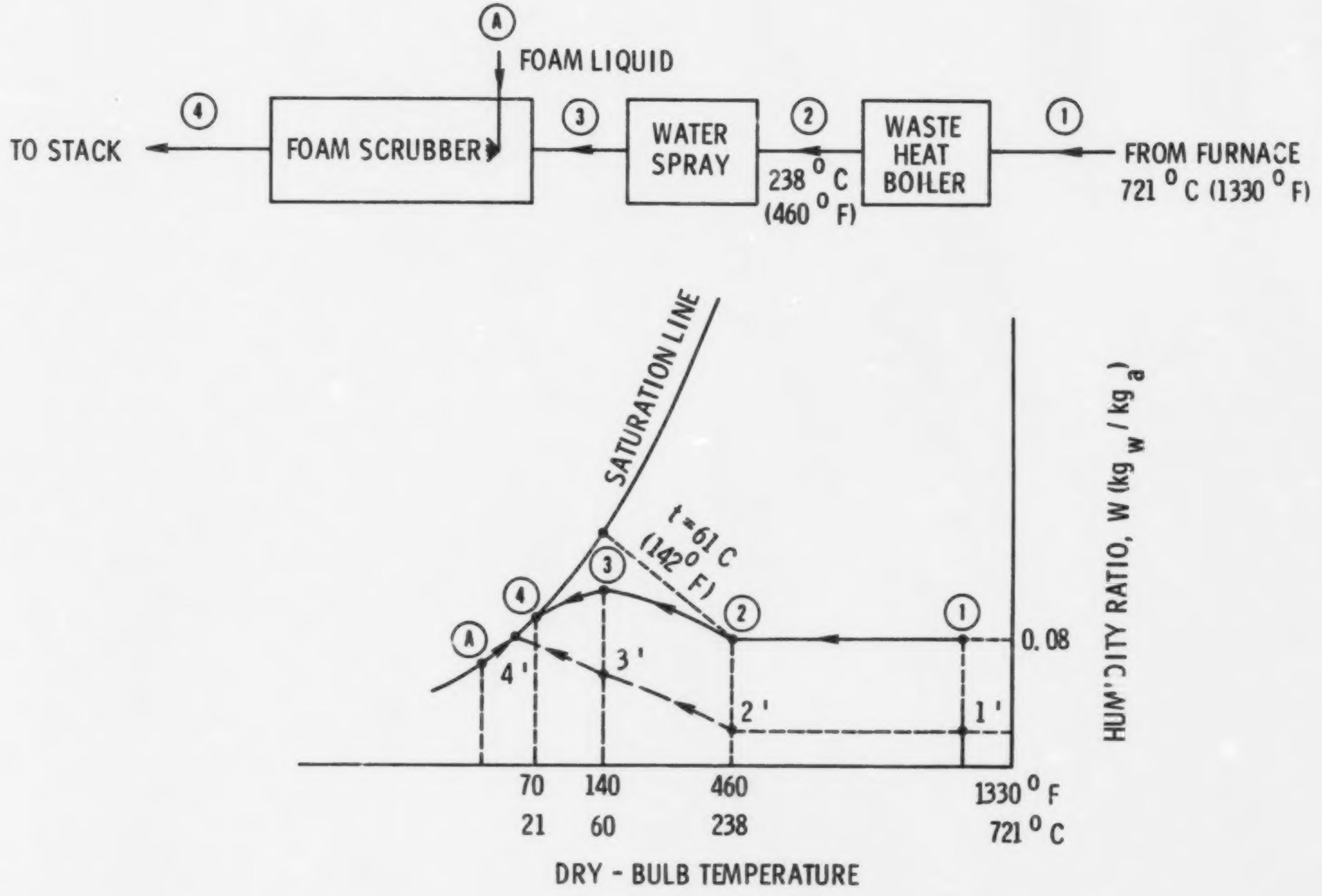
A
FOAM LIQUID
4
TO STACK
FOAM SCRUBBER
3
WATER SPRAY
2
238 0 C (460 0 F)
WASTE HEAT BOILER
1
FROM FURNACE 721 0 C (1330 0 F)
SATURATION LINE
t =61 C (142 0 F)
A
4
3
2
1
4 '
3 '
2 '
1 '
0. 08
HUM'DITY RATIO, W (kg w / kg a)
70
21
140
60
460
238
1330 0 F
721 0 C
DRY - BULB TEMPERATURE

Figure 18. Schematic diagram of exhaust gas treatment.

to the film surface depending on the operating conditions of the foam scrubber.

In the typical foam scrubber psychrometric process shown in Figure 18 (i.e., process 3→4), the entering gas is not saturated. Due to the gas high humidity and colder foam liquid film, the process (3→4) is that of condensation and cooling which would enhance the particle capturing capability of a foam scrubber. If the entering gas is relatively dry (not saturated and low in humidity ratio), evaporation of water vapor can take place inside the bubble even though the foam liquid is colder than the gas as shown by the dashed line 3'-4' in Figure 18. Evaporation of foam liquid is detrimental to the diffusion of particles to the foam bubble surface. Apart from the pure diffusion process discussed previously, the particles in general move in the direction of the diffusion flux of the heavier gas component. This is called diffusiophoresis. It is possible that inside the evaporating bubbles, a dust free zone can exist in the boundary layer, thus, blocking the accumulation of particles on the foam surface by the pure diffusion process.

In the practical application of foam scrubbing, it is unlikely that the foaming liquid and particle laden gas will be at isothermal conditions. Under the influence of a temperature gradient in the gas, particles inside the bubble would move towards the lower temperature. This phenomenon is called thermophoresis.

It should be noted that both diffusiophoresis and thermophoresis processes stop soon after the bubble film and gas inside the bubbles reach equilibrium state. If the time required to reach the equilibrium state is comparable to the foam residence time in the scrubber, the diffusiophoresis and thermophoresis could become important factors for particle capturing.

Let us now consider a small particle with radius r_p and velocity V_p suspended in a gas which itself move with velocity V and in which a temperature gradient ΔT exists. Then the force exerted by the gas on such a particle is given by the following equations:[4]

$$F = -6\pi\mu r_p \frac{2\left(k+C_t \frac{\lambda}{r_p} k_p\right)}{\left(1+3C_m \frac{\lambda}{r_p}\right)\left(2k+k_p+2C_t \frac{\lambda}{r_p} k_p\right)} \frac{k}{5p} \nabla T \qquad (33)$$

where k_p = conductivity of particle

σ = coefficient depending on both gas and particle surface properties and temperature, $\approx 1/5$

$C_t = \frac{15}{8} \frac{2-\alpha_t}{\alpha_t}$

$C_m = \frac{2-\alpha_m}{\alpha_m}$

α_t = thermal accomodation coefficient

α_m = momentum accomodation coefficient

In the steady state, the force given by Equation 33 is equal to the friction of the particle, i.e.,

---

[4] Aerosol Science. Davies, C. N. (ed). New York, Academic Press, 1966. 468 p.

$$F = - \frac{6\pi\mu r_p V_p}{\left[1+A \frac{\lambda}{r_p} + Q' \frac{\lambda}{r_p} e^{-\frac{br}{2\lambda}p}\right]} \qquad (34)$$

The thermophoretic velocity of the particle is therefore:

$$V_p = - \frac{\left[1+A\left(\frac{\lambda}{r_p}\right)+ Q'\left(\frac{\lambda}{r_p}\right)e^{-\frac{br}{2\lambda}p}\right]2\left[\lambda+C_y\left(\frac{\lambda}{r_p}\right)k_p\right]}{\left[1 + 3C_m\left(\frac{\lambda}{r_p}\right)\right]\left[2k+k_p+2C_t\left(\frac{\lambda}{r_p}\right) k_p\right]} \frac{k}{5p} \nabla T \qquad (35)$$

It was first suggested by Stefan that there must exist a hydrodynamic flow directed away from the evaporating and towards the condensing surface near a surface of an evaporating or condensing body. The velocity of this hydrodynamic flow (Stefan flow), U, is given by the following equation applicable for a binary mixture:

$$U = - \frac{D}{p_2} \frac{dp_1}{dx} \qquad (36a)$$

where p_1, p_2 = partial pressures of the vapor and air, and

$$\frac{dp_1}{dx} = - \frac{dp_2}{dx} \qquad (36b)$$

Particle matter near a condensing or evaporating surface might be expected to move with a velocity of about that of Stefan flow. However, the diffusion current of the vapor and gas have a modifying effect on the velocity of the particles. For small particles in a binary gas mixture, Waldmann and Schmitt[4] derived the particle velocity as follows:

$$V'_p = - \frac{\sqrt{m_1} - \sqrt{m_2}}{y_1 \sqrt{m_1} + y_2 \sqrt{m_2}} . D \frac{dy_1}{dx} \qquad (37)$$

where m_1, m_2 = mass of vapor and gas
y_1, y_2 = molar fraction of vapor and gas

This means that the particle moves in the direction of the diffusive flux of the heavier gas molecules.

Adding V'_p to the Stefan velocity, U, the diffusiophoretic velocity of particle becomes:

$$V_p = V'_p + U = - \frac{\sqrt{m_1}}{y_1 \sqrt{m_1} + y_2 \sqrt{m_2}} \frac{D}{p_2} \frac{dp_1}{dx} \qquad (38)$$

Before we estimate the effect ot thermophoresis and diffusiophoresis we must estimate the magnitude of ΔT and Δy in the practical engineering application. It must be emphasized that because of the limited relative amount of gas and liquid mass involved in the process, ΔT and Δy in Equations 35 and 36 are not constant values; rather, they diminish to zero in a relatively short period and vary within the bubble from point to point.

It is always desirable to saturate the gas stream entering a wet scrubber with water vapors. A common method is water quenching. The efficiency of this type of spray varies with the design, the quantity and pressure of the spray water and other operation factors. The following are, approximately, the efficiencies obtainable with commercial air washers of average construction in which the same water is continuously recirculated without being either heated or cooled (see Figure 19).

Single bank of sprays: $\eta_w = 65\%$
Two banks of sprays: $\eta_w = 80\%$
Three banks of sprays: $\eta_w = 90\%$

where $$\eta_w = \frac{t_2 - t_3}{t_2 - t^*} = \frac{W_3 - W_2}{W_s^* - W_2} = 1 - e^{\frac{-h_D A_\psi V}{M_a}}$$

M_a = mass rate of flow of dry air
W = humidity ratio
h_D = convection mass transfer coefficient
A_ψ = surface area of water droplets
W_s^* = humidity ratio of saturated moist air
t^* = thermodynamic wet bulb temperature
V = volume of air washer

It is obvious that it is practically impossible to achieve 100% saturation with this kind of spray device. It is estimated that mass transfer coefficient $h_D A_\psi$ has a value of 1.33 $kg/s \cdot m^3$ [300 lb/(hr) (cu ft) (lb_w/lb_a)] for commercial air washers with a pressure drop of 498 Pa (2 in. of water) or less.

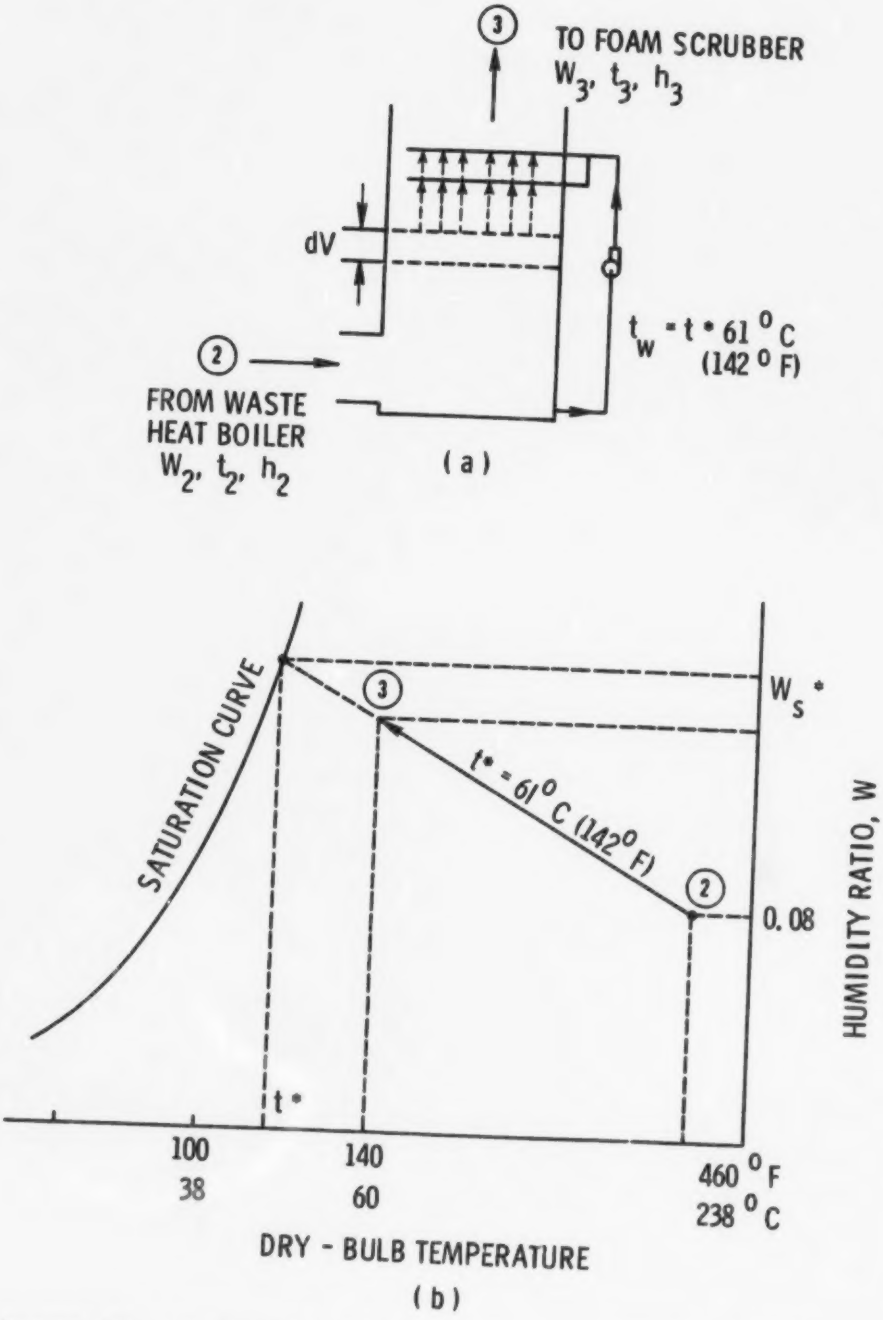
③
TO FOAM SCRUBBER
W_3, t_3, h_3
dV
$t_w = t^* 61\,^{\circ}C$
(142 °F)
②
FROM WASTE
HEAT BOILER
W_2, t_2, h_2
(a)
SATURATION CURVE
③
W_s^*
$t^* = 61^{\circ}C\ (142^{\circ}F)$
②
0.08
HUMIDITY RATIO, W
t*
100
38
140
60
460 °F
238 °C
DRY - BULB TEMPERATURE
(b)

Figure 19. Schematic diagram of air washer using directly recirculated spray water.

Instead of using recirculating water sprays as just shown above, one might use cold water sprays, possibly from a cooling tower, well water, or city water. For such a device, the process line, 2 - 3, would not follow a straight line (wet-bulb temperature line) as shown in Figure 19. The condition line would be like the one shown in Figure 18.

The equation describing the condition line on the psychrometric chart for the changes in the state for moist air passing the cold water spray can be expressed as follows:

$$\frac{dh}{dW} = L_e \left(\frac{h-h_{s,w}}{W-W_{s,w}}\right) + \left(h_{g,w} - 1061\ L_e\right) \qquad (39)$$

where h = enthalpy of moist air

L_e = Lewis number usually between 0.8 and 1.0 and depending on air velocity and ratio of thermal diffusivity and water vapor diffusivity

$h_{g,w}$ = specific enthalpy of saturated moist air evaluated at t_w

$W_{s,w}$ = humidity ratio of saturated moist air evaluated at t_w

$h_{s,w}$ = enthalpy of saturated moist air at t_w

To obtain an accurate solution for Equation 39 on the psychrometric chart, a step-by-step construction of the condition line is necessary. If the humidity ratio of the gas entering the foam scrubber is sufficiently high, there is no need for 100% saturation to achieve effective thermophoresis and diffusiophoresis for the removal of small particles inside the bubbles. Process 3→4 shown in Figure 18 is that of cooling and condensation of unsaturated hot humid gas in cool foam bubbles. In this case the thermophoretic and diffusiophoretic forces are additive. On the other hand, supersaturation with respect to water vapor may result in the modification of the particle size distribution (formation of larger size particles), thus, increasing the importance of the gravitational settling or decreasing the importance of the pure diffusional process.

Previous experimental results of the thermophoretic velocity as a function of temperature gradient are shown in Figure 20.[4] For estimation of initial thermophoretic velocities of particles we may assume:

Gas temperature = 60°C

Foam liquid temperature = 20°C

Hence, for 1 mm diameter foam bubbles, the initial temperature gradient $(300/T)\ dT/dx$ is about 800, which is extremely high (see Figure 20) indicating significant initial thermophoretic particle velocities. The exact temperature history of bubble liquid film and the gas inside the bubble are extremely difficult to quantify. However, we can estimate the time required to reach the final equilibrium temperature of the solution for the sudden emersion of a spherical gas bubble in a constant temperature liquid bath. With a thermal diffusivity, α, of $2.2 \times 10^{-5}\ m^2/s$ ($0.8587\ ft^2/hr$) and a Nusselt number of unity, calculation shows that it requires only 0.02 second for the central temperature of the gas bubble to reach 99% of the final temperature. This means that thermophoretic velocities go to zero in 0.02 second from the start of bubble formation.

Experimental results in diffusiophoretic velocity agree very well (±5%) with theory described by Equation 38 as shown in

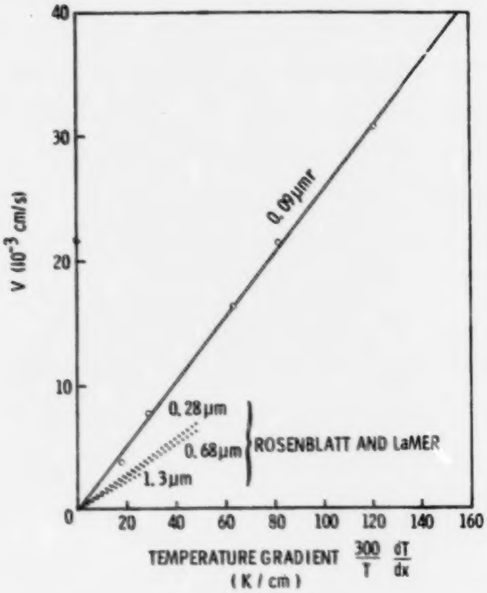

Figure 20. The thermophoretic velocity in air as a function of temperature gradient.

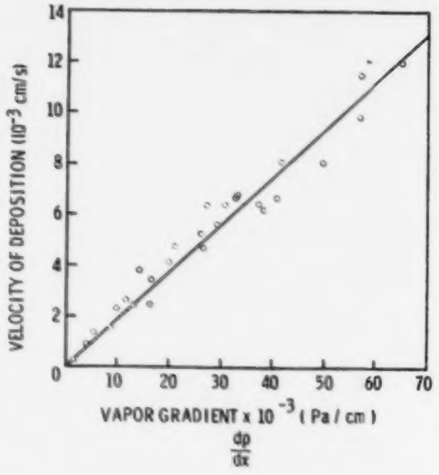

Figure 21. The diffusiophoretic velocity in air as a function of water-vapor pressure gradient.

Figure 21. It is seen that the maximum diffusiophoretic velocity is in the order of 0.1 mm/s. Similarly, for the thermophoresis process we can estimate the time required for the dry gas inside the bubble to reach an equilibrium saturation vapor pressure. With the diffusion coefficient of water vapor in air at $D = 0.24\ \mathrm{cm}^2/\mathrm{s}$ and a Schmidt number of unity, a quick calculation shows that it requires about 0.08 second for the central vapor pressure of the gas bubble to reach 99% of saturation. This is about 4 times slower than the gas reaches equilibrium temperature. With a diminishing vapor gradient the total displacement of a particle within the bubble by diffusiophoretic velocity would be far less than 0.1 x 0.08 = 0.008 mm.

4.3.3 Electrostatic Force

In addition to the previously mentioned thermophoresis and diffusiophoresis, electrostatic effects are also important in the particle collection by foam. Since particulate emissions from industrial effluents are highly charged, let us consider the effect of electrostatic charge on the collection of small particles by a foam scrubber.

As shown in Figure 22, the foam bubble can be considered conductive and grounded at all times. Imaginary charges, therefore, are always created opposite to charged particles regardless of the charge sign. By Coulomb's law of electrostatic forces, the attracting or repelling force between the charged particle and opposing surface is:

$$F_{\mathrm{Coulomb}} = \frac{1}{4\pi\varepsilon} \frac{\sigma^2}{\delta^2} \tag{40}$$

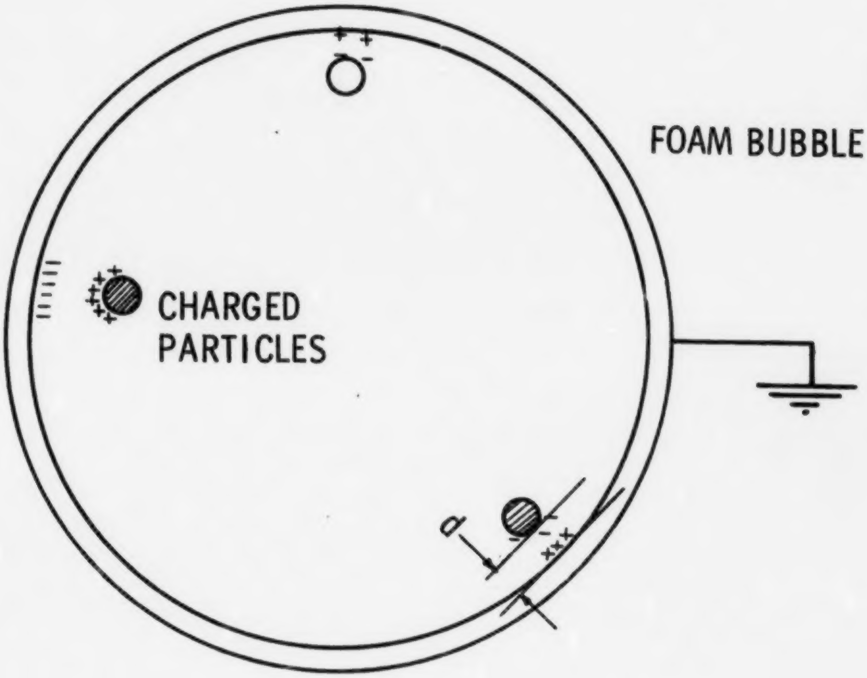
FOAM BUBBLE
CHARGED PARTICLES
a

Figure 22. Schematic of electrostatic force between particles and bubble wall.

where δ = distance between particles and surface

σ = number of charges on a particle

ε = permittivity of gas

In cgs system, Equation 40 becomes:

$$F_{\text{Coulomb}} = \frac{(\sigma e)^2}{k\delta^2} = \frac{(4.8 \times 10^{-10})^2\ n^2}{k\delta^2}\ \text{dynes/cm}^2 \qquad (41)$$

where e = 1 electron charge = 4.8×10^{-10} cgs esu

k = dielectric constant of gas

Equation 41 indicates the electrostatic force is inversely proportional to the square of distance between the bubble surface and the particle. While this force may be negligible when the particle is away from the bubble film, the attractive force between the particle and the bubble wall could become significant in the final step of the diffusion process as $\delta \to 0$, $F_{\text{Coulomb}} \to \infty$.

SECTION 5

EXPERIMENTAL WORK

Many experiments were performed in order to develop additional knowledge of foam scrubber performance. These experiments included particle collection efficiency determinations, investigations of optimum conditions for foam generation, investigations of various techniques of foam destruction, and foam characteristics measurements, e.g., foam stability, bubble size, foam density, and foam viscosity. In several cases we had to develop and devise a new technique to perform some of the experiments in order to obtain data representative of the foam scrubbing process. Descriptions of these techniques as well as some of the initial foam characterization results obtained before we were able to optimize the foam scrubber operation with respect to particle collection do not have a direct bearing on the particle collection efficiency data presented later in this section. We feel, however, that these descriptions may be useful in further development of fine particle foam scrubbing process since they provide some quantitative or qualitative indications for the relationships of variables influencing the foam characteristics. In order not to interfere with the main text of this report the descriptions will be presented in several appendixes and referred to throughout the main text.

5.1 EXPERIMENTAL FOAM SCRUBBER

The experimental apparatus to investigate the performance of a foam scrubber was constructed and is shown in Figure 23. The test scrubber can be supplied with compressed and filtered air. Before entering the foam generator, the air can pass through a humidification chamber and become saturated with moisture. The air can also be humidified using a dry steam generator (not shown in Figure 23). Humidified air is then passed through a rotameter and into the foam production and scrubbing section made of about 0.1 m (4 inches) I.D. plexiglass pipe. The aerosol is introduced at an orifice to insure thorough mixing. Downstream of the orifice, the surfactant solution supplied by a metering pump is sprayed onto the stainless steel screen. Foam is generated by the interaction of the air and liquid passing through the screen. Theoretical aspects of foam generation using a screen were presented in Section 4.1.

The foam then proceeds down the pipe of variable length (up to 6 m) and into the destruction chamber. A portion of the scrubber and the destruction chamber are shown in Figure 24.

5.2 FOAM GENERATION

It was initially felt that a 40 to 60 mesh screen would be of sufficient fineness to generate foam with the desired bubble diameter (approximately 1 mm). However, visual observation of foam made with the 60 mesh screen indicated that this foam consisted of bubbles about 6 mm in diameter. Since the bubble diameter is a critical factor for particle collection, some fine screens, 250 mesh and 325 mesh, have been investigated. The size of foams produced with different screens and surfactants and with different operating conditions will be

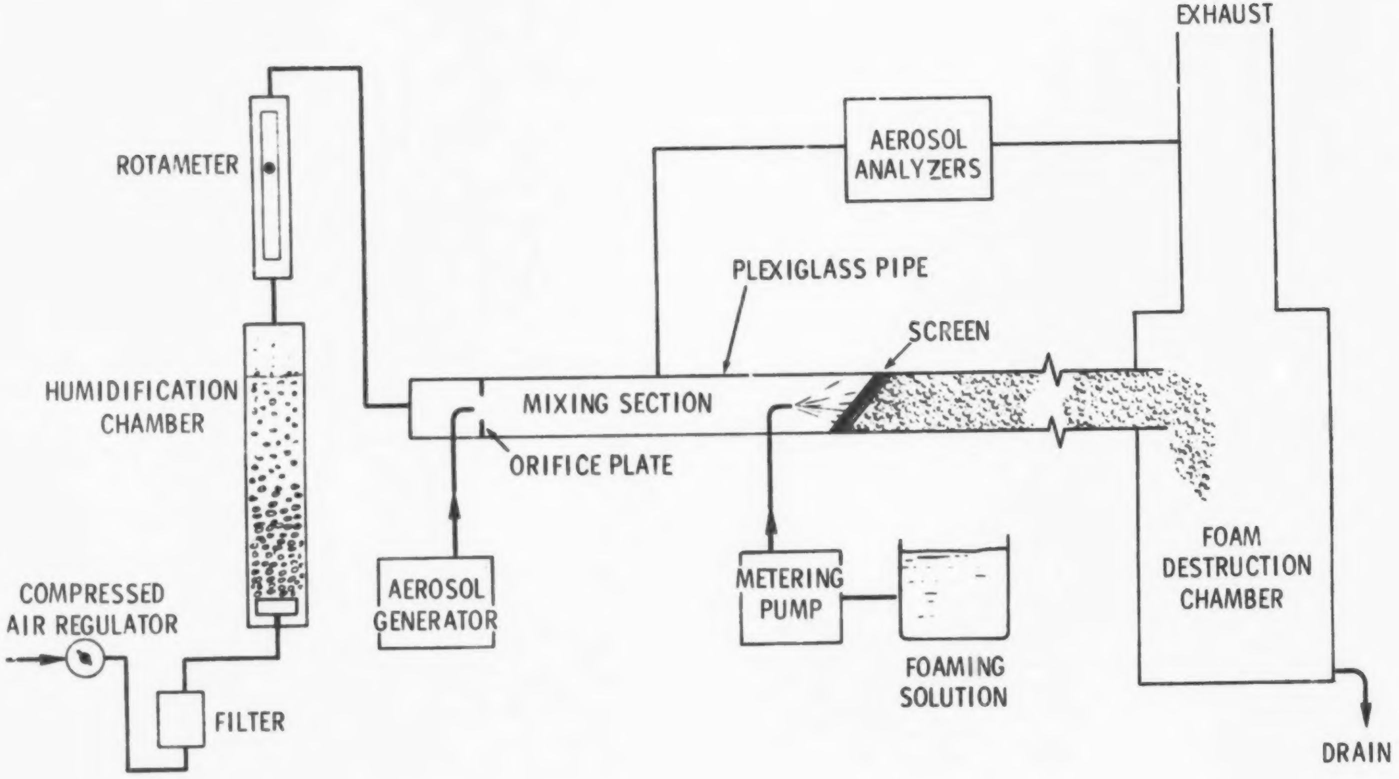
EXHAUST
ROTAMETER
AEROSOL ANALYZERS
PLEXIGLASS PIPE
SCREEN
HUMIDIFICATION CHAMBER
MIXING SECTION
ORIFICE PLATE
COMPRESSED AIR REGULATOR
AEROSOL GENERATOR
METERING PUMP
FOAM DESTRUCTION CHAMBER
FOAMING SOLUTION
FILTER
DRAIN

Figure 23. Experimental foam scrubber.

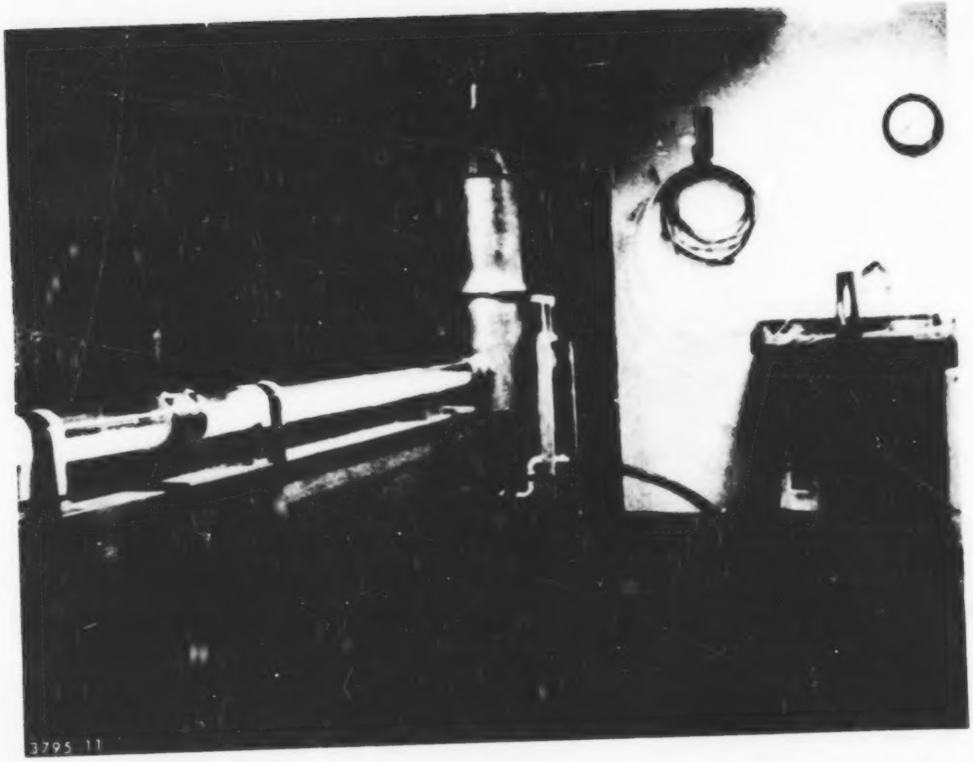

Figure 24. Destruction chamber of the foam scrubber

further discussed in Appendixes A and B. The majority of the particle collection measurements were performed with the 250 mesh screen.

5.3 FOAM DESTRUCTION

The design of the foam destruction chamber permitted the investigation and determination of the minimum destruction energy requirements for several destruction approaches. The chamber is schematically shown in Figure 25; its physical appearance was shown in Figure 24. According to the theory, the foam generation process is associated with the formation of new surface and consumption of energy. On the contrary, the reversed process of foam destruction is associated with energy release. This means that foam should have sufficient energy to self-destruct.

The difficulty in destroying foam is directly related to the foam stability which appears as a function of surfactant concentration and foam generation conditions. At a given surfactant concentration and foam generation conditions which influence the foam density (wetness) and the foam bubble size, one should be able to produce foams with the same stability. The wet foams, however, undergo continuous drainage and change in their density. Generally, the drier foams are less stable. In the foam scrubber process therefore the foam stability will be a function of residence time. Since the foam drainage is caused by gravitational forces, the physical arrangement of the scrubber, that is, whether the major portion of the scrubber is horizontal, vertical, or inclined, will also have some influence on the stability of foam exiting the scrubber.

Ideally, the foam should possess marginal stability and collapse by itself immediately after leaving the foam scrubber.

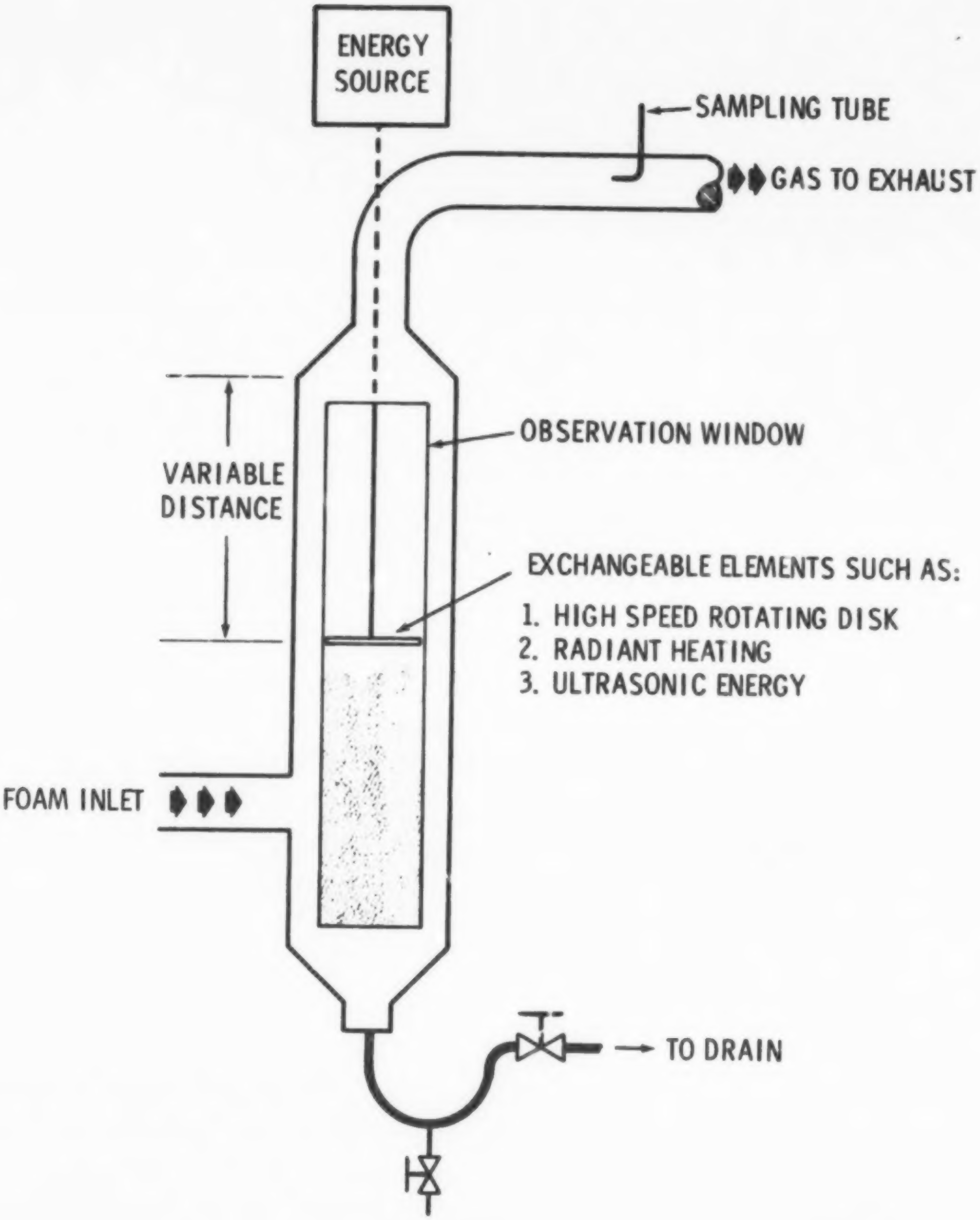
ENERGY SOURCE
SAMPLING TUBE
GAS TO EXHAUST
VARIABLE DISTANCE
OBSERVATION WINDOW
EXCHANGEABLE ELEMENTS SUCH AS:
1. HIGH SPEED ROTATING DISK
2. RADIANT HEATING
3. ULTRASONIC ENERGY
FOAM INLET
TO DRAIN

Figure 25. Foam destruction chamber.

This would eliminate the foam destruction step and any energy requirements associated with it. In practical foam scrubber application, however, the self-destruction of foam would be difficult to control due to the presence of gaseous and particle impurities that can highly influence the foam stability in a not exactly predictable manner. We have observed the self-destruction of foam to be a relatively slow process of collapsing first the small bubbles into larger bubbles which is followed by the larger bubbles collapsing to still larger bubbles. Because the bubble size is a very important parameter for fine particle collection, once the larger size bubbles are formed, the particle collection efficiency is markedly reduced. Early collapse of foam would simply mean that either insufficient collection of particles would result or longer scrubber residence times would need to be provided. Since the major collection mechanisms utilized in the foam scrubber are slow and require residence times as high as 30 - 60 seconds any additional increase of the residence time appears undesirable. This means that at least at present some form of foam destruction is needed.

Five foam destruction techniques were investigated during this program and included liquid spray, thermal destruction, ultrasonic destruction, compressed air spray, and high speed rotating disk. The high speed rotating disk was found to be the most effective device for foam destruction as to the energy requirements and possibility of foam liquid recycle. Consequently, the high speed disk was selected and used in particle collection determinations. Additional discussions on foam stability and its measurement are presented in Appendix C. Related information on foam destruction techniques and foam density determination is presented in Appendixes D and E, respectively.

5.4 SURFACTANT SELECTION

Four surfactants have been selected for foam scrubber evaluations. Tergitol TMN-6, made by Union Carbide, was chosen because it was used successfully in our previous coal dust suppression work utilizing foam. As suggested by our consultant, Aerosol OT produced by American Cyanamid possesses exceptional foaming characteristics and was therefore included in our study. Alkanol DW, made by DuPont, a sodium alkylaryl sulfonate, was selected because it is a good general purpose surfactant and is characterized as a medium quality foaming agent. Sterox NM, made by Monsanto, was also chosen because it is a high foaming general purpose surfactant. We feel that these four surfactants well represented the surface active agent market in the United States, and were good candidates for initiation of foam scrubbing work. Table 3 contains a list of the four surfactants with some of their characteristics.

5.5 PARTICLE MONITORING EQUIPMENT

Three particle counters were utilized on this program for aerosol characterization and the determination of fine particle collection efficiency by foam scrubbing. The counters were a nuclei condensation counter, an optical counter, and an electrical aerosol analyzer. The instruments have a combined capability to measure aerosol particles in the size range from 0.003 μm to about 30 μm. Because the counters have limited counting capacity a sample dilution system was devised and used in connection with the counters. Additional description of the aerosol sampling instruments and their capabilities is provided in Appendix F.

Table 3. SURFACTANT TYPES

Surfactant	Manufacturer	Composition	Chemical type	Concentration, %	Comments
Tergitol TMN	Union Carbide Corp., Plastics Div.	Trimethyl nonyl polyethylene glycol ether	Nonionic	90	Wetting and re-wetting agent
Sterox NM	Monsanto Co., Inorganic Chemicals Div.	Alkyl phenol ethylene oxide adduct	Nonionic	99.5	General purpose detergent (melting point 30-35°C)
Alkanol DW	E.I. du Pont de Nemours & Co., Inc.	Sodium alkylaryl sulfonate	Anionic	28	General use detergent; du Pont says it is in tight supply at the present time
Aerosol OT (75%)	American Cyanamid Co., Industrial Chemicals, Div.	Dioctyl ester of sodium sulfosuccinic acid	Anionic	75	Fruity pungent odor

5.6 EXPERIMENTAL AEROSOL GENERATION

Two types of aerosol particles were used during the bench scale tests of foam scrubber for collection efficiency. They were dioctyl phthalate and polypropylene glycol. Relative to water the two particle types possess different wettability properties, the dioctyl phthalate being essentially nonwettable and the polypropylene glycol being wettable and miscible with water in any proportions. The experimental aerosols were generated by means of a condensation aerosol generator developed at the University of Minnesota by Liu, Whitby, and Yu,[5] and illustrated in Figure 26.

5.7 FOAM SCRUBBER FINE PARTICLE COLLECTION EFFICIENCY

Particle collection efficiencies were obtained for the two particle types by measuring the aerosol concentration just prior to the surfactant spray nozzle and after the foam was destroyed in the destruction chamber. (Refer to Figure 23.) The difference in particle counts was used as a measure of particle collection in the foam scrubber. The measurements were made for different particle sizes as permitted by the particle counters used.

The destruction of foam resulted in formation of additional fine aerosol particles. This is associated with bubble bursting and liquid droplet dispersion at the time of foam destruction. Upon droplet evaporation any non-volatile material

---

[5] Liu, B. Y. H., K. T. Whitby, and H. H. S. Yu. A Condensation Aerosol Generator for Producing Monodispersal Aerosols in the Size Range of 0.036 to 1.3 Microns. (Presented at the 6th Inst. Conf. on Condensation Nuclei. Paris. May 1966). J. de Recherches Atmos. (Paris.) No. 3:397-406 (1966).

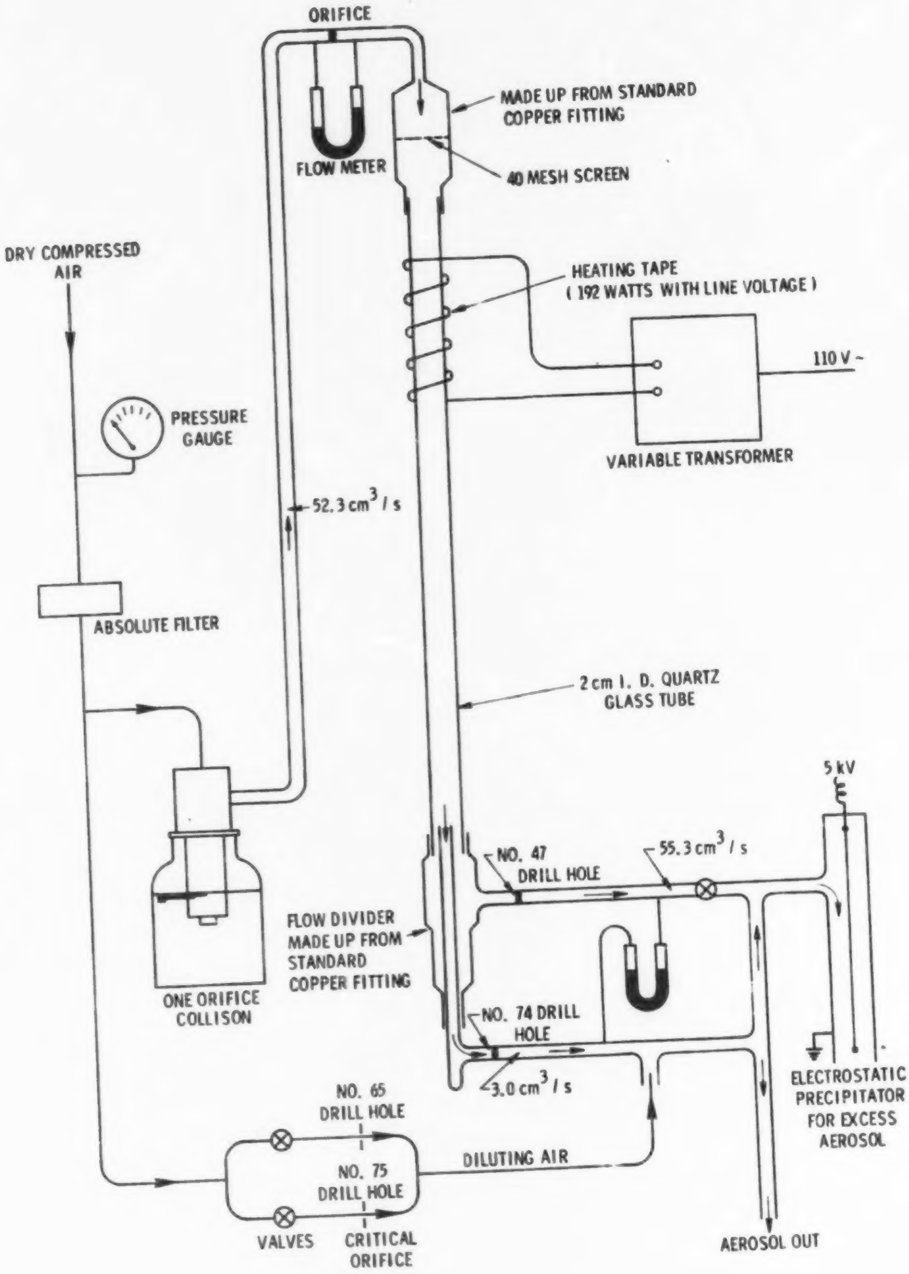
ORIFICE
MADE UP FROM STANDARD COPPER FITTING
FLOW METER
40 MESH SCREEN
DRY COMPRESSED AIR
HEATING TAPE (192 WATTS WITH LINE VOLTAGE)
110 V ~
PRESSURE GAUGE
VARIABLE TRANSFORMER
52.3 cm^3 / s
ABSOLUTE FILTER
2 cm I. D. QUARTZ GLASS TUBE
5 kV
NO. 47 DRILL HOLE
55.3 cm^3 / s
FLOW DIVIDER MADE UP FROM STANDARD COPPER FITTING
ONE ORIFICE COLLISON
NO. 74 DRILL HOLE
3.0 cm^3 / s
ELECTROSTATIC PRECIPITATOR FOR EXCESS AEROSOL
NO. 65 DRILL HOLE
NO. 75 DRILL HOLE
DILUTING AIR
VALVES
CRITICAL ORIFICE
AEROSOL OUT

Figure 26. Monodispersed aerosol generating system.

present in the liquid drops remains in the gas stream as a particle. Some additional data of number of particles produced from foam destruction are presented in Appendix G. During the tests evaluating the scrubber collection efficiency the destruction disk was operated so as to minimize the secondary particle formation.

In order to evaluate the fine particle collection occurring in the foam scrubber the concentration of the secondary particles at foam destruction was determined by operating the scrubber with no input aerosol and counting the particles after the foam was destroyed. This established the baseline of particulates which was then subtracted from the counts obtained under identical scrubber operating conditions and with a characterized aerosol input. Typically, the input aerosol concentration was maintained at a level which would hold the number of particles generated at foam destruction to about 2 - 10% of the input aerosol in the investigated size range.

Collection determinations were observed with different scrubber residence times. The scrubber residence times were varied by changing the scrubber length. At the same time the air flow velocity through the scrubber was maintained constant. This arrangement permitted performance of collection measurements with identical foam characteristics. Typical collection data using the high speed disk for the foam destruction are presented in Table 4. The results are summarized in a graphical form in Figures 27 and 28. Because the collection of fine particles in foam takes place mainly by diffusion and sedimentation the collection efficiency is a strong function of scrubber residence time. Both Figures 27 and 28 demonstrate curves asymptotically approaching 100% collection with an increase of scrubber residence time which

Table 4. SAMPLE DATA FOR DOP PARTICLE COLLECTION WITH FOAM SCRUBBER USING ROTATING DISK - HIGH QUALITY FOAM

Experiment number	Operating conditions						Results			
	Concentration of Tergitol, %	Air flow rate, 10^{-3} m^3/s (cfm)	Residence time, s	Dilution ratio	Surfactant solution flow rate, cm^3/s	Input DOP concentration, 10^6 particles/cm^3	Parameter	Particle concentration, μm		
								0.18 - 0.32	0.32 - 0.56	0.56 - 1.0
1[a]	1	1.137 (2.41)	40	30/1	5.83	2.25	Input aerosol	1.0×10^6	6.30×10^5	1.92×10^5
							Aerosol & foam	5.19×10^5	3.06×10^5	1.00×10^5
							Baseline - foam only	7.92×10^4	2.30×10^4	1.02×10^4
							% Collected	56.4	55.1	54.6
2[b]	1	1.370 (2.91)	30	30/1	5.83	0.55	Input aerosol	1.61×10^5	1.81×10^5	1.14×10^5
							Foam & aerosol	1.35×10^5	9.30×10^4	5.05×10^4
							Baseline - foam only	7.53×10^4	2.93×10^4	1.09×10^4
							% Collected	63.0	64.8	65.3
3[c]	1	1.370 (2.91)	30	30/1	5.83	2.59	Input aerosol	1.20×10^6	2.94×10^5	5.89×10^4
							Foam & aerosol	6.44×10^5	1.75×10^5	4.00×10^4
							Baseline - foam only	8.99×10^4	3.00×10^4	1.04×10^4
							% Collected	53.3	50.7	49.9
4[d]	4	1.137 (2.41)	40	30/1	5.83	3.35	Input aerosol	1.64×10^6	6.99×10^5	1.63×10^5
							Aerosol & foam	7.32×10^5	3.15×10^5	8.73×10^4
							Baseline - foam only	3.48×10^5	1.22×10^6	3.36×10^4
							% Collected	76.6	72.6	67.1
5	2	1.137 (2.41)	40	30/1	5.83	3.28	Input aerosol	1.70×10^6	7.23×10^5	1.58×10^5
							Aerosol & foam	6.60×10^5	2.86×10^5	7.47×10^4
							Baseline - foam only	2.73×10^5	1.00×10^5	2.74×10^4
							% Collected	77.2	74.3	66.0
6	2	0.541 (1.15)	84	30/1	5.83	3.13	Input aerosol	1.40×10^6	7.50×10^5	2.00×10^5
							Aerosol & foam	3.96×10^5	2.10×10^5	6.33×10^4
							Baseline - foam only	1.44×10^5	5.10×10^4	1.49×10^4
							% Collected	82.1	78.7	75.8
7	2	1.137 (2.41)	13	30/1	5.83	2.72	Input aerosol	1.41×10^6	6.15×10^5	1.49×10^5
							Aerosol & foam	7.44×10^5	3.24×10^5	9.27×10^4
							Baseline - foam only	1.11×10^5	4.20×10^4	1.05×10^4
							% Collected	54.9	54.2	45.7
8	2	1.137 (2.41)	13	None	5.83	1.06	Input aerosol	4.71×10^5	1.41×10^5	3.20×10^4
							Aerosol & foam	3.06×10^5	8.27×10^4	1.86×10^4
							Baseline - foam only	7.38×10^4	1.93×10^4	4.91×10^3
							% Collected	50.6	54.2	57.1

[a] Coarse foam, somewhat unstable. This experiment as a comparison with high quality foam data below.

[b] Coarse foam, somewhat unstable. Aerosol generated from 10% DOP solution.

[c] Coarse foam, somewhat unstable. Aerosol generated from 2% DOP solution.

[d] Baseline high because of high disk speed with 4% Tergitol. Uniform, small-celled, stable foam.

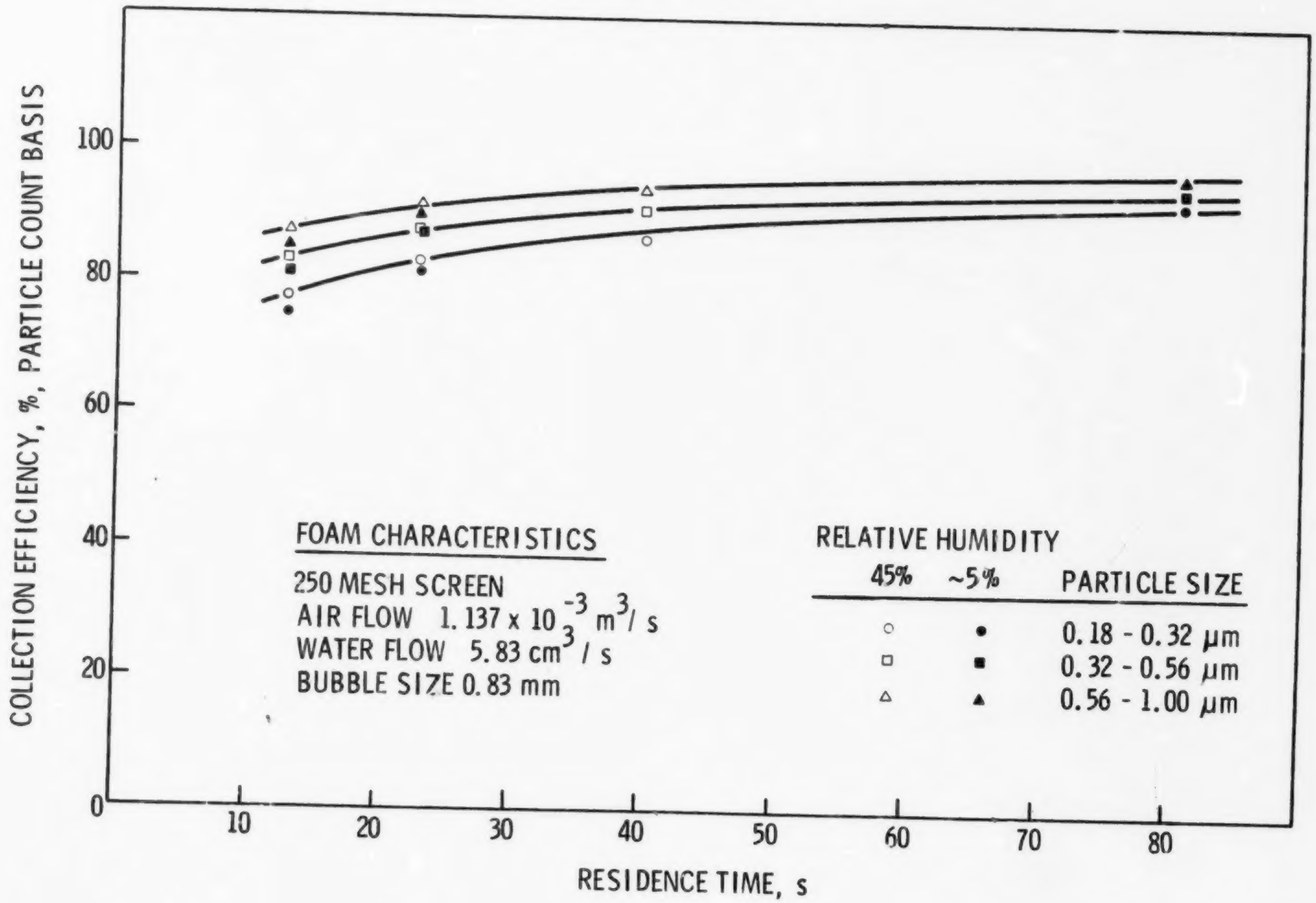

Figure 27. Foam scrubber collection efficiency of polypropylene glycol 425 using 2% Tergitol foam with rotating disk for foam destruction.

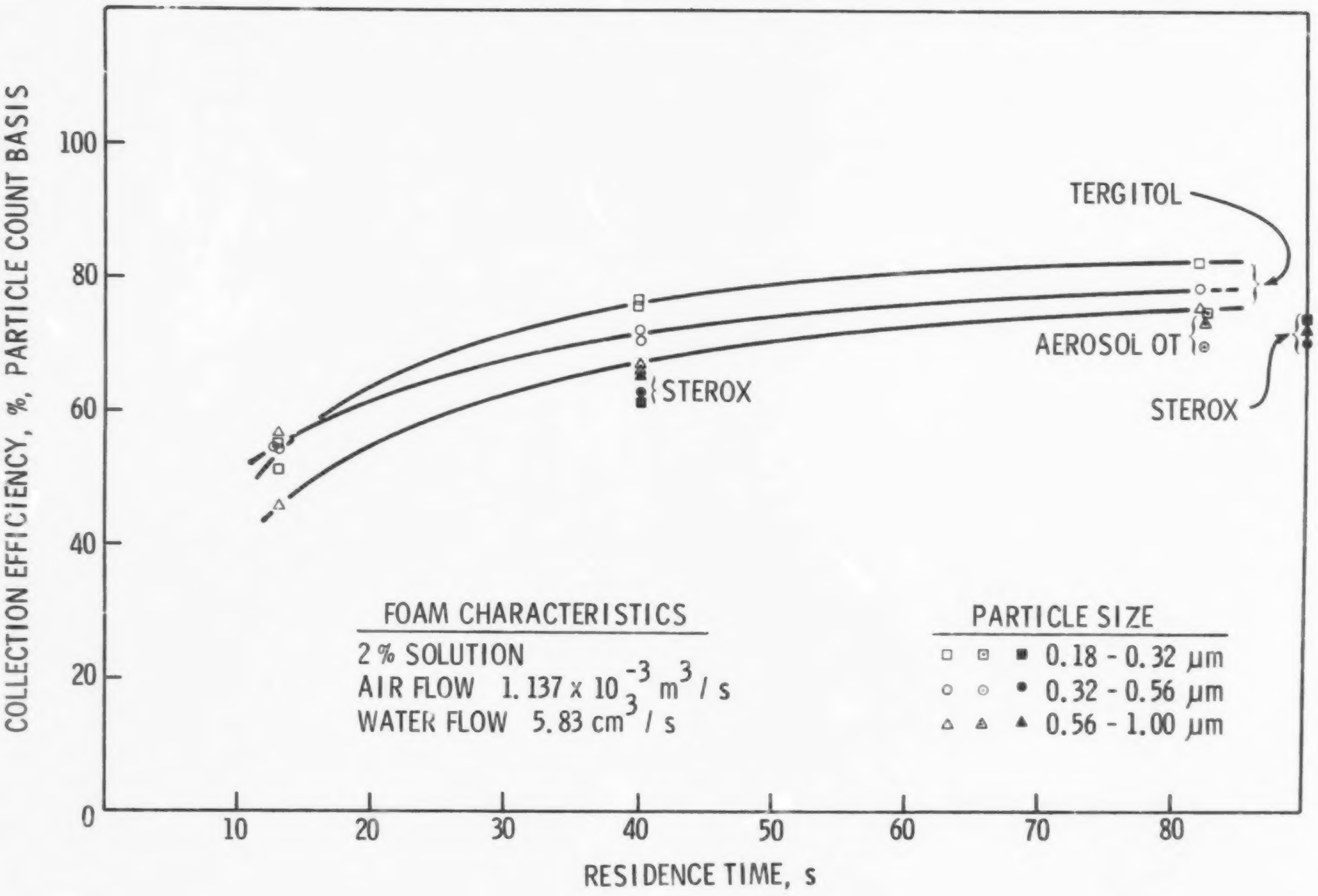

Figure 28. Collection of DOP aerosol using foam scrubbing with rotating disk for foam destruction.

agrees with the theoretically predicted curves reasonably-well (see Figures 6, 12, 13, and 14). Bubble diameter in all cases was 0.8 mm nominal. Somewhat higher collection efficiencies than those predicted have been observed using polypropylene glycol (wettable) aerosol especially at the lower scrubber residence times (Figure 27). This indicates that the compatibility between particles and the foam as for example suggested by the aerosol wettability is an important factor to consider in optimization of foam scrubber design and operation. Figure 28 shows several additional data points obtained with the DOP aerosol and different surfactants including Tergitol, Sterox, and Aerosol OT. These points further support the factor of aerosol/foam compatability since some changes in collection efficiency were noted due to the change of surfactant. Even though the collection efficiencies were found generally lower than those observed using Tergitol foam, proper surfactant selection might improve DOP collection and approach the efficiency that was observed for polypropylene glycol aerosol.

Also, a comparison of the collection data persented in Figures 27 and 28 suggests that there might be somewhat different collection rate control factors in the cases of DOP and polypropylene glycol aerosols. While the small size particles showed better collection efficiency than large size particles using DOP aerosols, this trend was found to be reversed for particles of polypropylene glycol.

Figure 27 also includes two sets of data measured with different humidity in the scrubber. Two relative humidity levels, 5% and 45%, were investigated using glycol aerosol and Tergitol foam. More humid input air increased the particle collection by about 1 - 2% for residence times of 13 and 26 seconds. Since the accuracy of the particle concentration measurement is believed to be about 10 - 20% it is not certain whether the effect of humidity is or is not significant.

The effect of bubble size on collection efficiency was also evaluated. The 60 mesh screen was used to generate coarser foam with the other operating parameters kept constant. The size of cells for the 60 mesh screen was photographically determined to be about 3.9 mm. The observed collection rates are presented in Figure 29. The collection rates are significantly less than the values determined for the small-celled foam (0.83 mm). The DOP aerosol showed a collection rate of about 40% with a particle size between 0.56 and 1.0 μm and 80 second residence time (75% collection was observed with the small-celled foam). The glycol achieved about 84% collection under similar conditions (98% with small-celled foam). Two data sets are also displayed using a large-celled 1% Alkanol foam. While this foam improved collection of DOP aerosol, the collection of polypropylene glycol aerosol was essentially unchanged.

The operating conditions which have been used in our experiments give an air (or foam) velocity in the scrubber of about 0.15 m/s (0.5 ft/s). It is postulated that a higher average velocity might influence the collection rate, especially at the point of foam generation where higher turbulence could enhance the effect of collection by impaction. Consequently, the velocity was increased by a factor of three to about 0.45 m/s (1.5 ft/s). At the same time the scrubber was lengthened to 5.5 m (18 ft) so that a 13 second residence time remained unchanged. The collection results for both DOP and the polyglycol were essentially the same as for the 13 second residence time at the lower air velocity.

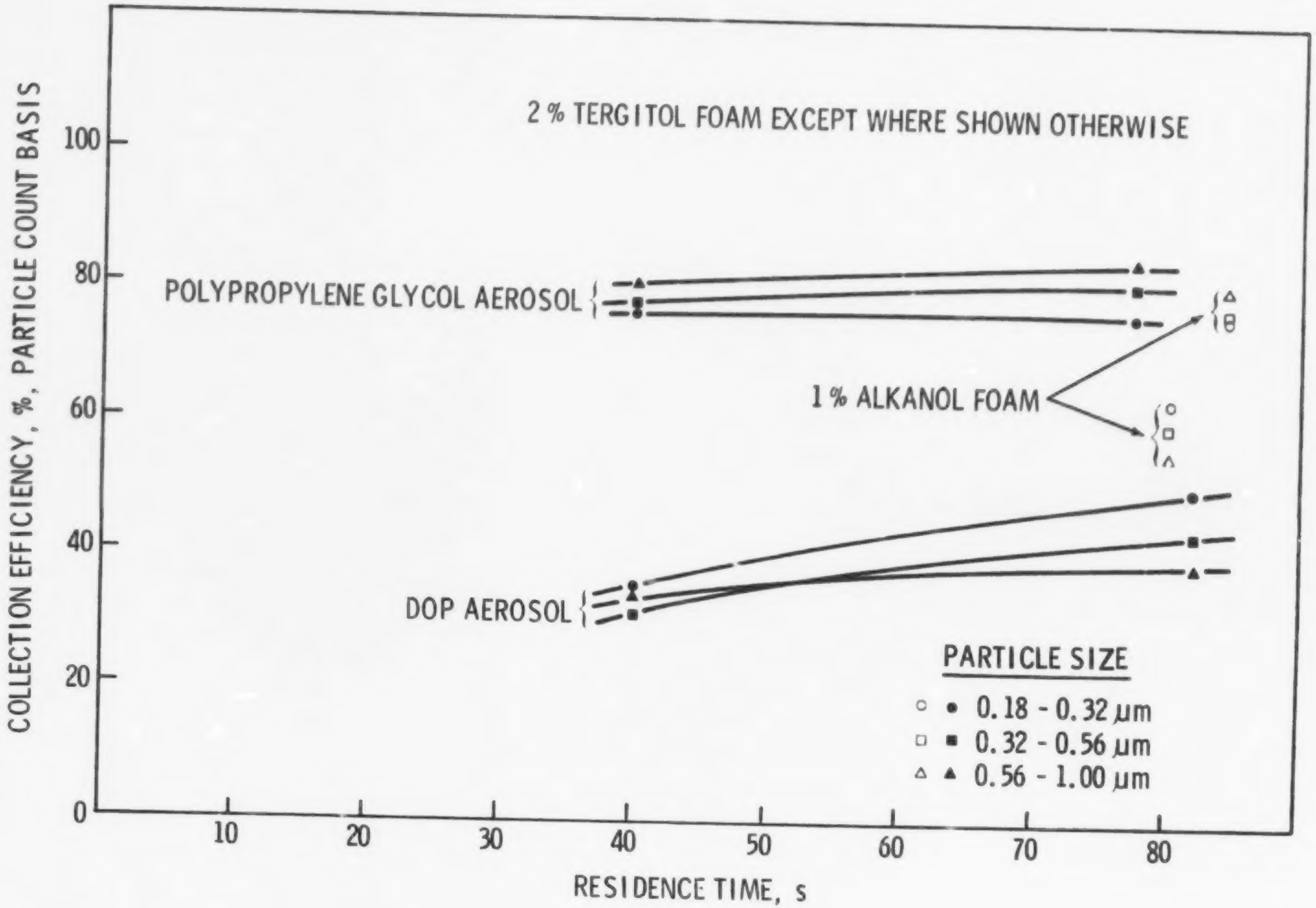

Figure 29. Foam scrubber collection efficiency of polypropylene glycol 425 and DOP using large-celled (3.9 mm) foam.

This supports the theoretical evaluations presented in Section 4 which indicated that the collection rates during the foam formation will be negligible and that the majority of particles will have to be collected by diffusion and sedimentation mechanisms.

There does, however, appear to be a point where collection efficiency is enhanced by capture of particles in the foam generation step. This occurs at high liquid to gas ratios causing the foam scrubber to behave similar to a wet scrubber. Figure 30 shows the effect of distilled water sprayed on the 250 mesh screen in relation to collection efficiency of DOP particles in the size range between 0.7 and 1.0 μm. No collection of particles is seen for liquid to gas ratios below 5,130 cm^3/m^3 (38.4 gal/1,000 ft^3). Thus, the collection efficiencies for foam scrubbing reported above primarily represent the mechanisms of diffusion and sedimentation.

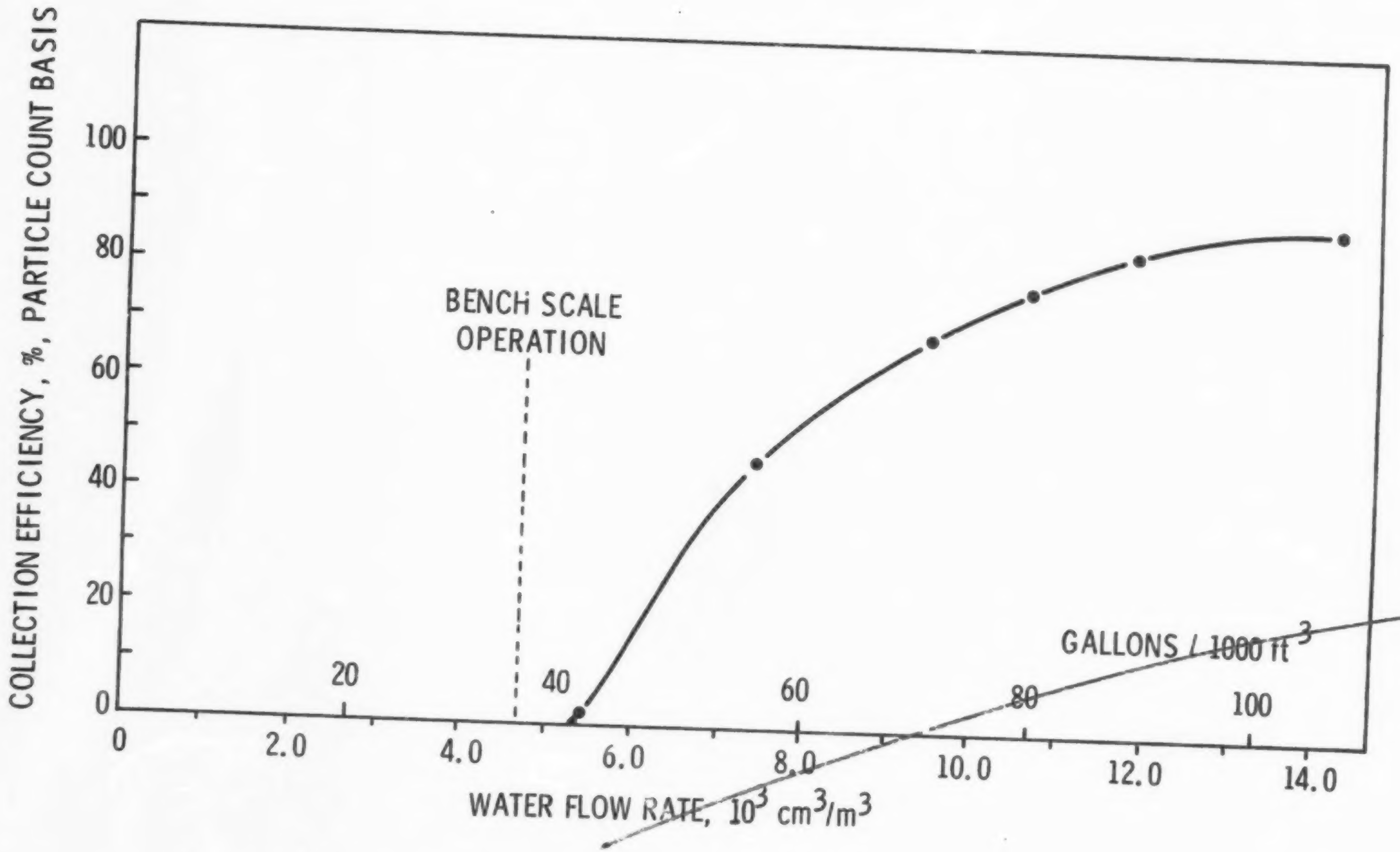

Figure 30. Collection efficiency values for distilled water sprayed on the screen versus water flow rate, DOP particle size: 0.7 - 1.0 μm.

SECTION 6

FOAM SCRUBBER ECONOMICS

Based upon the data collected during the bench scale evaluation of foam scrubbing, a cost model was generated to evaluate the economics of this fine particulate removal technique. The costs generated were compared with costs for particulate control using conventional techniques: high efficiency electrostatic precipitation, fabric filtration, and high energy wet scrubbing. Before presenting the cost estimates and comparisons, their limitations must be comprehended.

6.1 ACCURACY OF ESTIMATE

The accuracy of the foam scrubbing cost estimates is limited by the amount of information gained during the bench scale testing. This information was used to estimate the costs of a foam scrubber process with a handling capacity several magnitudes larger. Hence, the accuracy of the estimates for the foam scrubber is judged to be about ± 50%. Additional information to determine the foam scrubber costs was taken from Modern Cost-Engineering Techniques edited by H. Popper[6] and Plant Design and Economics for Chemical Engineers by

---

[6] Modern Cost-Engineering Techniques. Popper, H. (ed). New York, McGraw-Hill Book Company, 1968. 850 p.

M. S. Peters and K. D. Timmerhaus.[7] The costs for conventional control equipment were obtained from three journal references: Dust Collection Equipment by G. D. Sargent,[8] A Systematic Procedure for Determining the Cost of Controlling Particulate Emissions from Industrial Sources by N. G. Edmisten and F. L. Bunyard,[9] and Estimating the Costs of Gas-Cleaning Plants by J. R. F. Alonso.[10]

Even though the economic data for the conventional devices should be representative of fabric filter, high energy scrubber, and high efficiency electrostatic precipitation, the corresponding collection efficiencies of these devices in the fine particle range are questionable. They all are defined as high efficiency collectors based on total particle mass collection. Since fine particles in most industrial gases represent only a small fraction of the total particle mass (e.g., an estimated 68% of fine particles in the range between 0.01 and 3 µm from pulverized coal fired power plants are in the 1 - 3 µm range on a mass basis, while the same size range represents less than 1% of particles on a number basis),[11] these devices may not remove fine particles even if a very high overall mass collection efficiency (99%+) is obtainable as claimed. As a result, we can be comparing the economics of a foam scrubber device collecting fine particles with a conventional collector whose collection efficiency in the fine particle range is not very significant. Nevertheless, the economic data for the three conventional control techniques are based on extensive past experience in design, construction, and operation and are believed to be 25 - 30% accurate.

---

[7] Peters, M. S., and K. D. Timmerhaus. Plant Design and Economics for Chemical Engineers, 2nd Edition. New York, McGraw-Hill Book Company, 1968. 850 p.

[8] Sargent, G. D. Dust Collection Equipment. Chemical Engineering. 76:130-150, January 27, 1969.

[9] Edmisten, N. G., and F. L. Bunyard. A Systematic Procedure for Determining the Cost of Controlling Particulate Emissions from Industrial Sources. Journal of the Air Pollution Control Association. 20:446-452, July 1970.

[10] Alonso, J. R. F. Estimating the Costs of Gas-Cleaning Plants. Chemical Engineering. 78:86-96, December 13, 1971.

[11] Shannon, L. J., P. G. Gorman, and M. Reichel. Particulate Pollutant System Study. Vol. II - Fine Particle Emissions. Midwest Research Institute. Kansas City. Environmental Protection Agency (Durham), Contract CPA 22-69-104 (PB 302 521). August 1, 1971. 348 p.

6.2 BASE COLLECTION EFFICIENCIES

To substantiate the questionability of collection efficiencies for the three conventional devices in the fine particle range the following discussion is presented. In a study of fine particulate emissions performed by Midwest Research Institute,[11] collection efficiency data for the conventional devices to the submicrometer particle size range were extrapolated. These are presented in Figure 31. For convenience the collection data from bench scale experiments for the foam scrubber are also included.

The collection efficiencies for wet scrubbers and fabric filters in the particle size between 0.1 and 1 μm can be sufficiently supported by experimental data. Data from at least 10 scrubbers and six fabric filters of different designs were compiled to produce the extrapolated curves. The curve for fabric filters was produced using data which ranged between about 0.5% and 65% penetration of 0.1 μm particles. Thus, this curve represents a questionable average with a relatively large spread rather than a typical fabric filter operation. Wet scrubbers show a fairly steep curve with the collection efficiencies in fine particle size range quickly

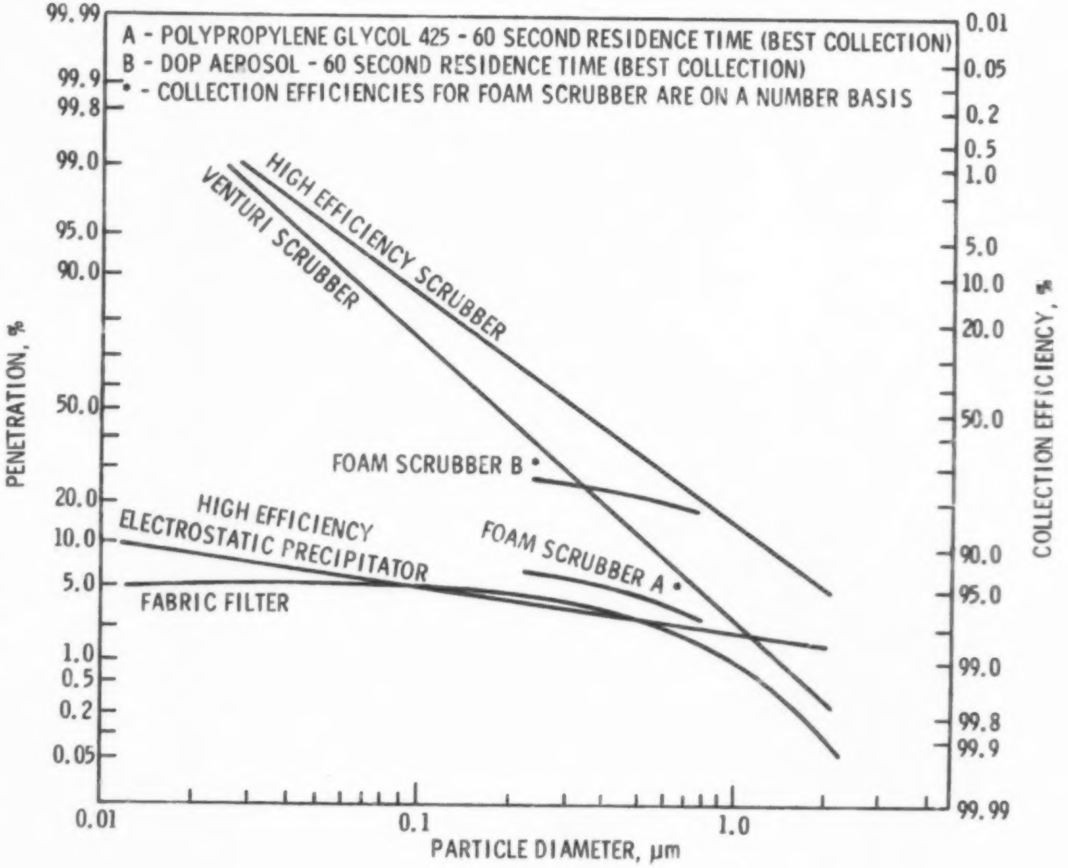

Figure 31. Extrapolated fine particulate control efficiencies.

decreasing with the decreasing particle size. The collection curves for the foam scrubber do not extend below 0.1 μm particle size, but as indicated by the theoretically calculated collection efficiencies (see Figures 9 through 17) reasonably high collection of particles in this range may be expected. The extrapolated collection curve of electrostatic precipitation to particle size range between 0.1 and 1 μm can be supported by only one experimental datum measured for particles of about 0.7 μm. The rest of the experimental data were taken in the range above 1 μm.

In conclusion, the collection of fine particles by the three conventional devices is questionable and will need further experimental verification. This may lead to changes in the cost estimates if these devices should collect significant amounts of particles in fine particle size range. The changes are more likely to increase than to decrease the costs presented here. The costs for foam scrubber are based on bench scale tests and can increase or decrease in the future. To obtain meaningful comparison of capital and operating cost estimates for particulate control alternatives, the estimates should be based upon consistent parameters and have similar accuracy. However, a preliminary economic analysis of foam scrubbing can be useful by providind order-of-magnitude comparisons with conventional control techniques and identifying the critical cost sensitive areas to provide direction for further experimental work. But the limitations of these estimates and comparisons should not be overlooked. The economic analysis of foam scrubbing and comparison with the three conventional control devices follow. General assumptions applicable to all cost estimates are listed in Table 5 followed by the assumptions for each specific type of control equipment in Tables 6 through 9.

Table 5. COST ASSUMPTIONS

General

Capital and operating costs do not include waste treatment and disposal

Gas temperature, gas composition, grain loading, and control efficiency were not considered as variables due to insufficient information concerning their influence on cost

Time reference 1975 Marshall and Stevens index 440

Chemical Engineering fabricated equipment index 203

Capital

Cost scaling exponent 0.6

Installation charge includes field installation, startup cost, working capital, and interest on construction loan

Operating

Stream time 8,000 hours/yr

Pump and air mover efficiency 50%

Utility costs

electricity \$0.015/kWh

water \$0.079/m^3 (\$0.30/10^3 gal)

Depreciation - 7% installed cost

Capital charges - 10% installed cost (includes interest, taxes, insurance, overhead, general and administration, etc.)

Table 6. FOAM SCRUBBING ASSUMPTIONS

Capital

Minimize surface area of scrubber (length = diameter) with maximum diameter of about 9 m (30 ft) - if larger add another scrubber train

Scrubber - 6.35 mm (1/4") carbon steel with cost as function of weight (spray nozzle 45 kg, 100 lb)

Screen - \$215/m^2 (\$20/ft^2)

Foam destruction system (10% of scrubber cost)

Residence time 10 - 50 seconds

Surfactant makeup vessel or surge vessel with recycle 1/2 hour capacity

Pump requirement - 500 cm^3/m^3 (38 gal/1,000 acf) (either feed or recycle)

Installation charge - 150% purchase cost

Operating

Pressure drop 2.2 kPa (9" H_2O)

Solution nozzle pressure 138 kPa (20 psig)

Labor 1.5 man @ \$6/hour

Control laboratory labor and operating materials 30% operating labor cost

Surfactant solution recycle - none, 90%, 99%

Energy required for foam destruction - 847 watts/m^3 (24 watts/ft^3)

Surfactant - 2% solution utilized for Tergitol

Cost on 100% basis - Tergitol \$1.43/liter (\$5.40/gal)
Aerosol \$1.27/liter (\$4.80/gal)
Sterox \$0.53/liter (\$2.0/gal)
Alkanol \$3.17/liter (\$12.00/gal)
use 1% solution

Table 7. ELECTROSTATIC PRECIPITATION ASSUMPTIONS

Capital

References listed in text

Installation charge - 70% purchase cost

Operating

Maintenance, labor and materials \$64/m^3 s^{-1} (\$0.03/acfm)

Pressure drop 249 Pa (1.0" H_2O)

Contact power 9 watts/m^3 (0.00034 hp/acfm)

For costs based on installed cost use high end of range

Table 8. FABRIC FILTER ASSUMPTIONS

Capital

References listed in text

Installation charge - 75% purchase cost

Operating

Maintenance, labor and materials \$170/m^3 s^{-1} (\$0.08/acfm)

Pressure drop 1.99 kPa (8.0" H_2O)

For costs based on installed cost use high end of range

Table 9. HIGH ENERGY WET SCRUBBER ASSUMPTIONS

Capital

References listed in text

Installation Charge - 200% purchase cost

Operating

Maintenance, labor and materials \$127/m^3 s^{-1} (\$0.06/acfm)

Pressure drop 14.9 kPa (60" H_2O)

Liquid head 1.79×10^5 Pa (26 psig)

Liquid circulation 2.67 m^3/1,000 m^3 (20 gal/10^3 acf)

Makeup water 6.68×10^{-5} m^3/m^3 (0.03 gal/acfm hr)

For costs based on installed cost use high end of range

6.3 RESULTS

The results of the capital cost estimates are presented in Table 10 and Figure 32. Table 10 presents foam scrubbing capital cost as percentage of total costs and as a function of residence time for a 23.6 m^3/s (50,000 acfm) unit, and Figure 32 depicts the capital costs for foam scrubbing as well as conventional controls as a function of unit capacity. Table 10 shows that the largest capital cost is incurred for the surfactant mixing vessel (from 35% to 61% of total cost). This is due to the large quantity of solution required for treatment [5,100 cm^3/m^3(38 gal/10^3 ft^3)]. A 57,000 gal vessel is required for 1/2 hour storage capacity. Figure 32 indicates that capital costs for foam scrubbing are similar to the costs for electrostatic precipitation, the most expensive conventional control device.

Table 11 and Figure 33 present the results of the operating cost analysis. Foam scrubbing operating costs as a percentage of total operating costs are presented in Table 11 as a function of surfactant recycle for a 23.6 m^3/s (50,000 acfm) unit. The operating cost is independent of residence time since the operating costs based on installed equipment cost are minimal compared to the cost of the surfactant (76 - 99+%). Costs for this estimate are based on using Tergitol. Other surfactant costs were listed in Table 6. Figure 33 presents a comparison of operating costs for foam scrubbing with the conventional collection methods. Even with 99% recycle, the operating cost of foam scrubbing is an order of magnitude greater than the most expensive conventional method (high energy wet scrubbing).

For foam scrubbing to be competitive with other particulate control equipment, operating costs must be reduced. A

Table 10. FOAM SCRUBBING CAPITAL COSTS FOR 23.6 m^3/s (50,000 ACFM) UNIT AS A FUNCTION OF RESIDENCE TIME

Component	Residence time, s				
	10	20	30	40	50
	Capital cost as % of total				
Scrubber	21	26	31	33	33
Screen	12	16	22	24	26
Destruction system	2	3	3	3	3
Mixing (or storage) vessel	61	51	41	37	35
Feed (or recycle) pump	4	4	3	3	3
TOTAL purchase cost	100	100	100	100	100

Table 11. FOAM SCRUBBING OPERATING COSTS FOR 23.6 m^3/s (50,000 ACFM) UNIT AS A FUNCTION OF SURFACTANT CYCLE

Component	Percent recycle		
	0	90	99
	Operating cost as % of total		
Labor	<1	1	7
Materials			
Surfactant	99+	97	76
Other	<1	<1	1
Utilities	<1	2	13
Depreciation	<1	<1	1
Capital charges	<1	<1	2
TOTAL operating cost	100	100	100

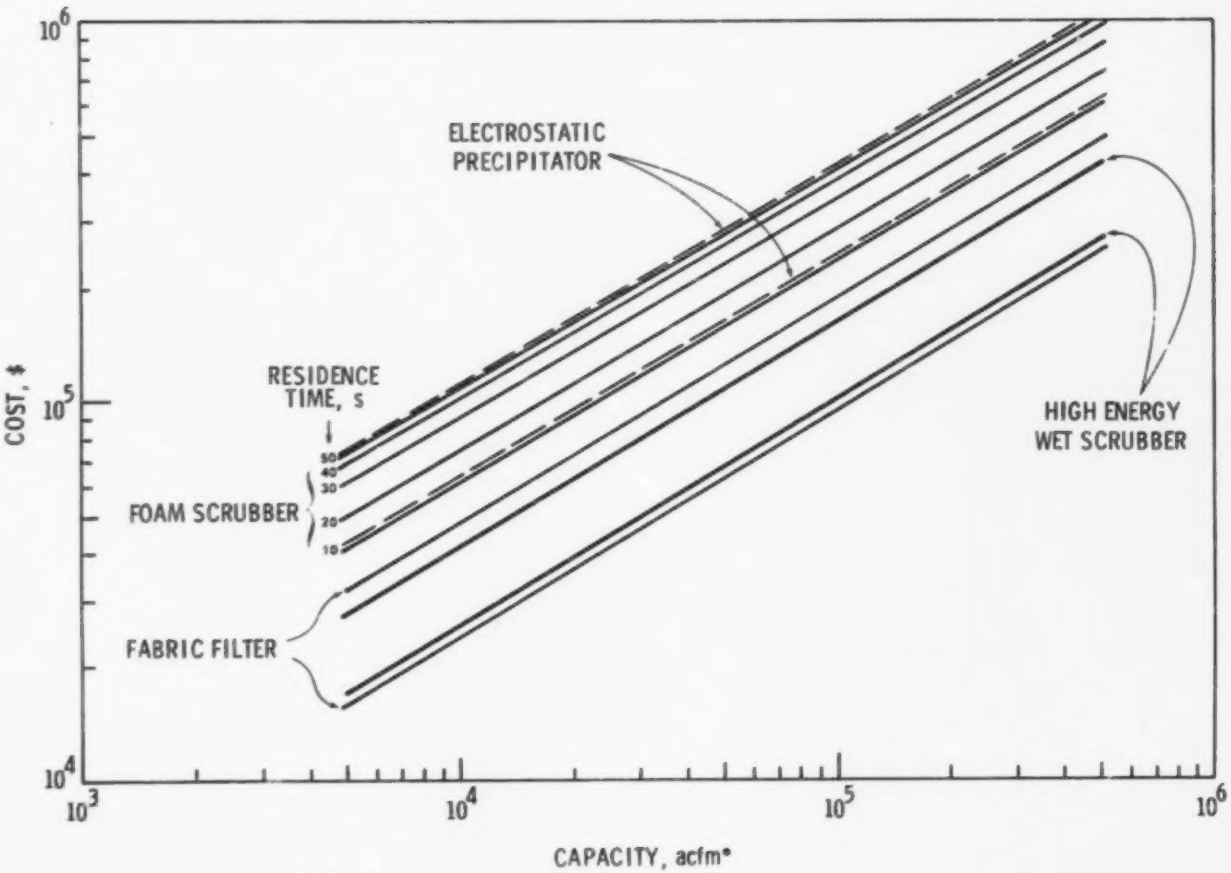

*1 acfm = 4.719 x 10^{-4} m^3/s

Figure 32. Capital cost for fine particulate control.

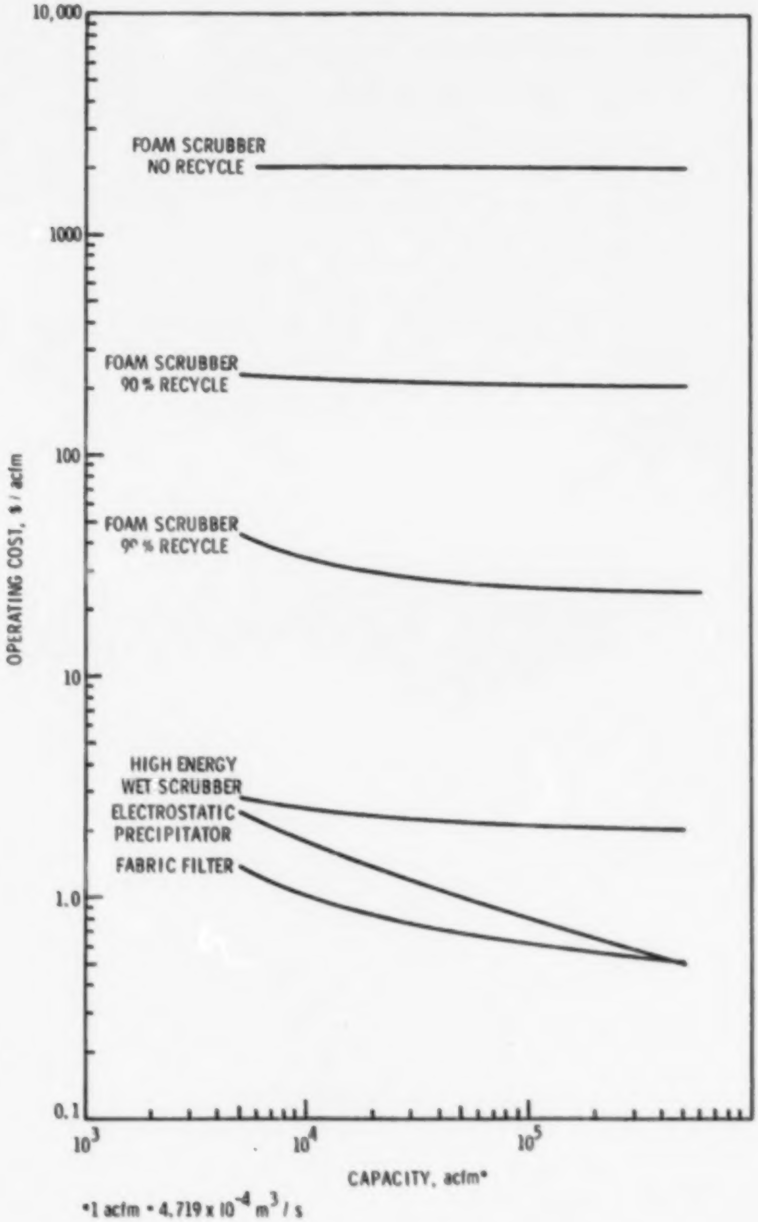

Figure 33. Operating cost for fine particulate control.

critical area in which operating cost reduction can be sought is the expenditure for surfactant. Reducing this expenditure may be accomplished by any one or combination of the following ways: using less expensive surfactant, increasing recycle of surfactant, using more dilute surfactant solution, or reducing the liquid to gas ratio. If savings in surfactant cost can be accomplished by these methods, foam scrubbing will become economically more attractive and may become cost competitive with conventional particulate control methods.

SECTION 7

REFERENCES

1. Shannon, L. J. Control Technology for Fine Particulate Emissions. Midwest Research Institute. Kansas City. U.S. Environmental Protection Agency, EPA-650/2-74-027 (PB 236 646). May 1974. 225 p.

2. Yu, H. S., and E. M. Sparrow. Flow Development in a Channel Having a Longitudinally Moving Wall. Journal of Applied Mechanics. 37(2):498-507, June 1970.

3. Bird, R. B., W. E. Stewart, and E. N. Lightfoot. Transport Phenomena. New York, John Wiley and Sons, Inc., 1960. 780 p.

4. Aerosol Science. Davies, C. N. (ed). New York, Academic Press, 1966. 468 p.

5. Liu, B. Y. H., K. T. Whitby, and H. H. S. Yu. A Condensation Aerosol Generator for Producing Monodispersal Aerosols in the Size Range of 0.036 to 1.3 Microns. (Presented at the 6th Inst. Conf. on Condensation Nuclei. Paris. May 1966). J. de Recherches Atmos. (Paris). No. 3:397-406 (1966).

6. Modern Cost-Engineering Techniques. Popper, H. (ed). New York, McGraw-Hill Book Company, 1976. 538 p.

7. Peters, M. S., and K. D. Timmerhaus. Plant Design and Economics for Chemical Engineers, 2nd Edition. New York, McGraw-Hill Book Company, 1968. 850 p.

8. Sargent, G. D. Dust Collection Equipment. Chemical Engineering. 76:130-150, January 27, 1969.

9. Edmisten, N. G., and F. L. Bunyard. A Systematic Procedure for Determining the Cost of Controlling Particulate Emissions from Industrial Sources. Journal of the Air Pollution Control Association. 20:446-452, July 1970.

10. Alonso, J. R. F. Estimating the Costs of Gas-Cleaning Plants. Chemical Engineering. 78:86-96, December 13, 1971.

11. Shannon, L. J., P. G. Gorman, and M. Reichel. Particulate Pollutant System Study. Vol. II - Fine Particle Emissions. Midwest Research Institute, Kansas City. Environmental Protection Agency (Durham), Contract CPA 22-69-104 (PB 203 521). August 1, 1971, 348 p.

12. Mahalingam, R., H. S. Surate, and J. A. Brink, Jr., High Expansion Foam Flow Analyses. Washington State University. (Presented at the AIChE 78th National Meeting. Salt Lake City. August 1976.)

13. Bikerman, J. J. Foams. New York, Spring-Verlag, 1973. 337 p.

14. Bransky, D. W., and F. F. Diwoky. Removal of Sulfuric-Acid Fog by Bubble-Phase Absorption. Refiner and Natural Gasoline Manufacturer. 19:191-195, June 1940.

15. Boucher, R. M., and A. L. Weiner. Foam Control by Acoustic and Aerodynamic Means. British Chemical Engineering. 8:808-812, December 1963.

16. Personal communciation. Branson Ultrasonics Co. October 1975.

17. McCabe, W. L., and J. C. Smith. Unit Operations of Chemical Engineering. New York, McGraw-Hill, 1967, p. 217.

18. Goldberg, M., and E. Rubin. Mechanical Foam Breaking. Ind. and Eng. Chemistry Process Design and Development. 6(2):195-200, April 1967.

19. Rubin, E., and M. Golt. Foam Breaking with a High Speed Rotating Disk. Ind. and Eng. Chemistry Process and and Development. 9(2):341-344, April 1970.

20. Liu, B. Y. H., R. N. Berglund, and J. K. Agarwal. Experimental Studies of Optical Particle Counters. Atmospheric Environment. 8:717-732, July 1974.

21. Liu, B. Y. H., K. T. Whitby, and Y. H. Pui. A Portable Electrical Aerosol Size Analyzer for Size Measurement of Submicron Particles. (Presented at the 66th Annual Meeting of the Air Pollution Control Association. Chicago. June 23, 1973), 15 p.

22. Quon, J. E., and R. A. Phillips. A Laboratory Investigation of a Foam Phase Air Cleaning Device. (Presented at the 148th National Meeting of the American Chemical Society. Chicago. September 1964), 15 p.

23. Willeke, K., K. T. Whitby, W. E. Clark, and V. A. Marple. Size Distributions of Denver Aerosols - A Comparison of Two Sites. Atmospheric Environment, 8:609-633, June 1974.

APPENDIX A

DETERMINATIONS OF FOAM BUBBLE SIZE

The theoretical deviations for particle collection indicated that the bubble size is a very influencing parameter for particle collection efficiency. Therefore, there was a need to define the foam bubble size in order to investigate the conditions under which fine bubble foams can be generated.

The foam bubble size determinations were made using a photographic technique. In order to eliminate optical distortion of curved pipe wall we have designed a plexiglass pipe element which has a flat viewing section. All our bubble size measurements were made using this section and through flat plexiglass. Photographs were taken with a 35 mm camera fitted with an extension tube attachment for close-up photography to measure approximately 1 mm bubbles. A series of shots were required at various lighting conditions to determine optimum light conditions for bubble resolution. Each photo was evaluated by the random selection of 10 bubbles. These 10 bubbles were measured and their mean volumetric diameter calculated. This was accomplished by converting the 10 measured diameters to volume figures (assuming spherical bubbles) and then averaging these for a mean volume. The mean volume was then converted back to a mean volumetric diameter.

Early work on bubble size involved experiments which should establish the influencing parameters on bubble size. Parameters investigated were air flow rate, liquid flow rate, surfactant type and concentration, and screen mesh size. The results of our experiments are presented in Table A-1.

Several general trends can be observed from data in Table A-1. The dependence of air flow rate on bubble size can be

Preceding page blank

Table A-1. MEAN BUBBLE DIAMETER FOR VARIOUS FLOW CONDITIONS

Surfactant		Flow rates		Liquid gas ratio, $cm^3/m^3 \times 10^{-3}$	Screen mesh size	Mean volumetric bubble diameter (mm)
Concentration, %	Name	Water cm^3/s	Air $m^3/s \times 10^{-3}$			
4	Tergitol	18.08	1.076	16.8	250	0.84
4	"	11.42	1.076	12.6	250	0.87
2	"	18.08	1.076	16.8	250	0.94
1	"	11.42	1.076	10.6	250	1.10
1	"	11.42	1.680	6.8	250	0.91
1	"	11.42	2.320	4.9	250	0.82
1	"	18.08	0.077	23.5	250	1.09
1	"	18.08	1.076	16.8	250	0.99
1	"	18.08	1.350	13.4	250	0.92
1	"	18.08	1.680	10.8	250	0.79
1	"	18.08	2.001	9.0	250	0.77
1	"	18.08	2.320	7.8	250	0.74
1	"	20.70	1.076	19.2	250	0.92
1	"	15.30	1.076	14.2	250	0.93
1	"	10.05	1.076	9.3	250	0.93
1	"	4.80	1.076	4.5	250	0.94
0.5	"	18.08	1.076	16.8	250	1.01
1	Aerosol	18.08	1.076	16.8	250	0.85
1	Aerosol	18.08	1.680	10.8	250	0.81
1	Aerosol	18.08	2.320	7.8	250	0.77
2	Sterox	18.08	1.076	16.8	250	0.90
1	Sterox	18.08	1.076	16.8	250	0.99
1	Sterox	18.08	1.680	10.8	250	0.94
1	Sterox	18.08	2.320	7.8	250	0.89
2	Alkanol	18.08	1.076	16.8	250	0.70
1	Alkanol	18.08	1.076	16.8	250	0.83
1	Alkanol	18.08	1.076	16.8	250	0.76
1	Tergitol	11.42	1.076	10.6	60	2.94
1	Tergitol	11.42	1.680	6.8	60	2.58
1	Tergitol	11.42	2.320	4.9	60	2.54
1	Tergitol	18.08	1.076	16.8	350	0.76
1	Tergitol	18.08	1.680	10.8	350	0.62
1	Tergitol	2.320	2.320	7.8	350	0.66

demonstrated by Figure A-1. The curve indicates that the mean bubble diameter decreases with an increasing air flow rate. As lone as the foam generation screen is maintained properly wet, the increased water flow rate seemed to decrease the mean air flow rate bubble size. This effect, however, appeared rather insignificant and very much within the experimental error of foam bubble size determinations. The screen has been observed to be the most critical parameter affecting bubble size. A 60 x 60 mesh screen under stable condition produced foam with bubble diameter of about 2.5 - 3 mm. A 250 x 250 mesh screen produced foam of about 1 mm diameter, and 350 x 350 mesh screen produced bubbles about 0.7 mm in diameter. The effect of screen size on the foam bubble size is represented by Figure A-2.

Figure A-3 shows the effect of surfactant concentration on bubble size. An increasing concentration of Tergitol tends to reduce the mean bubble size. An additional effect of surfactant concentration was observed at low surfactant concentrations (about 0.1%). At these low concentrations the foam is unstable or marginally stable and the bubbles tend to be much larger than when higher surfactant levels are used and stable foams are produced. No further investigation of these marginal conditions was made since large bubble foams were of no interest to this program.

In conclusion, the most directly influencing parameters on bubble size are air flow rate, surfactant concentration, and the screen size. However, only the screen size changes the bubble size significantly (factor of 5) while the flow rate and surfactant concentration exhibit less significant (about a 10 - 20%) change in bubble size.

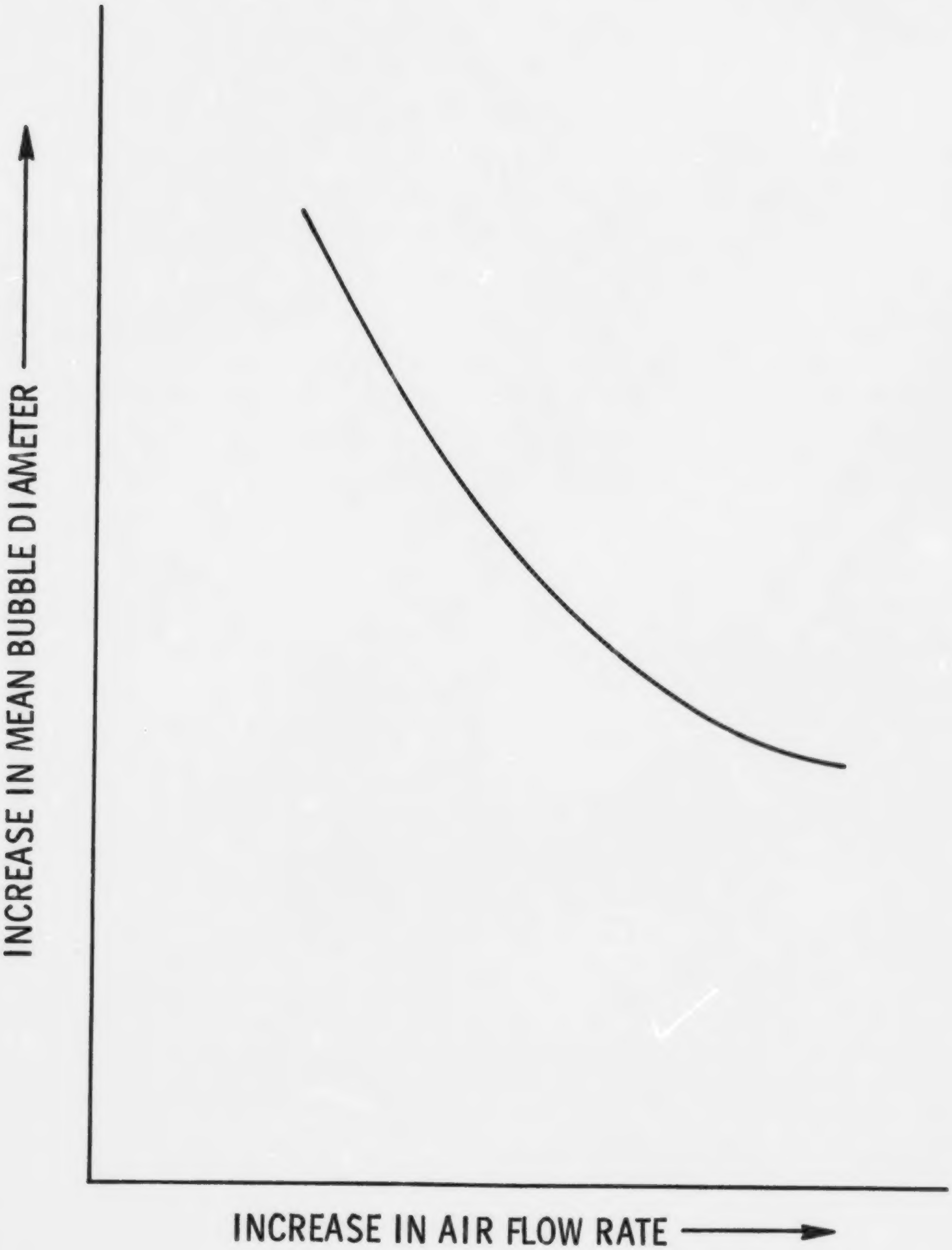

Figure A-1. Bubble diameter versus air flow rate observed for 1% Tergitol foam.

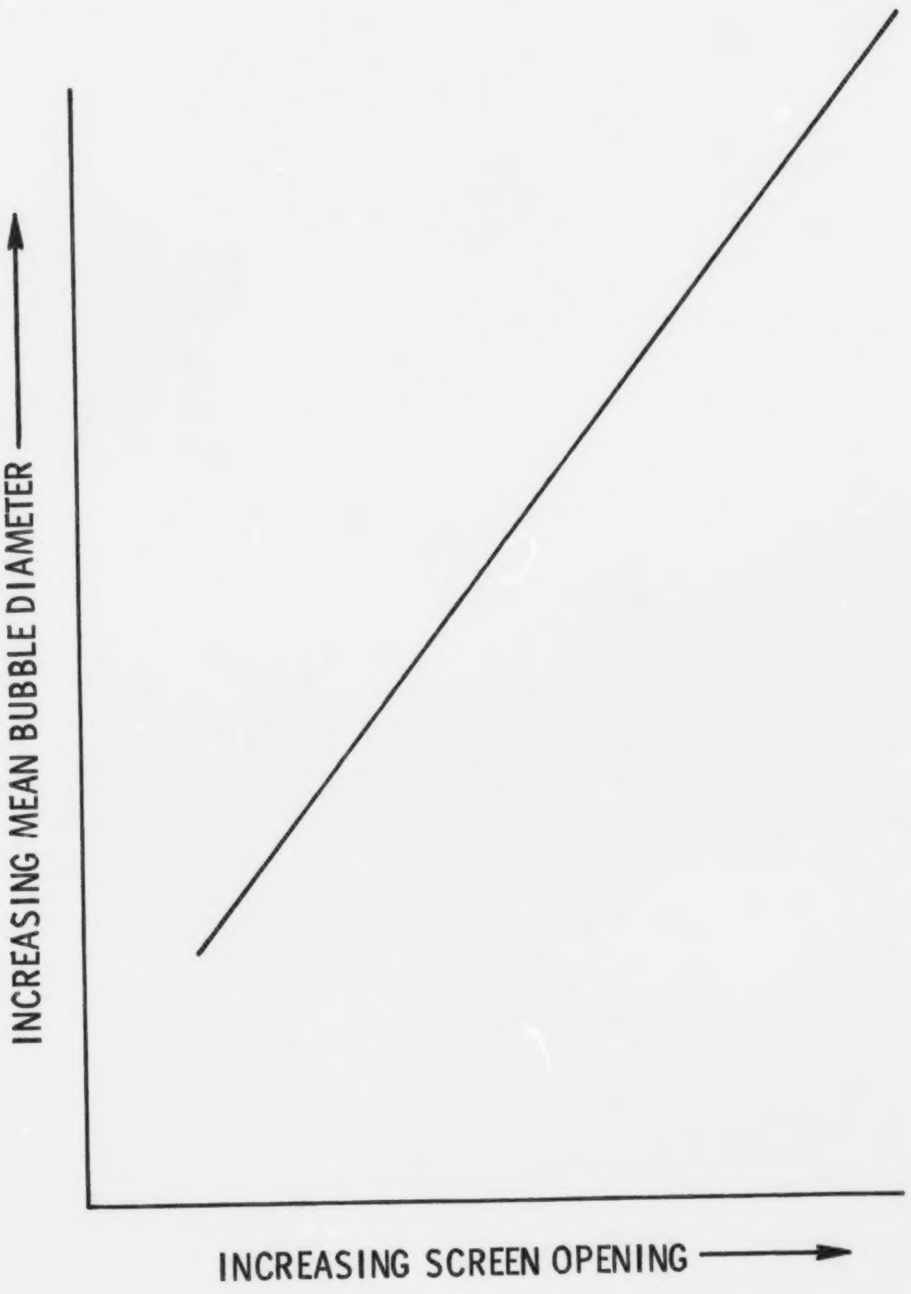

Figure A-2. Bubble diameter versus screen opening for 1% Tergitol foam constant air and liquid flow.

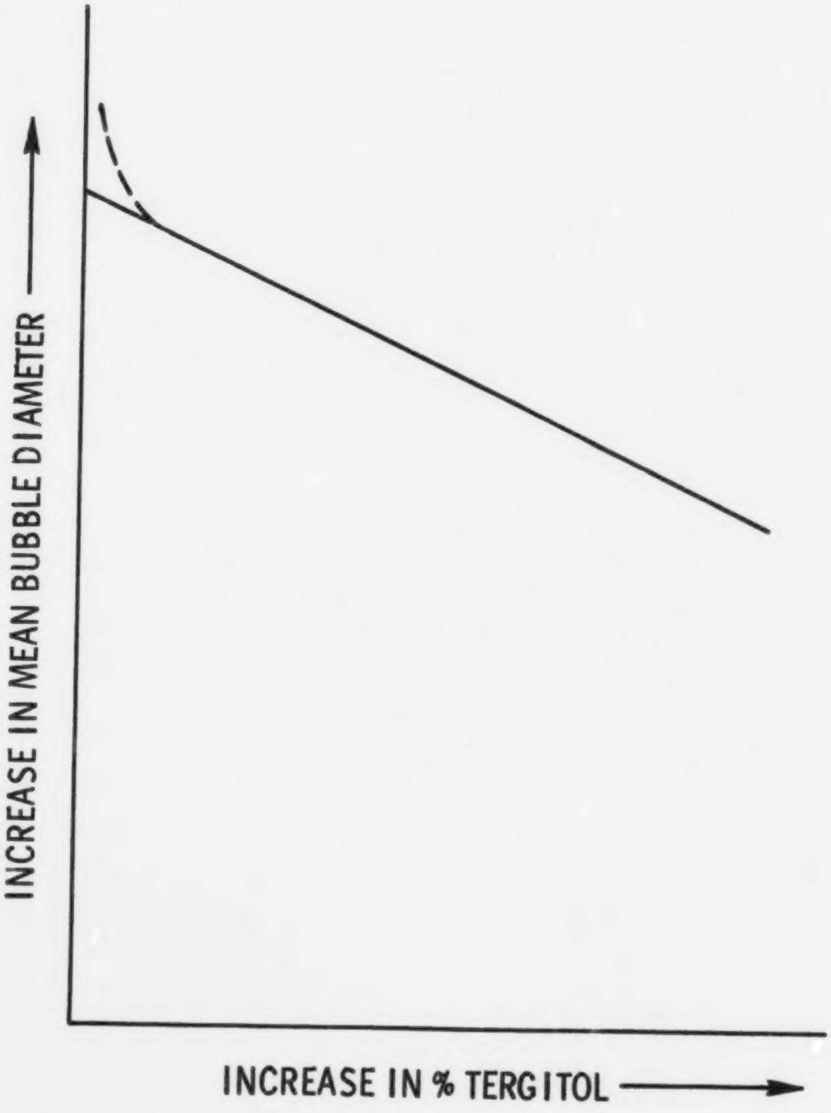

Figure A-3. Bubble diameter versus surfactant concentration.

In the later part of the program we were able to improve the technique of foam generation to an extent that much lower liquid flow rates were needed to produce foams of satisfactory stability. This was accomplished mainly through the physical position of the liquid spray nozzle in relation to the foam generation screen. The position of the nozzle was adjusted manually on the "try and see" basis. With the nozzle in certain positions a uniform and stable foam was produced. We feel that this position was in the exact center of the duct with the nozzle spray pattern covering the whole screen. Exact measurements of the nozzle positions were not made because of the limited access to the nozzle location.

The measurements of foam bubble size were repeated with the reduced liquid flow rates and the data obtained suggest that the position of the spray nozzle can significantly influence the foam bubble size as well as its stability. Table A-2 summarizes the results determined under specific operating conditions. Comparison of the data in Tables A-1 and A-2 will indicate the significance of nozzle position on the foam characteristics. Even though correlating the data from both tables may lead to some discrepancies, general trends between air flow rate, surfactant concentration, screen size, and foam bubble size discussed earlier in this appendix are believed real since they were gotten with the spray nozzle in a specific position. Examples of typical photos used to determine foam bubble size are shown in Figure A-4.

One weakness of the correlations and data presented here is that the foam was photographed through the plexiglass wall and only the bubbles against the wall could be analyzed. The validity of the results therefore rests mainly in indicating the foam bubble size range as well as the influencing bubble size. Assuming that the bubbles on the duct walls

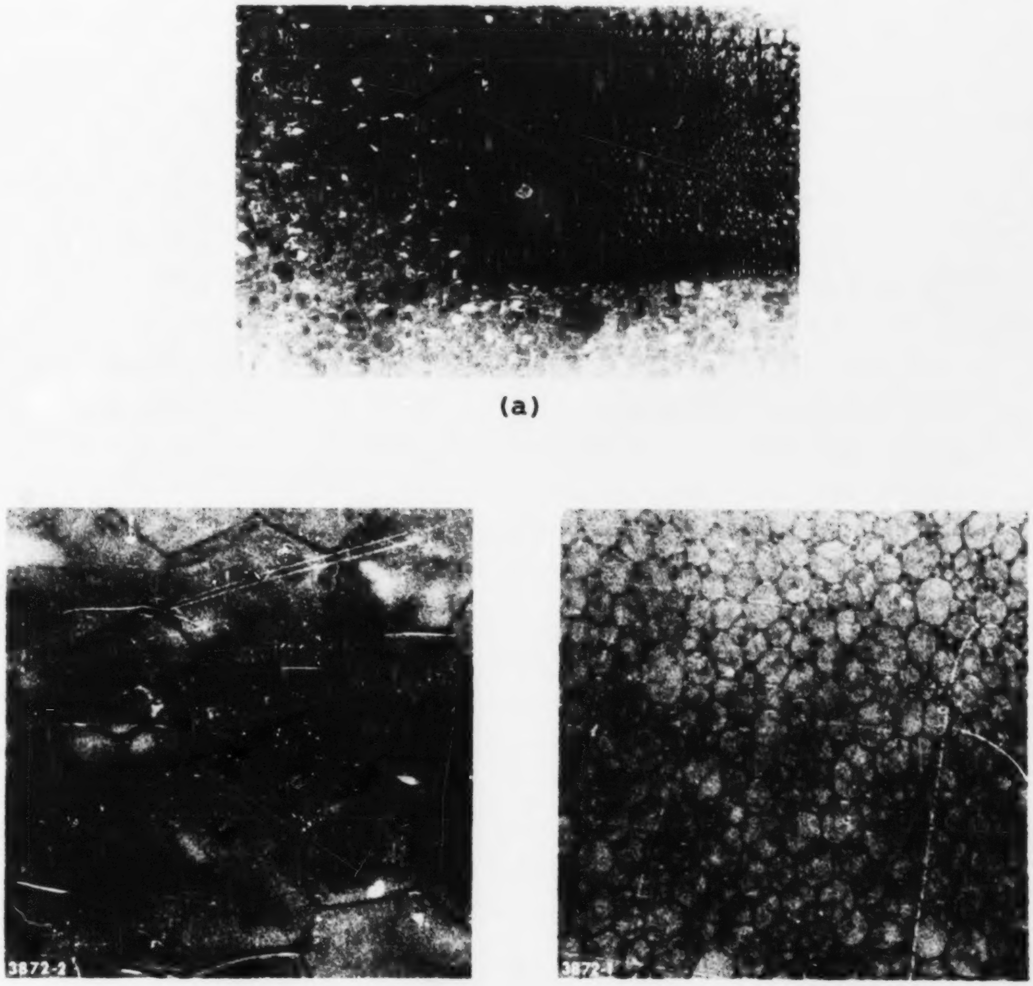

(a)

(b)

(c)

(a) Tergitol foam, 1% solution; air flow 1.076 x 10^{-3} m^3/s; liquid flow 11.4 cm^3/s; 250 mesh screen; volumetric mean bubble diameter 1.10 mm; scale graduated in fractions of an inch

(b) Tergitol foam, 2% solution; air flow 1.137 x 10^{-3} m^3/s; liquid flow 5.83 cm^3/s; 60 mesh screen; volumetric mean bubble diameter 3.90 mm

(c) Tergitol foam, 1% solution; air flow 1.137 x 10^{-3} m^3/s; liquid flow 5.83 cm^3/s; 250 mesh screen; volumetric mean bubble diameter 0.84 mm

Figure A-4. Photos of foam for bubble size determinations

Table A-2. BUBBLE SIZE OF FOAM GENERATED WITH TERGITOL[a]

Percent Tergitol	Screen size	Arithmetic mean bubble size, mm	Bubble size range, mm
1	250 mesh	0.84	0.60 - 1.10
2	250 mesh	0.82	0.65 - 1.05
2	325 mesh	0.72	0.40 - 1.05
2	60 mesh	3.90	3.00 - 4.60

[a] Water flow 5.83 cm^3/s; air flow 1.137×10^{-3} m^3/s (38.4 gal/1,000 acfm).

are same or proportional in size to the bubbles in the main foam flow the correlations would have broader application. Th evaluations of qualitative and quantitative differences between the bubbles on the wall and in the main stream were not the objective of this program and would probably require very sophisticated experiments and a separate research effort. It has been observed that during high flow rates the bubbles in the vicinity of the wall exhibit laminar flow while those in the center of the flow regime may exhibit turbulent flow. The turbulence then results in coarser bubbles which migrate to the center of the flow regime. The correlations presented, however, were based on no significant turbulence observed in the foam flow. Additional discussion of foam turbulence is presented in Appendix B.

APPENDIX B

TURBULENT FLOW OF FOAM

The minimum air velocity required for foam formation was empirically determined using the bench scale scrubber with the 250 mesh screen. The air flow was first turned off and then the water sprayed onto the screen. The air flow was very gradually increased until foam formation was just observed across the entire screen face. At this air flow rate the foam was clearly exhibiting plug flow. A slight variation was observed with the various surfactants. However, no variation was seen by varying the water delivery rate which is in agreement with our observations relative to the negligible influence of liquid flow on bubble size. This is probably because the excess water simply drains off the screen. The measurements of minimum air velocities are presented below.

Surfactant	Water flow rate	v minimum
1% Tergitol	11.42 cm^3/s	2.03×10^{-2} m/s (4 ft/min)
1% Tergitol	18.08 cm^3/s	2.03×10^{-2} m/s (4 ft/min)
1% Alkanol	11.42 cm^3/s	2.54×10^{-2} m/s (5 ft/min)
1% Aerosol	11.42 cm^3/s	2.34×10^{-2} m/s (4.6 ft/min)

It has been observed that the air flow has an effect on the bubble size uniformity. An air flow of 1.076×10^{-3} m^3/s (2.28 cfm) with a 1% Tergitol solution spray produces a reasonably uniform bubble size across the flow patterns (see Figure B-1a). A 2.317×10^{-3} m^3/s (4.91 cfm) flow rate with the same solution gives a large number of coarse bubbles in the center of the flow with the coarser bubbles being primarily in the more turbulent section of the flow and the smaller bubbles accumulating in the laminar flow near the wall (Figure B-1b). The Reynolds numbers for the air flow

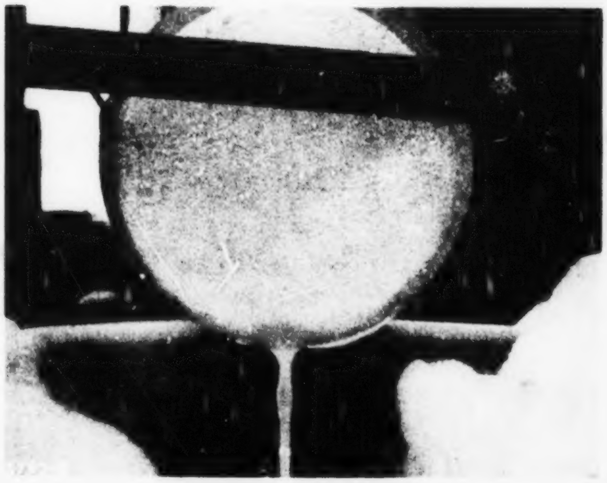

Figure B-1a. Air flow,
1.076×10^{-3} m^3/s (2.28 cfm)
1% Tergitol

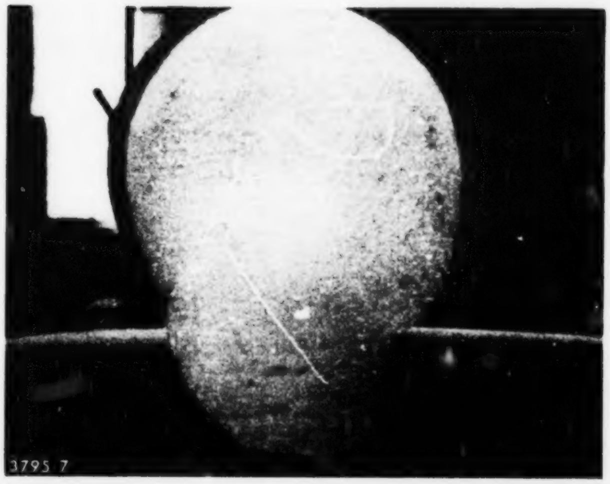

Figure B-1b. Air flow,
2.317×10^{-3} m^3/s (4.91 cfm)
1% Tergitol

at 1.076 x 10^{-3}, 1.685 x 10^{-3}, and 2.317 x 10^{-3} m^3/s (2.28, 3.57, and 4.91 cfm) are 8,840, 13,430, and 19,100, respectively. All of these values are in the transition region considering gas flow. Our observations of foam flow at 2.317 x 10^{-3} m^3/s (4.91 cfm), however, revealed significantly more turbulence in the center of the flow than that observed with 1.076 x 10^{-3} m^3/s (2.28 cfm) flow.

Similar phenomena were observed for the other surfactants except the Alkanol DW. At the 2.317 x 10^{-3} m^3/s (4.91 cfm) flow rate as well as the 1.076 x 10^{-3} m^3/s (2.28 cfm) flow rate, Alkanol exhibits uniform, consistent bubbles across the flow field (see Figures B-2a and B-2b). This foam tends to be more stiff and rigid. In effect it seems to exhibit a higher bulk foam viscosity. Readings were taken to several foams with a Brookfield FVT viscometer and the values are presented graphically in Figure B-3. The results of viscosity measurements indicate that the Alkanol foams are more viscous than the other foams at a 1% concentration. The values of viscosity are relative only and are not meant to be a determination of absolute foam viscosity. The apparent foam viscosity in Figure B-3 appears as a strong function of rate of shear indicated by the rotational speed of the viscometer plate.

This phenomenon is in agreement with the findings of others, e.g., Mahalingam who observed that foam viscosity is characteristically non-Newtonian and increases with decreasing shear rate.[12] Since these viscosity measurements were not considered absolute and are a function of shear they were

---

[12] Mahalingam, R., H. S. Surate, and J. A. Brink, Jr., High Expansion Foam Flow Analyses. Washington State University. (Presented at the AIChE 78th National Meeting. Salt Lake City. August 1974.) 34 p.

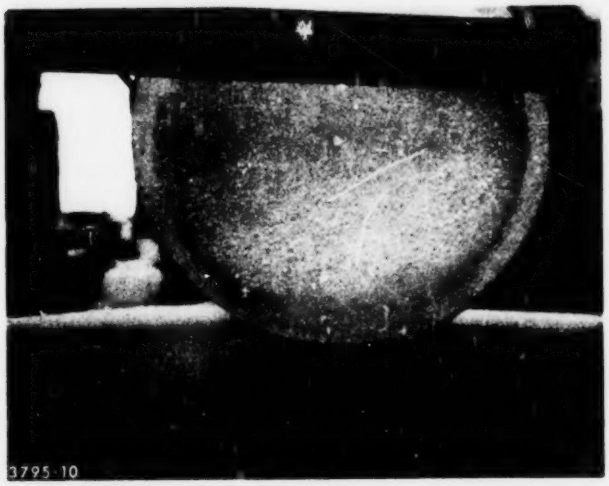

Figure B-2a. Air flow,
1.076×10^{-3} m^3/s (2.28 cfm)
1% Alkanol

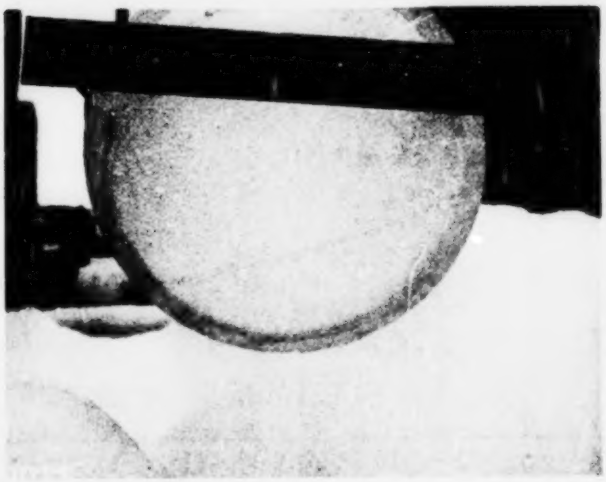

Figure B-2b. Air flow,
2.317×10^{-3} m^3/s (4.91 cfm)
1% Alkanol

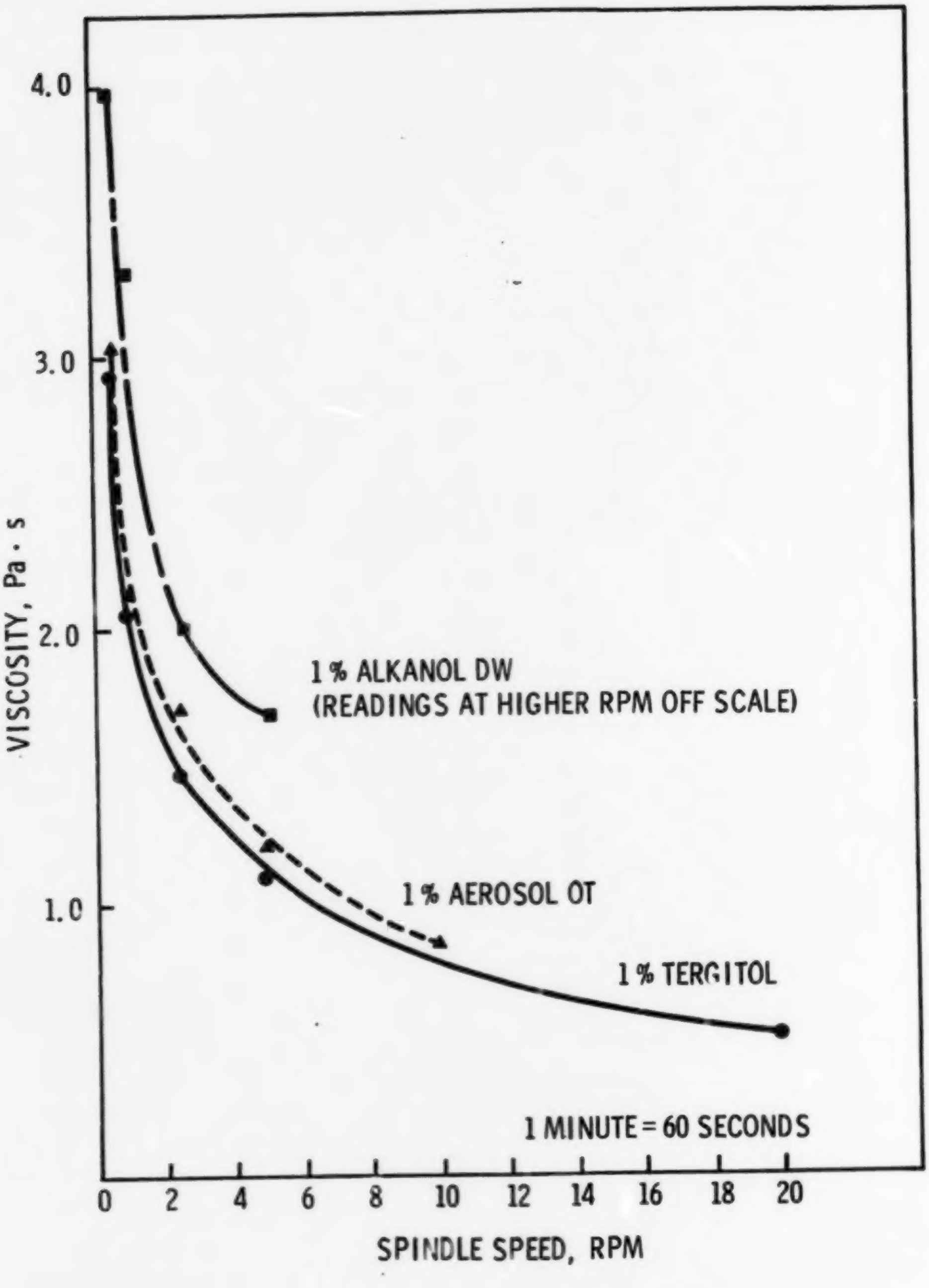

Figure B-3. Foam viscosity measured on Brookfield viscometer.

not included in the Reynolds number calculations mentioned above.

Measurements were taken to determine the minimum air velocity at which the turbulence effect (the presence of large coarse bubbles in the foam) is observed. The data are given in Table B-1. As the air flow rate is increased the turbulence effect becomes more pronounced, i.e., the coarse bubbles become larger and more frequent. The method for the threshold velocity determination is described below.

The water flow rate was held constant at 18.08 cm^3/s (1,085 ml/min), and the surfactant concentrations varied between 0.5% and 4%. The air flow rate was gradually incrementally increased until turbulence developed. It should be pointed out that this is not a sharply defined point but rather the beginning of a transition region. It should also be noted that even at low flow rates some surfactants exhibit a certain amount of large bubbles while others do not. Alkanol appears also to be superior to the other surfactants in its resistance to large bubble formation.

The validity of the data presented in this appendix is in the observation of two gas velocities which determine the range of optimum foam generation. The minimum velocity is required to produce uniform foam of satisfactory quality and has been theoretically defined as the velocity needed to detach a bubble from the generation screen. As the velocity increases, more and more turbulence is observed in the nucleus of the flow which results in coarse bubble formation. The latter phenomenon is further complicated by higher shear forces which reduce the apparent foam viscosity and produce flow with a higher Reynolds number.

Table B-1. THRESHOLD AIR FLOW RATES

Surfactant	Concentration, %	Threshold air flow rate	
		$m^3/s \times 10^{-3}$	cfm
Tergitol TMN	0.5	Very low	
	1	1.298	2.75
	2	1.519	3.22
	4	1.822	3.86
Aerosol OT	0.5	1.345	2.85
	1	1.68	3.57
	2	1.519	3.22
	4	1.217	2.58
Sterox NM	0.5	1.076	2.28
	1	1.345	2.85
	2	1.68	3.57
	4	1.68	3.57
Alkanol DW	1	2.66	5.65

APPENDIX C

FOAM STABILITY

The foam stability is an important variable affecting the overall performance of the scrubber. The foam must resist any destructive interaction of particulates and any tendency for the individual cells to destruct and coagulate into larger cells during scrubber operation. At the same time, it is desirable to operate the scrubber at a minimum surfactant concentration to minimize destruction requirements and surfactant costs.

Several techniques to measure foam stability were examined in order to evaluate this important property of foam. These techniques included the static measurements in a graduated cylinder and foam destruction using a water spray. Both of these techniques were found to have some limitations as to their applicability to foam conditions existing in the foam scrubber. A method involving destruction of foam using sand was devised and felt to be sufficiently independent of other variables influencing foam stability measurements. A detailed discussion of the results interpretation is presented here.

Most classical studies on foam stability have investigated broad classes of foaming agents and involved filling a container with foam and measuring the volume change with time as the foam collapsed.[13] Two methods can be employed here: (1) covering the top of the container to eliminate the evaporative effects, and (2) allowing the container to remain open. The second method is based on the convective and evaporative destruction on the foam surface. These are stability measurements under essentially static conditions as opposed to flow in a pipe where the foam is subject to a more dynamically changing environment.

---

[13] Bikerman, J. J. Foams. New York, Springer-Verlag, 1973. 337 p.

The ideal method of measuring the stability for our purpose would be to have an infinitely long pipe and simply record the time required for a significant amount of foam destruction. Since this is not a practical method much effort was expended attempting to statistically measure the stability of the foams produced and correlate the measured values with observations of foam flow in our bench scale scrubber.

The foam was first put into a 1,000 cm^3 graduate (this is only slightly more difficult than putting the toothpaste back in the tube). The graduate was then covered with a dampened cloth to eliminate any external effect. Gravitational effects gradually caused the water to drain from the bubble walls and collect in the bottom of the graduate. Some typical drainage curves for Tergitol are presented in Figure C-1. The foam soon resembles a shadowy sheath of entangled surfactant molecules. The stability in this case is probably dependent on intermolecular forces, and the degree of molecular entanglement. The destruction observed did not proceed at a consistent rate and large sections of the foam mass would suddenly destruct as if by an explosion.

Using this technique a reasonable degree of reproducibility was achieved with Tergitol and the values indicated that higher surfactant concentrations tend to increase the stability; this is what was observed in the flowing foam. For Aerosol OT, however, the reproducibility was much less, and a 0.1% foam which was very marginally stable for foam production gave a static stability reading of greater than

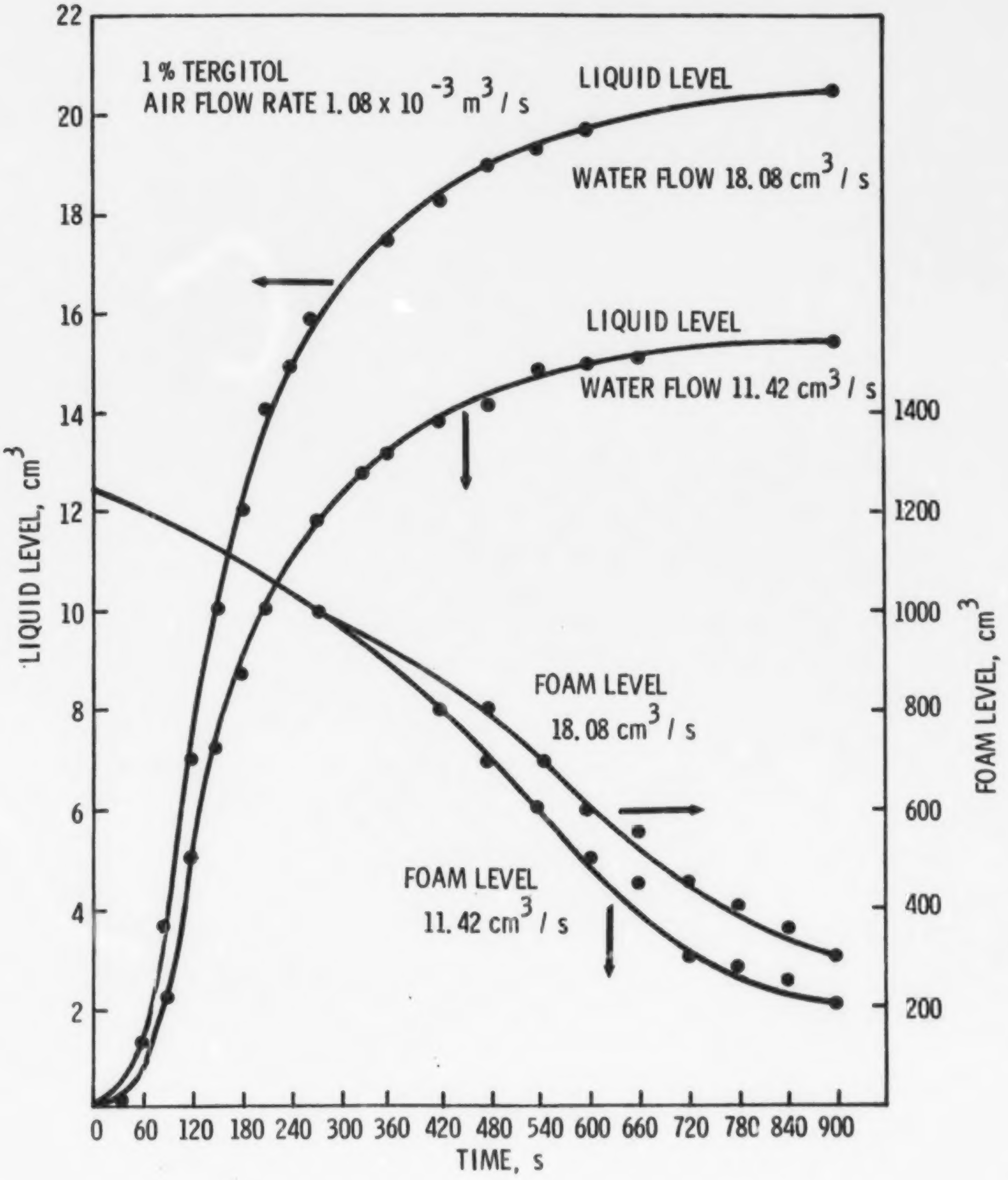

Figure C-1. Foam drainage rates.

5,400 seconds (90 minutes) with negligible destruction. A 1% solution of Aerosol on the other hand which is adequately stable for foam production required 600 - 1,200 seconds (10 - 20 minutes) for 500 cm^3 of foam loss. From the experimental results determined for destruction of 500 cm^3 of foam and summarized in Table C-1, it was felt that this method of measuring the stability did not correlate well with what is observed in foam production. More than one value presented in Table C-1 indicates duplicate runs.

It was attempted to measure the stability by leaving the top of the graduate open to the air and in some cases blowing air into the graduate. The results achieved were similar to those described above. Foams which were not adequately stable for tube flow exhibited the same or higher readings as foams which were stable enough.

It was decided to abandon measuring the stability under essentially static conditions and to look for a method which measured the foam's resistance to destruction by external forces. A new method was devised. A 0.21 m^3 (55 gallon) container with a bottom drain was filled with foam which was destroyed to 0.10 m^3 (25 gallon) level with a hand operated water spray. The time required to accomplish this was recorded as a measure of foam stability. The results also presented in Table C-1 (dynamic stability) were reproducible within several seconds and seemed to correlate well with foam behavior observed under flowing conditions.

The experimental data also indicate that increased surfactant concentration, increased foam wetness, and a decreased bubble size all tend to increase foam stability. Measurements with the 250 mesh screen indicate that a stability reading of approximately 40 - 60 seconds is required for stable foam

Table C-1. RESULTS OF EXPERIMENTAL MEASUREMENTS

Surfactant	Air flow rate $m^3/s \times 10^{-3}$	Air flow rate cfm	Water flow rate cm^3/s	Expansion ratio cm^3/g	Static stability seconds	Dynamic stability seconds	Comments
0.1% Tergitol							Stable foam not formed
0.5% Tergitol	1.076	2.28	10.08	89	312,315	21	Foam marginally stable bubbles 5mm - 10 mm
	1.68	3.57	10.08	99.5	420,432		
	2.32	4.91	10.08	130	330,345		
	1.076	2.28	11.42	107	258,270		
	1.68	3.57	11.42	121	312,333		
	2.32	4.91	11.42	149	375,480	18.5	
1% Tergitol	1.076	2.28	10.08	65	450,576	58,53	Approx 1 mm bubbles stability adequate
	1.68	3.57	10.08	90	510,516	44,45	
	2.32	4.91	10.08	123	630,555	45,53	
	1.076	2.28	11.42	84	396,375	42,41	
	1.68	3.57	11.42	138	420,390	38,37	
	2.32	4.91	11.42	192	456,492	37,39	
2% Tergitol	1.076	2.28	10.08	66	576	85,84	
	1.68	3.57	10.08	83	636		
	2.32	4.91	10.08	120	600		
	1.076	2.28	11.42	83.5	492		
	1.68	3.57	11.42	132	510		
	2.32	4.91	11.42	102.5	495	60,55	
5% Tergitol	1.076	2.28	10.08	--	--	135	
1% Tergitol (60 mesh screen)	1.076	2.28	11.42	132	--	21	Bubbles approximately 5mm - 10 mm in diameter
	1.68	3.57		157.5		20	
	2.32	4.91		194		19	
0.1 Aerosol OT	1.076	2.28	10.08	117	>5400	--	Marginally stable bubbles 5 mm - 10 mm
	1.68	3.57	10.08	132.5	>5400		
1% Aerosol OT	1.076	2.28	10.08	76	660,738	65	Approx 1 mm bubbles stability adequate
	1.68	3.57	10.08	11[illegible].5	1110		
	2.32	4.91	10.08	15[illegible]			
	1.076	2.28	11.42	98	1020		
	1.68	3.57	11.42	145.5	1197		
	2.32	4.91	11.42	205		45	
0.1% Alkanol DW	1.076	2.28	10.08	--	--	--	Stability adequate bubbles 5 mm - 10 mm
1% Alkanol DW	1.076	2.28	10.08	54.2	>5400	240,250	Approx 1 mm bubbles
	1.68	3.57	10.08	98.5	>5400		
	2.32	4.91	10.08	155			
	1.076	2.28	11.42				
	1.68	3.57	11.42				
	2.32	4.91	11.42				
0.1% Sterox NM	1.076	2.28	10.08	--	--	105,106	
	1.68	3.57	10.08			15	Marginal stability very large bubbles
	2.32	4.91	10.08				
1% Sterox NM	1.076	2.28	10.08	--	--	55	Approx 1 mm bubbles stability adequate
	1.68	3.57	10.08				
	2.32	4.91	10.08				
	1.076	2.28	11.42			60	
	1.68	3.57	11.42				
	2.32	4.91	11.42			47	

Note: All data taken with 250 mesh screen unless otherwise stated.

production. The 40 mesh screen, which produced about 5 mm bubbles, exhibited stable foam with only a 20 second spray-down time. One surfactant, Alkanol DW at 1% concentration, gave a foam which was about four times as stable as the other foams at 1%. This foam was so stable we had much difficulty destroying it. This may indicate that the 72% "inactive component" present in Alkanol may not be inactive as far as foam production is concerned. This is particularly interesting since Alkanol, a sodium alkylaryl sulfonate, was chosen because alkylaryl sulfonates are generally thought to be poor-to-medium foaming agents.

Speculating that perhaps foam which is more stable tends to hold the water longer and would exhibit a water drainage rate which is different from a less stable foam, drainage rate curves were prepared for foams of varying surfactant concentrations (see Figure C-2). It is seen that all of the foams exhibit about the same drainage rates in the time periods used in foam scrubbers. Therefore, the drainage rates do not appear to be the influencing factor for the observed differences in foam stability.

The water spray destruction method to determine foam stability became questionable when we had established correlations representing foam stability as a function of surfactant concentration. The foam stability seemed to proportionally increase with the surfactant concentration. This is contrary to the theory since the foam stability should be increasing while the foam surface is being saturated with the surfactant to form a monolayer. Once this phase is reached the foam stability will start to decrease. As a result, the foam stability correlation with concentration should contain a maximum. The proportional dependence of foam stability on the surfactant concentration using water spray for foam

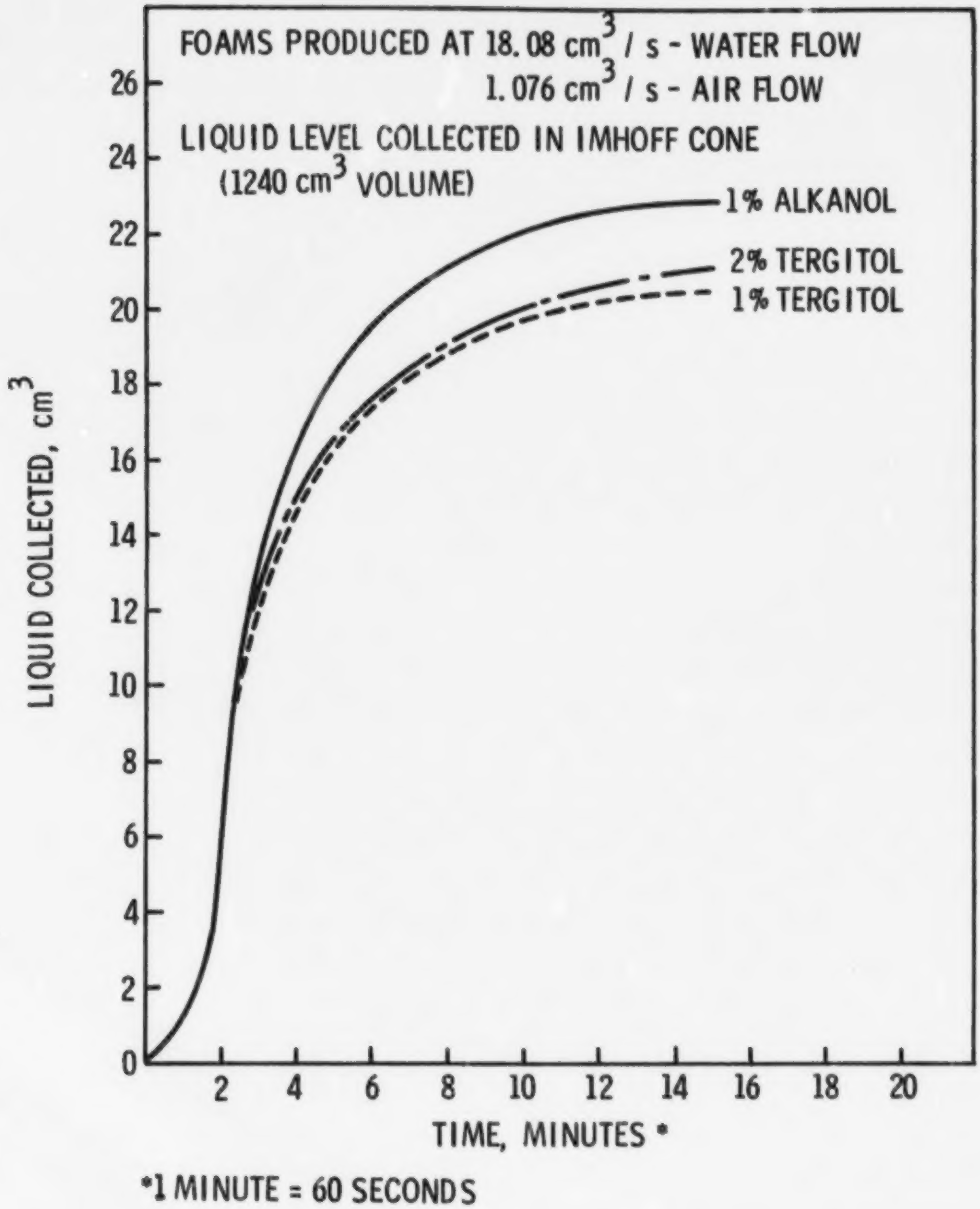

Figure C-2. Drainage rates for foams of varying stability.

destruction is perhaps due to the dilution of surfactant. Considering that there is a certain minimal concentration of surfactant at which the foam is reasonably destroyed with a water spray, the more concentrated foam will require more water to dilute this foam to reach this minimal concentration and a proportional relationship will result.

In order to determine foam stability, a method was needed which would destroy the foam with an inert material, one that does not interact with the foam. Sand was felt to be the most readily available material to satisfy this requirement. Consequently, a method was investigated whereby the sand was sprayed into a 3.8×10^{-3} m^3 (1 gallon) container of foam with a portable hand operated sand blast gun. The sand blast gun used (similar to a paint spray gun) is a Porta-Blast unit made by Lindberg Products Co., Placerville, California. The arrangement of the sand foam destruction method is shown in Figure C-3.

The sand was screened into a uniform fraction with 18 - 20 mesh U.S. Standard sieve screens. The screened sand was held in a separate container and fed into the sand spray by the suction force developed inside the gun. The gun nozzle did not provide a wide enough spray pattern for our purposes. Consequently, a brass pipe fitting was inserted in the gun to make a suitable nozzle and provide a suitable spray pattern. The fitting was 1/4" pipe to 3/8" Swagelok with the swage end outside the gun. The Porta-Blast gun was operated at 6.89×10^4 pascals (10 psig), and 1.12×10^{-3} m^3/s (2.40 cfm). The distance between the nozzle and the container was held at 40 cm and the spray time was fixed at 10 seconds. After spraying, the foam exhibited a level surface and the final height could be measured. The resultant height was reproducible to ±0.25 inch. The sand flow rate was measured and determined to be 4.83 g/s (290 g/min) ±10%.

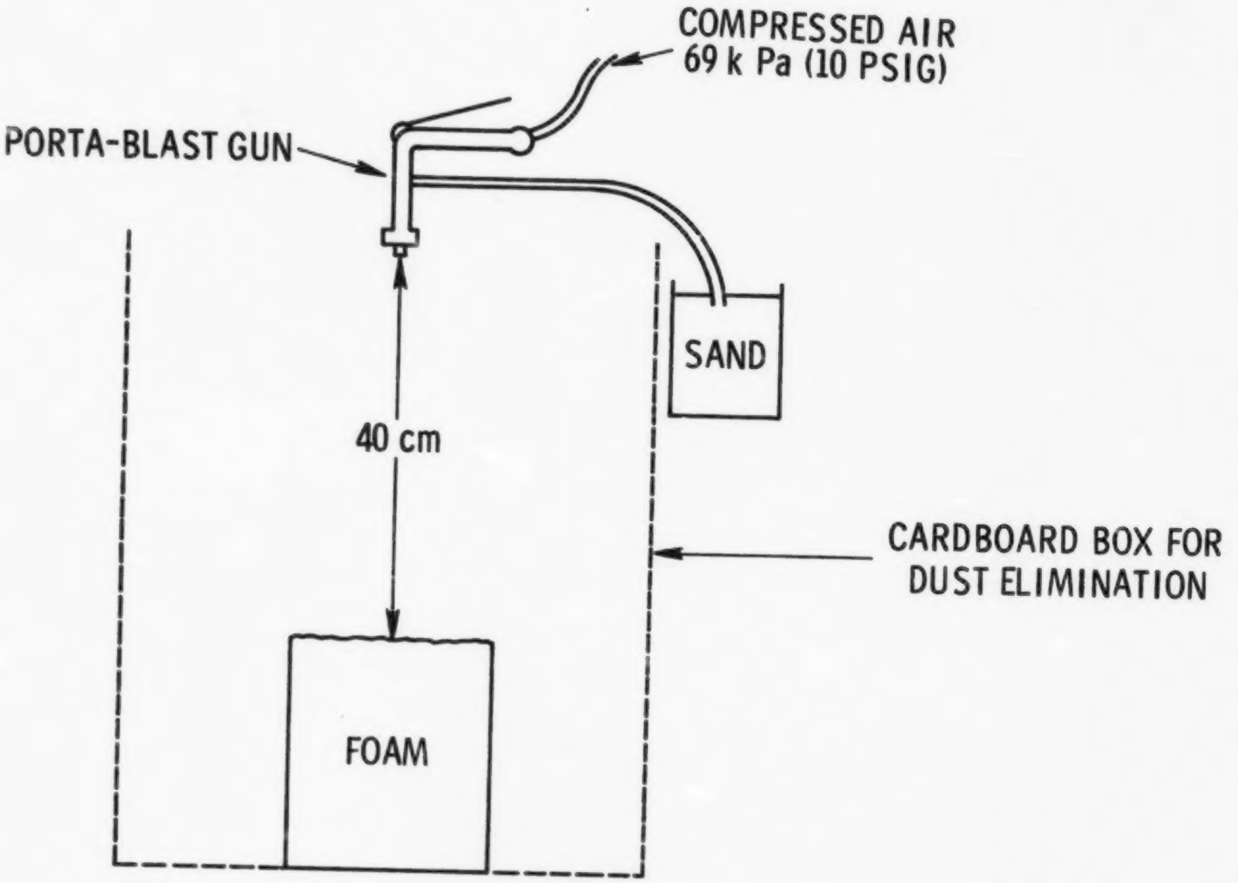
COMPRESSED AIR
69 k Pa (10 PSIG)
PORTA-BLAST GUN
SAND
40 cm
CARDBOARD BOX FOR
DUST ELIMINATION
FOAM

Figure C-3. Portable sand blast device used for foam stability measurement.

Reproducible results were achieved with this method. Visually observed quality of foam in the scrubber correlated well with the results obtained using sand for foam destruction. The resulting stability curve for Tergitol foams is presented in Figure C-4. The stability curve indicates that the Tergitol foam steadily increases in stability up to about 3 - 4% concentration and beyond this the stability levels off. Higher concentrations of Tergitol foams were not investigated since they were considered impractical for foam scrubber application.

We first attempted to uniformly impact the foam with sand by shaking the sand from a screen. This method appeared promising but it would not give consistent reproducible results. Sand was then screened into various uniform fractions using standard sieve screens. The uniform fraction of sand was then placed on the smallest sieve screen which would pass all of the particles and held over the container of foam. The sieve was vibrated with a mechanical vibrator to help insure a uniform delivery rate of sand. Various size fractions of sand were tried and various types of vibrators and shakers were also evaluated with different vibrational frequencies and amplitudes.

The height above the container and the time increment employed were also varied during evaluation of this method. However, the irregularly shaped sand particles tended to clog the sieve and consequently a uniform consistent sand flow rate could not be achieved with this technique. Circular glass beads were also investigated, but they passed easily through the screen without vibration.

It was noticed that foam stability tends to increase significantly with a reduction in bubble size. From purely

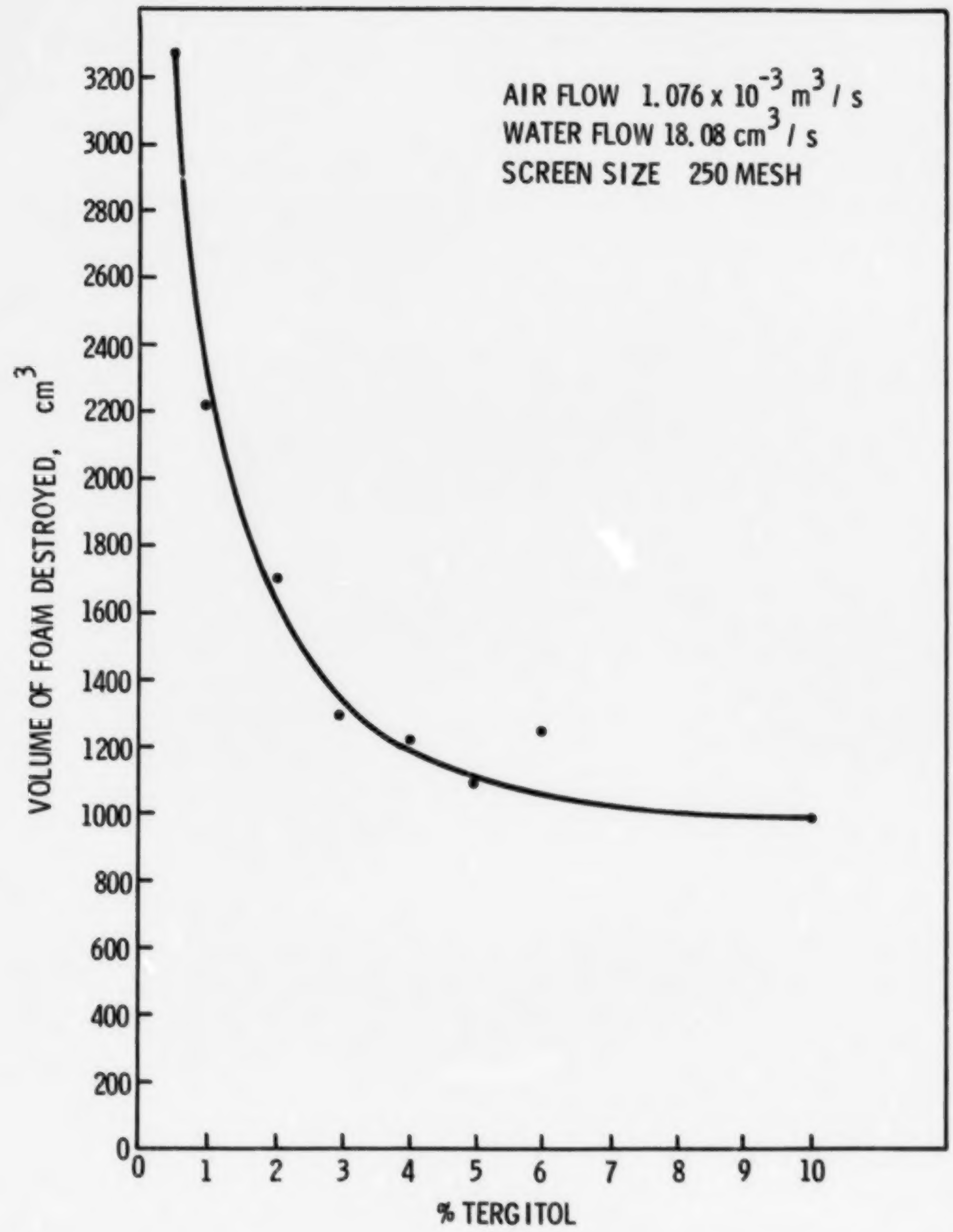

Figure C-4. Stability versus concentration for Tergitol foam.

geometric considerations, a reduced bubble diameter increases the number of cell units which must be destroyed. Table C-2 indicates the bubble volume as a function of bubble diameter. It can be seen that about two thousand 1 mm bubbles are required to occupy the volume of a 1/2 inch bubble or about fifteen thousand 0.5 mm bubbles are needed for the same volume. Smaller bubbles exhibit an increased stability simply because the reduced film area is more resistant to hole initiation.

Table C-2. BUBBLE VOLUME VS. DIAMETER

Bubble diameter		Volume, mm^3	Number of units per cm^3
inches	mm		
1/2	12.7	1,072.53	0.93
1/4	6.35	134.07	7.46
	5	65.45	15.28
1/8	3.17	16.68	59.95
	2.0	4.19	238.6
	1.0	0.52	1,910
	0.5	0.065	15,384

In the latter part of the program we were able to produce foam of sufficient quality for aerosol collection with liquid flow rates as low as 5.83 cm^3/s. Since our previous foam stability measurements did not include this condition, we have obtained additional measurements of the foam stability. As indicated above, in the earlier measurements the foam was destroyed using a 10 second spray of 18 - 20 mesh sand with a portable sandblast gun at 6.89×10^4 Pa (10 psig) with the nozzle placed 40 cm above the foam container. For the new conditions the foam was much less stable and a 10 second spray resulted in a complete destruction of the foam.

Consequently, the spray time was reduced to 5 seconds. The stability curves of the Tergitol foam for three scrubber residence times and three surfactant levels are presented in Figure C-5.

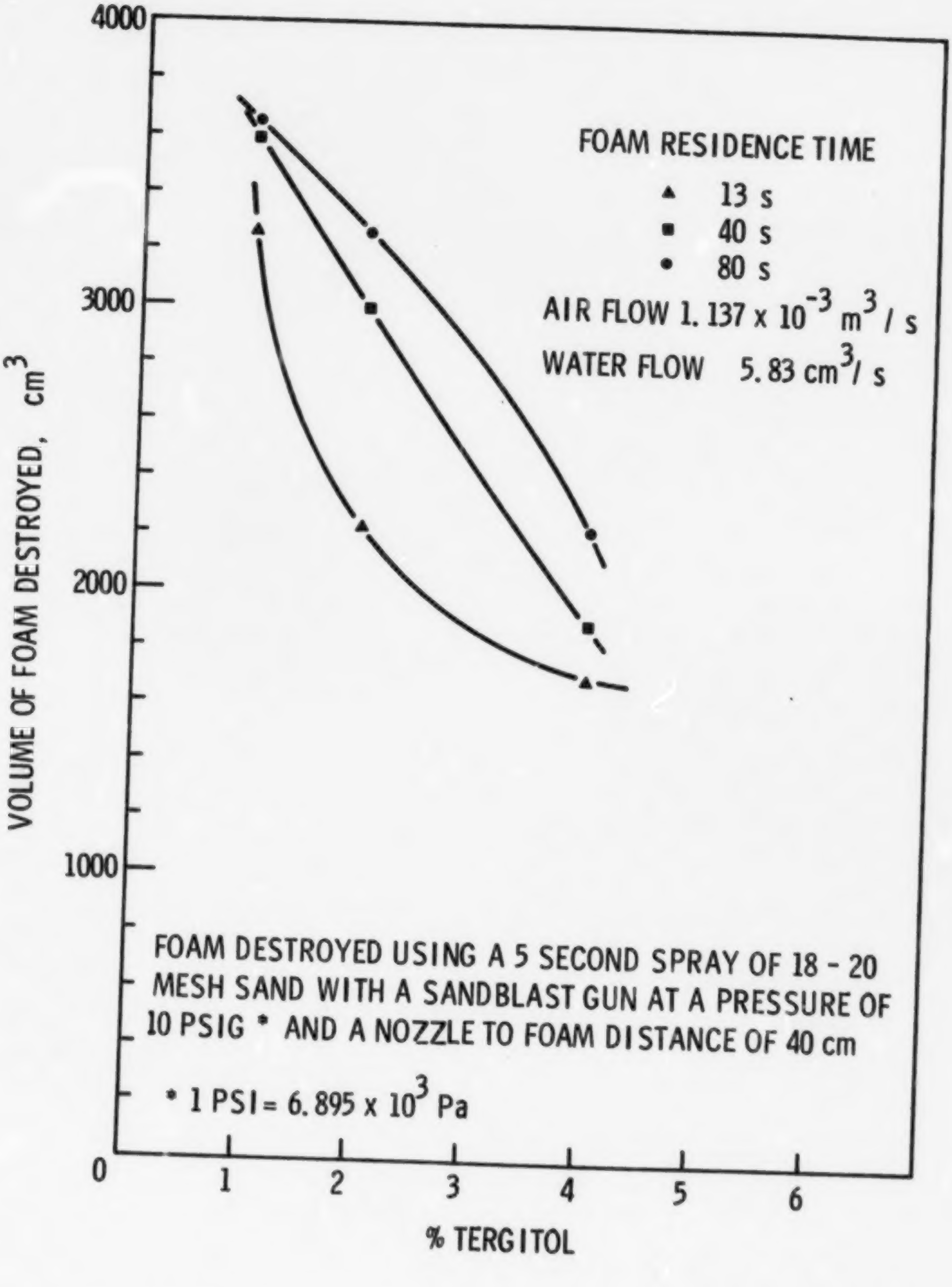

Figure C-5. Stability of foam generated using Tergitol with 250 mesh screen.

APPENDIX D

TECHNIQUES OF FOAM DESTRUCTION

A recycled surfactant solution that is sprayed into the foam can destroy foam.[14] For our purposes it was desired not to dilute the surfactant solution so it could be recycled for reuse. Consequently, a spray method was evaluated using the non-diluted surfactant solution.

The 1% Tergitol solution was fed through a positive displacement pump to a Fulljet spray nozzle (Spraying Systems Co.). The spray nozzle pressure was adjusted to give 5.15 x 10^5 Pa (60 psig). Data for 1% Tergitol foam are presented in Table D-1 and compared with the data obtained with pure water spray.

The data indicate that the recycled solution is not nearly as effective as pure water. It was also observed that the spray method is more effective for less stable foam and would be quite efficient for foam comprised of large, 6 mm or larger, bubbles. An increase in destruction rate is noted for an increased spray rate. The spray appears to destroy the foam easily at first, but as time proceeds the wet solution probably cannot drain off the foam as fast as it is delivered by the spray. Consequently, the spray begins to interact with the very "wet" foam and gives the appearance of generating more foam. In conclusion this method did not appear to be an effective method for foam destruction but it might have some potential for less stable foams or could possibly be used in conjunction with another method.

---

[14] Bransky, D. W., and F. F. Diwoky. Removal of Sulfuric-Acid Fog by Bubble-Phase Absorption. Refiner and Natural Gasoline Manufacturer. 19:191-195, June 1940.

Table D-1. DESTRUCTION WITH KNOCKDOWN SPRAY

Water flow, cm^3/s	Air flow, $m^3/s \times 10^{-3}$	Air flow, (cfm)	Knockdown spray	Knockdown spray flow rate cm^3/s	Spraydown time seconds	Destruction rate $m^3/s \times 10^{-2}$	Destruction rate (cfm)
18.08	1.076	2.28	Pure water	26.66	53,55	2.10	44.5
18.08	1.076	2.28	1% Tergitol	26.66	101,97	1.15	24.3
11.41	2.32	4.91	Pure water	26.66	33,36	3.27	69.7
11.41	2.32	4.91	1% Tergitol	26.66	54.57	2.02	43.3
18.08	1.076	2.78	Pure water	52.92	31,30	3.72	78.9
18.08	1.076	2.78	1% Tergitol	52.92	60,63	1.84	39.1

THERMAL DESTRUCTION

It was felt than an abrupt delivery of thermal energy to the foam might be effective for foam destruction. In our evaluation a ring burner, 0.152 m (6 inches) in diameter, was placed in the foam destruction chamber. A propane bottle was attached to the burner and the regulator adjusted for maximum propane gas flow. The propane gas flow was determined to be 0.166 g/s (10 g/min) by weighing the container before and after the experiment. Assuming complete combustion, the energy input for 10 lb/min of propane is 8,281 W (11.1 hp). The air intake on the burner was adjusted for a completely blue flame. Foam produced from 18.08 g/s of liquid and 1.076 x 10^{-3} m^3/s of air was introduced into the destruction chamber. The foam passed through the center of the flame and enclosed the burner and extinguished the flame. It was observed that as the foam encountered the flame the water was driven off and the dehydrated "foam" was able to encircle the burner. Modifications were made to the burner, such as a metal plate above the flame to deflect the heat down in the foam. Also, holes were drilled in the bottom of the burner to shoot flame down in the foam. These modifications did not significantly alter the results observed before.

A more effective method of thermal foam destruction was found using a steam coil. A 15 m (50 ft) length of 0.63 cm (1/4 inch) copper tubing was coiled into a 0.65 m (25 inch) long pipe section with diameter of 0.15 m (4 inches) and placed inside the destruction chamber. Steam at 1.03 x 10^4 Pa (15 psig) passed through the coil and resulted in a complete destruction of 1% Tergitol foam at an air flow of 1.076 x 10^{-3} m^3/s (2.28 cfm) and a water flow of 18.08 cm^3/s (1,085 ml/s). The condensed steam was collected at a rate of 85 cm^3/min. This corresponds to an energy load of 4.98 hp.

ULTRASONIC DESTRUCTION

The majority of the ultrasonic devices on the market employ the transmission of ultrasonic energy to incompressible materials. Foam by its nature is a compressible substance and in fact foam materials are used as acoustic insulators. Some studies have been done investigating frequencies from 0.7 to 29 kHz/s and intensities up to 150 db by passing air through high frequency horns and whistles.[15] An apparatus of this sort is shown in Figure D-1. The method destroyed foam but the maximum destruction rate achieved was 1.7×10^{-4} m^3/s (0.36 cfm) per 4.7×10^{-4} m^3/s (1 cfm) of air supplied to the sound source. As a result a 1,470 watt (2 hp) compressor would be required to destroy 4.7×10^{-4} m^3/s (1 cfm) of foam. Further evaluation of this approach revealed that the large air flow from the sound source tended to dehydrate the foam in some cases and produce a sticky material creating some operation problem.[16] Also, a soundproof chamber would probably be required for industrial applications. Perhaps a more promising technique to accomplish foam breakage is the use of an air jet as illustrated in Figure D-2.

We have investigated the application of an air jet to foam destruction using Deflectojet 8686-37 nozzle procured from Spraying Systems Company, Figure D-2. This nozzle simulated the flow pattern and the air jet action suggested in reference 15. Using the air jet in our destruction chamber resulted in a complete destruction of 1% Tergitol foam which was produced with a 1.076×10^{-3} m^3/s (2.28 cfm) air flow

---

[15] Boucher, R. M., and A. L. Weiner. Foam Control by Acoustic and Aerodynamic Means. British Chemical Engineering. 8:808-812, December 1963.

[16] Personal communication. Branson Ultrasonics Co. Oct. 1975.

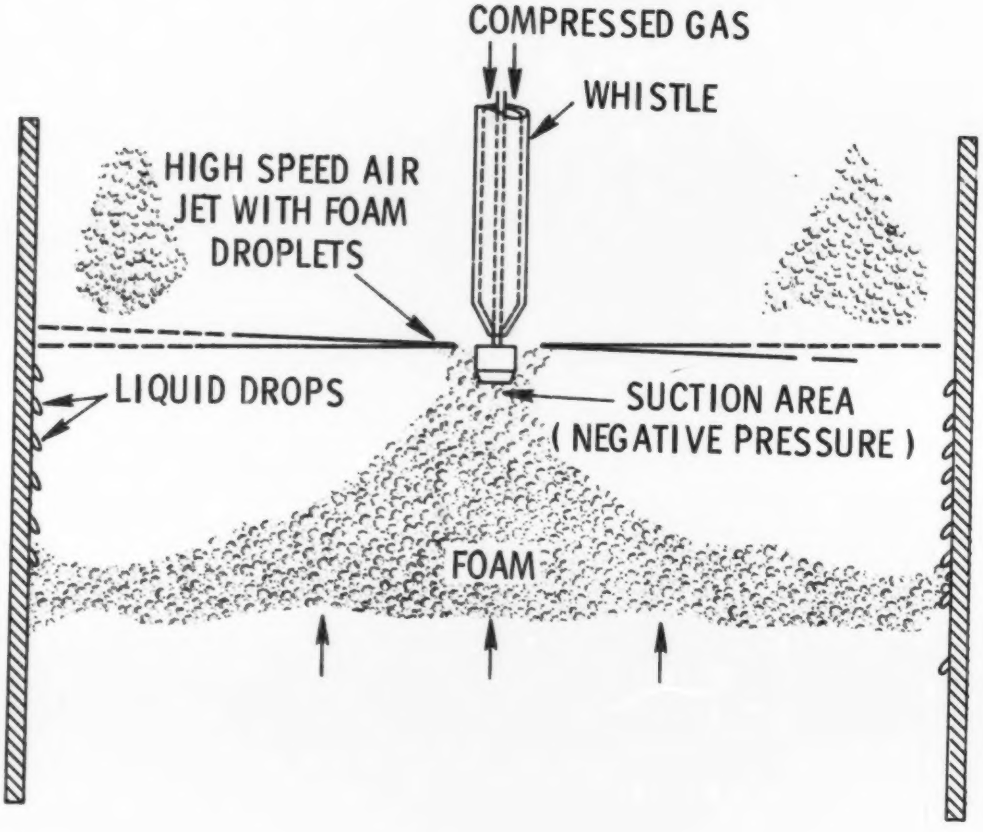
COMPRESSED GAS
WHISTLE
HIGH SPEED AIR JET WITH FOAM DROPLETS
LIQUID DROPS
SUCTION AREA (NEGATIVE PRESSURE)
FOAM

Figure D-1. Air jet whistle used by Branson for foam breakage.

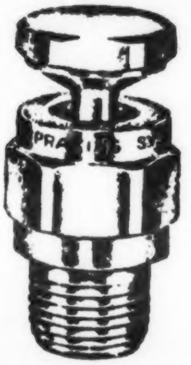

Hollow Cone Spray Pattern

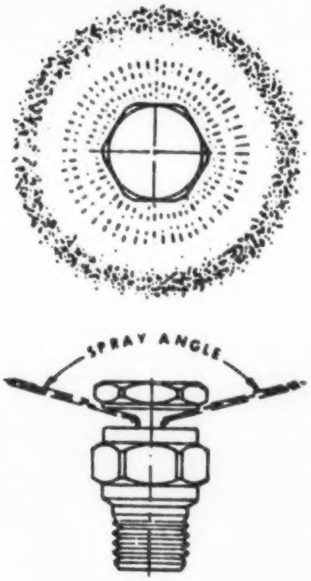

Figure D-2. Deflectojet nozzle from Spraying Systems Company. Nozzle has 180° spray angle.

and 18.08 cm^3/s water flow. The foam rate was gradually increased and at 1.345 x 10^{-3} m^3/s (2.85 cfm) the rate of destruction became slower than the foam flow rate. The air flow through the nozzle at this condition was measured to be 1.16 x 10^{-3} m^3/s (2.45 cfm) at 3.7 kPa (46 psi). This air flow corresponds to a compressor requirement of 261 W (0.35 hp) assuming a compressor efficiency of 80%.[17]

DESTRUCTION USING HIGH SPEED ROTATING DISK

A high speed rotating disk was investigated by Goldberg and Rubin[18] and by Rubin and Golt.[19] Their results indicated that disk speeds in excess of 2,500 rpm provided an effective technique for foam breakage. Their work also indicated the disk material was not critical and a Teflon disk exhibited quite effective foam destruction. We mounted a 0.24 cm (0.062 in.) thick Teflon disk on a 50 watt (1/15 hp) Bodine electric motor and placed the disk in the 0.1 m (4 in.) vertical plexiglass pipe which was located inside the destruction chamber.

The motor was operated at its rated output of 10,000 rpm. The disk was evaluated with 1% Tergitol foam, 1.076 x 10^{-3} m^3/s (4.91 cfm). The destruction was inadequate. It was felt that the disk-to-pipe clearance would be a critical parameter (as any undestroyed foam had to pass through this opening).

---

[17] McCabe, W. L., and J. C. Smith. Unit Operations of Chemical Engineering. New York, McGraw-Hill, 1967. p. 217.

[18] Goldberg, M., and E. Rubin. Mechanical Foam Breaking. Ind. and Eng. Chemistry Process Design and Development. 6(2):195-200, April 1967.

[19] Rubin, E., and M. Golt. Foam Breaking with a High Speed Rotating Disk. Ind. and Eng. Chemistry Process Design and Development. 9(2):241-244, April 1970.

Clearances from 0.05 - 0.15 cm (0.125 - 0.375 in.) were investigated and the effect of the clearance distance on the destruction rate was observed to be minimal. The disk was then modified by cutting some sections out of it as shown in Figure D-3. This modification greatly increased the efficiency of foam destruction. The modified disk (with a disk-to-wall clearance of 0.08 cm) efficiently destroyed 1% and 4% Tergitol foam at flow rates up to 3.6 x 10^{-3} m^3/s (7.5 cfm). The input power to the motor under no torque was measured at 50 watts (1/15 hp), while in use the power requirement was 60 - 65 watts.

A small pneumatic hand grinder (Buckeye 2.6, Model 510D) was used to spin the disk instead of the electric motor. The grinder listed a maximum speed of 24,000 rpm. Once again no attempt was made to optimize the rotational speed. The grinder was operated with air at 317 kPa (46 psi) and 1.84 x 10^{-3} m^3/s (3.9 cfm) and was as efficient as the disk driven by the electric motor. The compressor requirement for this air would be 410 watts (0.55 hp), which is significantly greater than the power needed for the electric motor. The success of the high speed disk indicated than an efficient implementation of shear forces is an effective technique for foam destruction. Since the high speed disk destroyed foam efficiently with the least energy consumption this technique was mainly utilized in our foam scrubber collection efficiency evaluations.

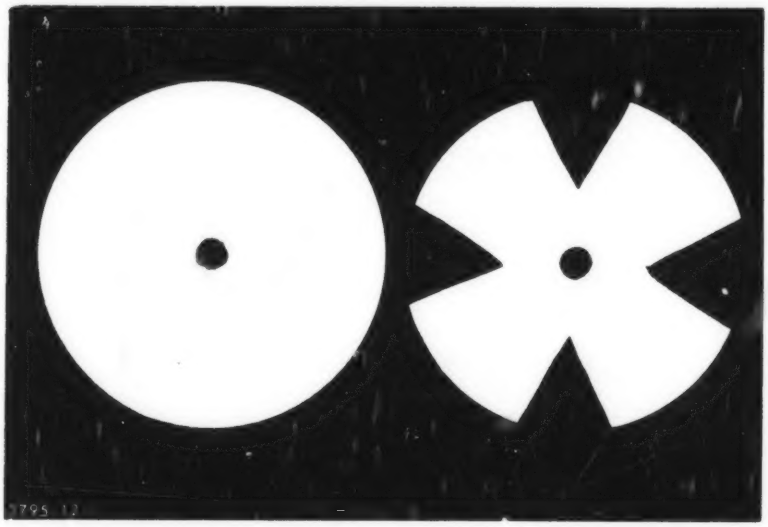

Figure D-3. Modified and unmodified Teflon disk

APPENDIX E

FOAM DENSITY

As indicated by our results above, the stability of foam with the same bubble size may vary with time. This is due to foam drainage. Fresh foam prepared with an adequate liquid spray will contain more surfactant liquid between the bubbles (wet foam) than the foam which was allowed to drain some of this solution (dry foam). The thickness of the bubbles may be considered as a measure of foam wetness. However, the difficulty in measuring the thickness of the foam films restricts the use of this variable. Similar results that could be considered a measure of foam wetness or wall thickness might be achieved by measuring the density of the foam.

A technique was developed to consistently and reproducibly measure the foam density. A 0.1 m (4 in.) flexible hose was attached to the plexiglass pipe about 1.52 m (5 ft) downstream from the foam production screen. A plastic container ($\sim$0.08 m^3) was then put on a platform so that it was above the level of the plexiglass pipe. This prevents water runoff from entering the container. The container is then filled with foam and weighed. From these measurements the expansion ratio defined as the volume of the container divided by the weight of the foam, or foam density, can be calculated. Expansion ratios for foams produced varied between about 50 and 200 cm^3/g. The data are presented graphically in Figures E-1 and E-2. The expansion ratio is simply the inverse of the density, and an expansion ratio of 100 has a bulk foam density of 0.01 g/cm^3.

The data indicate that the water flow rate is increased the expansion ratio is reduced. Increasing the surfactant concentration also tends to increase the density or reduce the

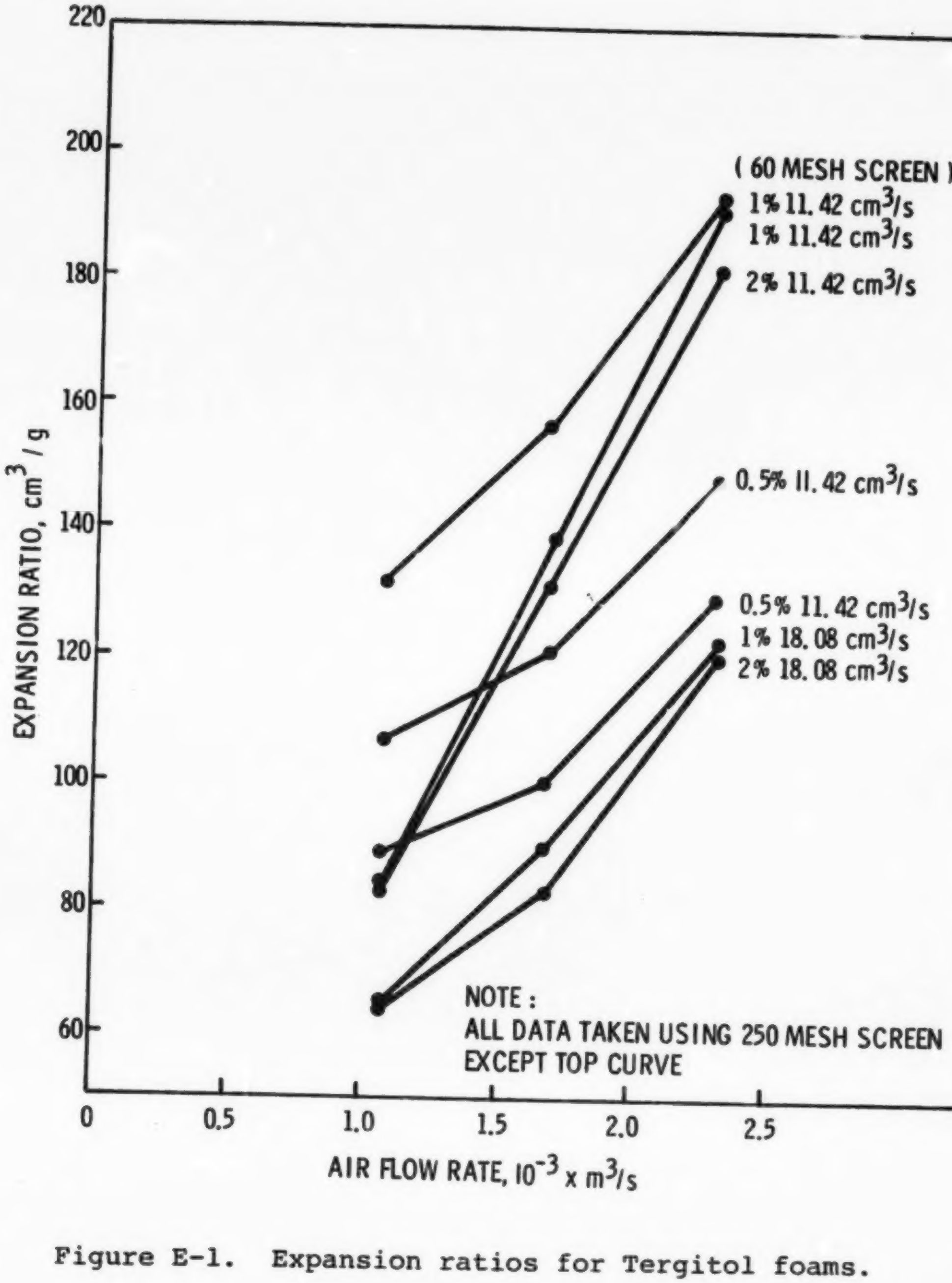

Figure E-1. Expansion ratios for Tergitol foams.

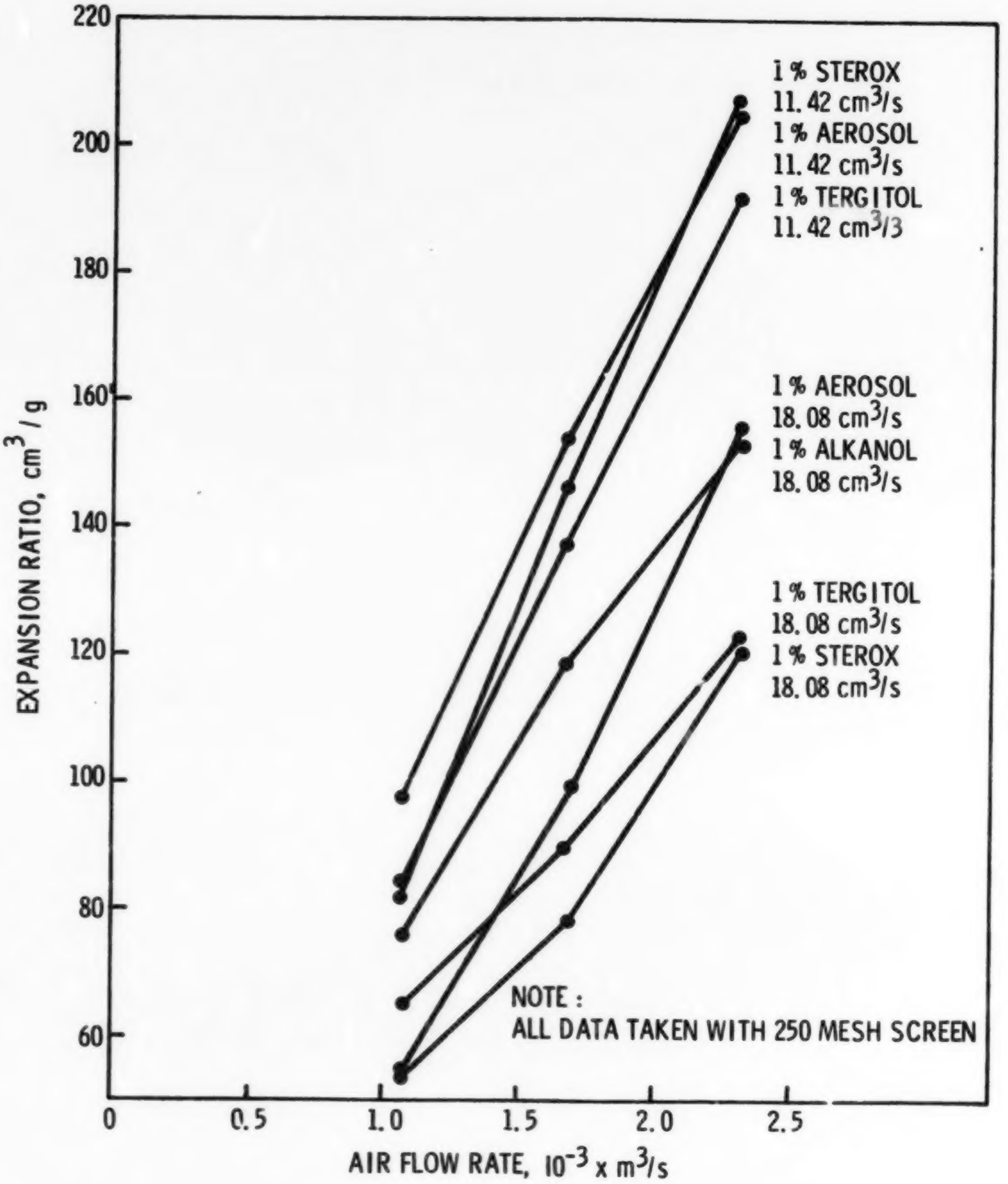

Figure E-2. Expansion ratios for several surfactants.

expansion ratio. Reducing the bubble size also tends to reduce the expansion ratio as is seen from the foam produced with the 60 mesh screen. An interesting observation is that increasing the bubble size (data with the 60 mesh screen and the 0.5% Tergitol) seems to reduce the slope of the curve. Data with very fine bubbles throughout the operating range (the Alkanol) increases the slope of the curve.

The possible explanation is that the larger bubbles which are definitely less stable than fine bubbles might undergo some destruction during the sampling.

APPENDIX F

INSTRUMENTATION FOR AEROSOL SAMPLING

Three types of particle count instruments were used for aerosol characterization and the determination of particle collection efficiency by the foam scrubber. The three instruments included a model Rich 100 Condensation Nuclear Monitor manufactured by the Environment/One Corporation, a Royco Model 220 Optical Counter from Royco Instruments, Inc., and a Model 3030 Electrical Aerosol Size Analyzer manufactured by Thermo Systems, Inc.

These three instruments characterize particles in the submicrometer size range desired for evaluation of foam scrubber operation. The condensation nuclei counter operates on the principle of utilizing the aerosol particles to nucleate condensation of water vapor and form larger particles which are analyzed by light attenuation phenomena. The condensation counter provides the total of all particles over 0.0025 μm in diameter, for concentrations above 300 particles/cm^3 (8.5 x 10^6/ft^3). Environment/One lists the accuracy of their instrument at ±20% with a repeatability of ±3%. The instrument computes a new reading about once per second and requires less than a minute to reach equilibrium in a new environment.

The Royco optical counter operates by projecting a light beam through the gas stream and detecting the particles by monitoring the light scatter with a photomultiplier tube. The particles are individually monitored by the photo tube and the detected light pulse is a function of particle size. Consequently, the output pulses from the tube can be counted and classified according to particle size at the same time. The instrument counts particles in five particle size classes: 0.3 - 0.5 μm, 0.5 - 0.7 μm, 0.7 - 1.0 μm, 1.0 - 2.0 μm, and

>2.0 μm. As reported by the manufacturer, the optical sensor has a maximum concentration limit, of 35 - 70 particles/cm^3 1 - 2 x 10^6 particles/ft^3). The accuracy of this instrument has been reported to approach 100%.[20]

The electrical analyzer generates a positively charged aerosol by passing the input gas through an electrically induced corona. The charged aerosol is then passed along a charged wire with known voltage. Particles less than a certain size are attracted to the wire and the remaining particles are collected on a charged plate. The voltage across the wire is incrementally varied and the charge collected upon the plate can be transformed into a size distribution of particles from 0.003 μm to 1.0 μm in 10 incremental steps. The accuracy of the instrument has been reported as "good" with a variability of 5% to 10%.[21]

SAMPLE DILUTION

The high aerosol concentrations which were employed in the investigations required the use of a dilution system so that the sample stream would not exceed the capacity of the optical and electrical aerosol monitors. The dilution system had a dilution capability from 25/1 and 500/1 and is illustrated in Figure F-1. The Cyclonair blower was used to pull the aerosol sample and the dilution air through the mixing section of the dilution apparatus.

---

[20] Liu, B. Y. H., R. N. Berglund, and J. K. Agarwal. Experimental Studies of Optical Particle Counters. Atmospheric Environment. 8:717-732, July 1974.

[21] Liu, B. Y. H., K. T. Whitby, and Y. H. Pui. A Portable Electrical Aerosol Size Analyzer for Size Measurement of Submicron Particles. (Presented at the 66th Annual Meeting of the Air Pollution Control Association. Chicago. June 23, 1973). 15 p.

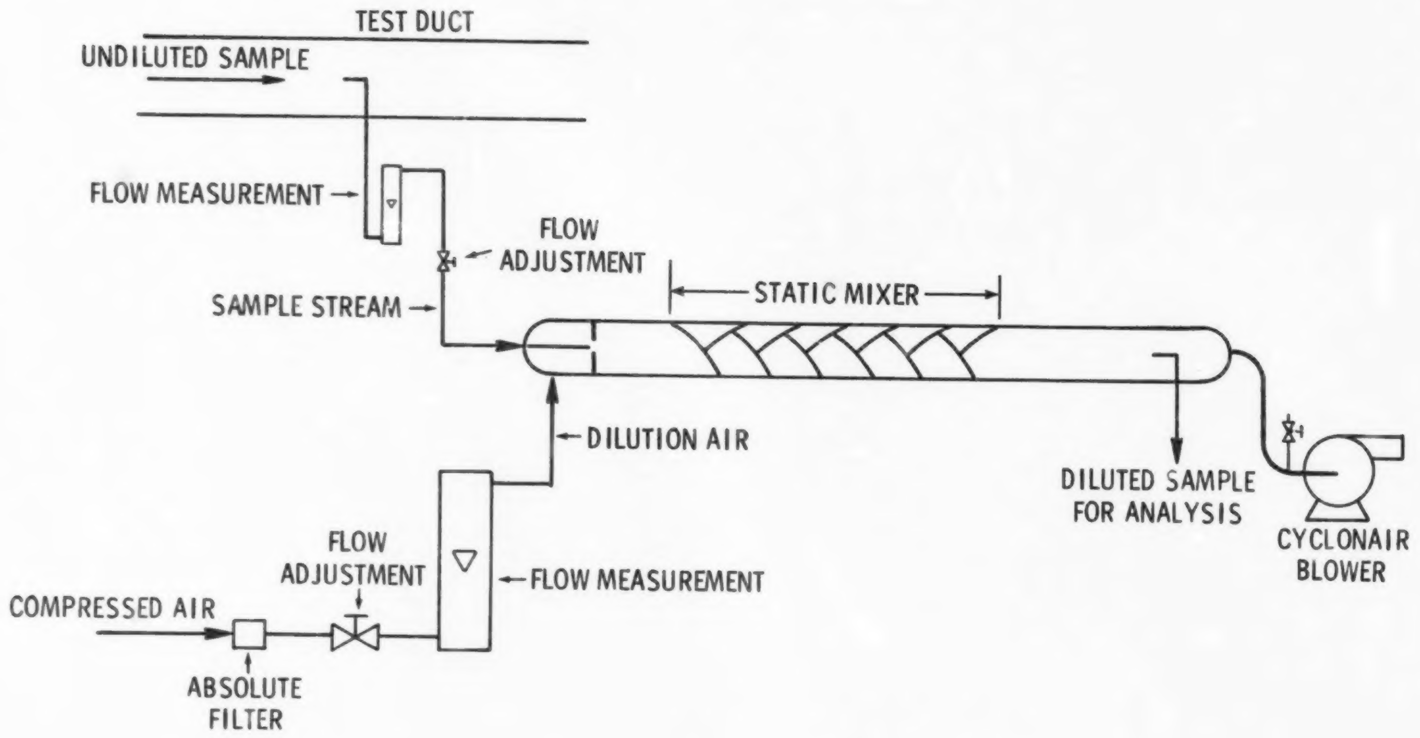
TEST DUCT
UNDILUTED SAMPLE
FLOW MEASUREMENT
FLOW ADJUSTMENT
SAMPLE STREAM
STATIC MIXER
DILUTION AIR
DILUTED SAMPLE FOR ANALYSIS
CYCLONAIR BLOWER
FLOW ADJUSTMENT
FLOW MEASUREMENT
COMPRESSED AIR
ABSOLUTE FILTER

Figure F-1. Sample dilution system.

The overall operation of the dilution system was checked by comparing the actual dilution ratio (as determined by the particle concentration measured with the condensation nuclei counter) with the theoretical dilution ratio (as determined from the rotameter settings). Figure F-2 indicates accurate dilutions up to the ratio of 400 to 1. The dilution system was also verified and its accuracy demonstrated by the use of three aerosol counters. Good agreement of all instruments was observed.

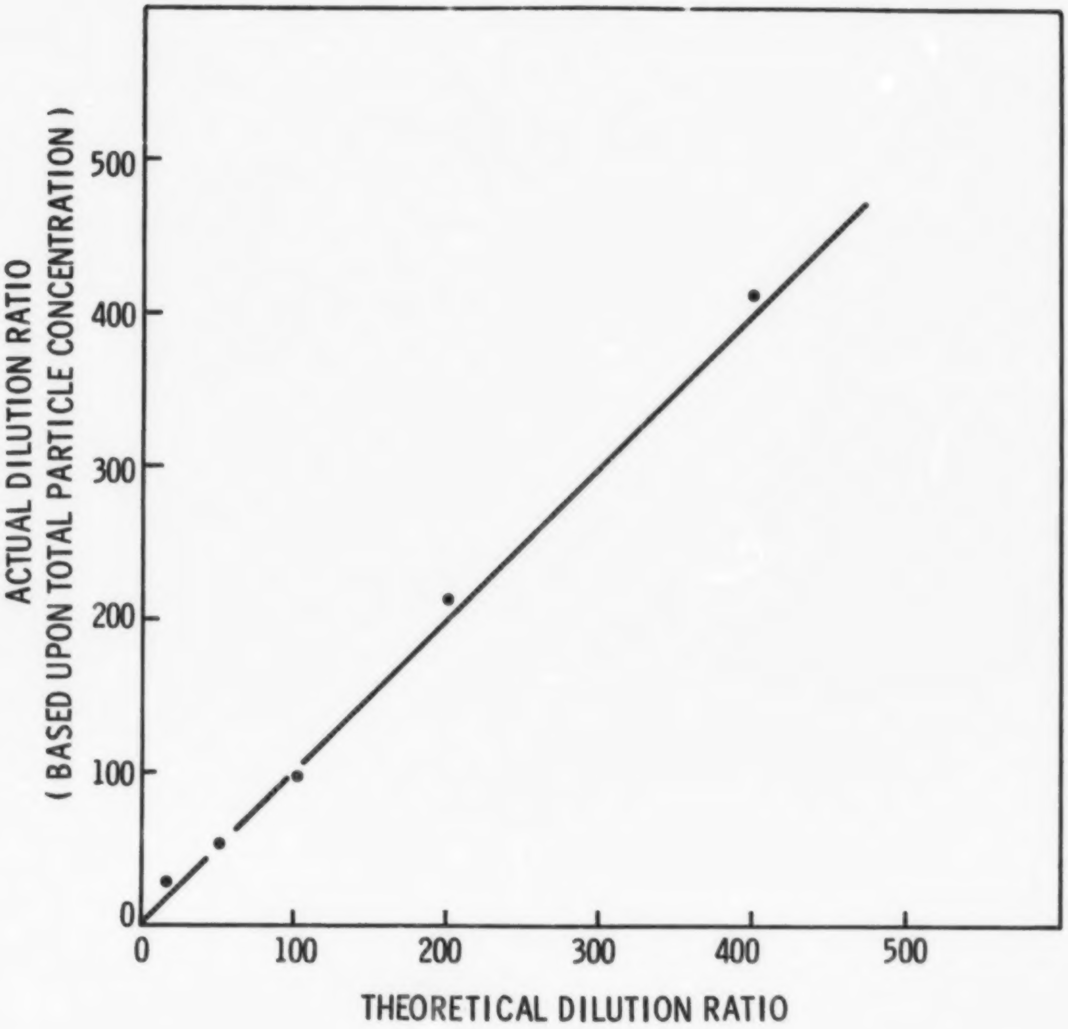

Figure F-2. Characterization of dilution system.

APPENDIX G

SECONDARY FORMATION OF PARTICLES FROM FOAM DESTRUCTION

Upon droplet evaporation any non-volatile material which is present in the liquid drop then remains in the gas stream as a particle. The destruction of foam is associated with the formation of fine aerosol. This has been observed by other investigators and confirmed in our experiments (e.g., Quon and Phillips[22] have indicated that a significant number of particles in the 0.3 to 2.0 μm range are produced when foam is destroyed by bubbling through isoamylalcohol). Destruction of foam results in bubble bursting and liquid droplet dispersion. While using the high speed rotating disk for foam destruction, it was observed that the number of particles generated varies with the disk speed and the foam density (see Figure G-1). The data indicate that for 2% Tergitol foam (o.37 x 10^{-3} m^3/s air flow, 5.83 cm^3/s water flow) at minimum destruction speed of 5,000 rpm, the baseline number of fine particles (ranging from 0.01 to 1.0 μm) was about 0.79 x 10^6 particles/cm^3. The number of these fine particles increased to about 1.65 x 10^6/cm^3 at a disk speed of 10,000 rpm. The foam used in this experiment consisted of about 1 mm cells and had a bulk density of 4.95 kg/m^3.

A significantly less dense foam was prepared using 1% Tergitol. Under the same flow conditions this foam appeared somewhat unstable and consisted of coarser, non-uniform cells (approximately 3 - 10 mm). The density could not be measured accurately because of the low foam stability. The baseline number of fine particles generated by disk destruction of

---

[22] Quon, J. E., and R. A. Phillips. A Laboratory Investigation of a Foam Phase Air Cleaning Device. (Presented at the 148th National Meeting of the American Chemican Society. Chicago. September 1964.). 15 p.

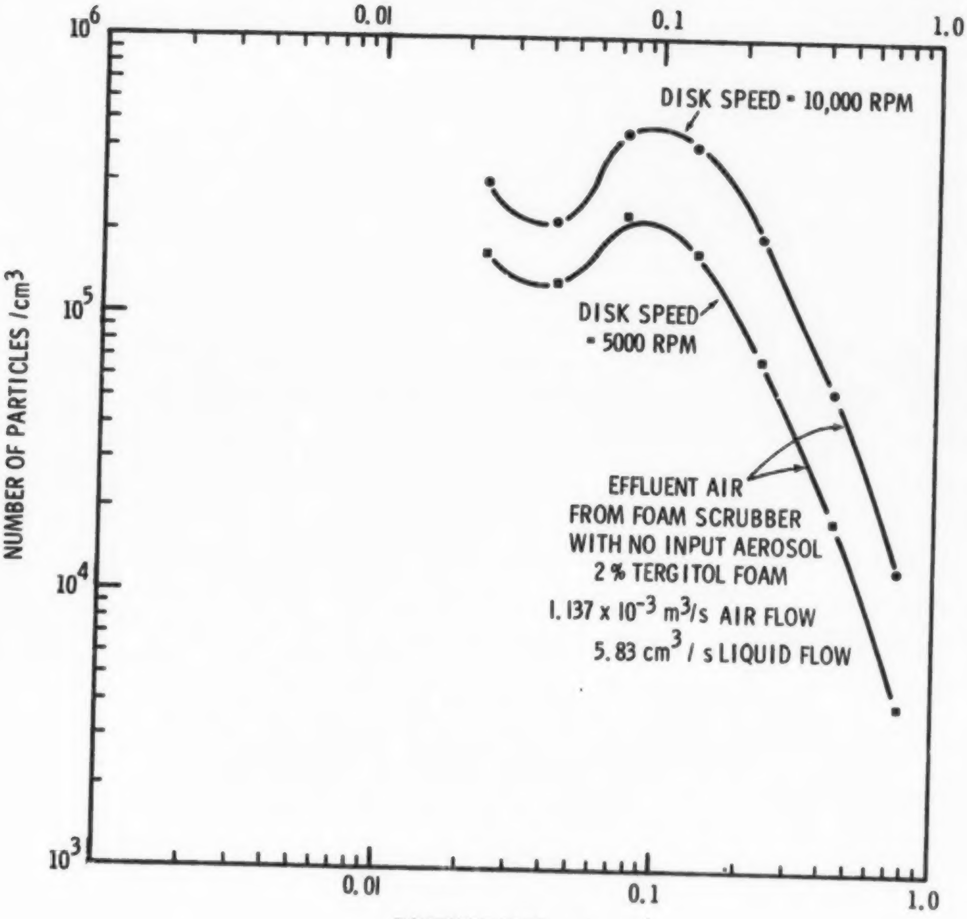

Figure G-1. Particles generated by foam destruction with rotating disk.

this foam varied from 0.34 x $10^6/cm^3$ at 5,000 rpm to 0.57 x $10^6/cm^3$ at 10,000 rpm. During actual collection efficiency determinations the disk was operated at the minimum destruction speed to reduce the particle baseline to a minimum.

Even though some emission of fine particles from foam destruction can be expected, our results should be regarded as very preliminary. We do not know whether or not the number of fine particles emitted from the foam destruction in the commercial operation would be proportionally higher relative to process capacity. Also, we feel that the design optimization of the disk foam destruction device in respect to fine particle emissions could substantially reduce this problem.